

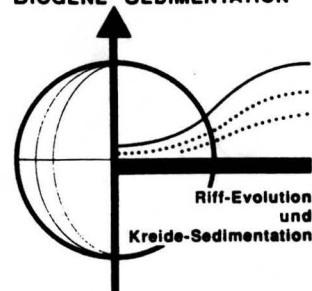
# Modern Cryptic Microbialite/Metazoan Facies from Lizard Island (Great Barrier Reef, Australia) Formation and Concepts

Joachim Reitner, Berlin

KEYWORDS: ORIGIN OF MICROBIAL CARBONATES – REEF CAVES – PELOID FORMATION – BIOFILMS - SPONGES – GREAT BARRIER REEF – RECENT

DFG-Schwerpunkt

BIOGENE SEDIMENTATION



## CONTENTS

### Summary

- 1 Introduction
- 2 Location of studied reef areas and sample sites
- 3 Material and methods
  - 3.1 Material
  - 3.2 Methods
    - 3.2.1 In vivo fluorochroming of hardtissue of sponges and microbialites
    - 3.2.2 Non fluorochroming stainings
    - 3.2.3 Fixation of sponges and microbialites
  - 3.3 Sample preparations
    - 3.3.1 Hardpart microtome
    - 3.3.2 Electron microscopy (TEM, SEM)
  - 3.4 Experiments within reef caves and aquaria
- 4 Definition of "Microbialite"
  - 4.1 Previous studies on Microbialites - a short overview
- 5 Cryptic microbialites of the Lizard Island Section
  - 5.1 Spatial facies distribution within shallow water reef caves of Lizard Island and North Direction Island
  - 5.2 Structure of cryptic microbialites
    - 5.2.1 Outer surfaces
    - 5.2.2 Vertical facies succession
  - 5.3 Interpretation
- 6 Microbialite formation
  - 6.1 Microbialite mineralization model based on organic macromolecules
  - 6.2 Calcifying soluble and insoluble matrices within microcavities and pocket-like structures
  - 6.3 In situ peloid formation
  - 6.4 Sponge tissue diagenesis - micropeloid formation
  - 6.5 Biofilms and microbes
    - 6.5.1 Calcified microbes
    - 6.5.2 Fe/Mn biofilms
  - 6.6 Geochemistry and stable isotopes
    - 6.6.1 Geochemical parameters
    - 6.6.2 Cements
    - 6.6.3 Stable isotopes
- 7 Proposed relationship between "bacterio-sponges" and biofilms of cryptic microbialites
  - 7.1 Bacteria in sponges
  - 7.2 Heterotrophic bacteria within studied cave sponges
    - 7.2.1 Proposed function of symbiotic heterotrophic bacteria

- 7.2.2 Hypothetic relationship between "bacterio-sponges" and biofilms
  - 8 Problems of microbialite formation - the alkalinity question
  - 9 Are modern microbialites from Lizard Island a model for ancient sponge reefs? - a perspective
  - 10 Conclusions
- References

## SUMMARY

From shallow water caves of fringing reefs related to continental islands of the Lizard Island Section thrombolitic micritic microbialites were observed. The microbialites exhibit always a light decreasing facies succession. The succession starts with a corallal community and ends with light independent microbial biofilms and benthos (coralline sponges). The sessile mineralized benthos community is constructed of crustose foraminifera, serpulids, thecidean brachiopods, bryozoans, and coralline sponges. The observed benthic community is very similar to those one observed in cryptic habitates of Aptian and Albian reefs of northern Spain.

For longtime studies of the microbialite formation and growth rates of coralline sponges the specimens were stained in vivo, within their natural habitat with histochemical fluorochromes and nonfluorescent agents. Main results are a very slow growth of the microbialite and associated sponges (50-100  $\mu\text{m}/\text{y}$ ). Only few calcifying microbes are participants during microbialite formation. Calcifying acidic organic macromolecules are mainly responsible for microbialite formation by cementing detrital material. Fe/Mn-bacterial biofilms are responsible for strong corrosion of the microbialite. Beside the corrosive activity of the Fe/Mn-bacterial biofilms boring sponges (*Aka*, *Cliona*) are the main destructors.

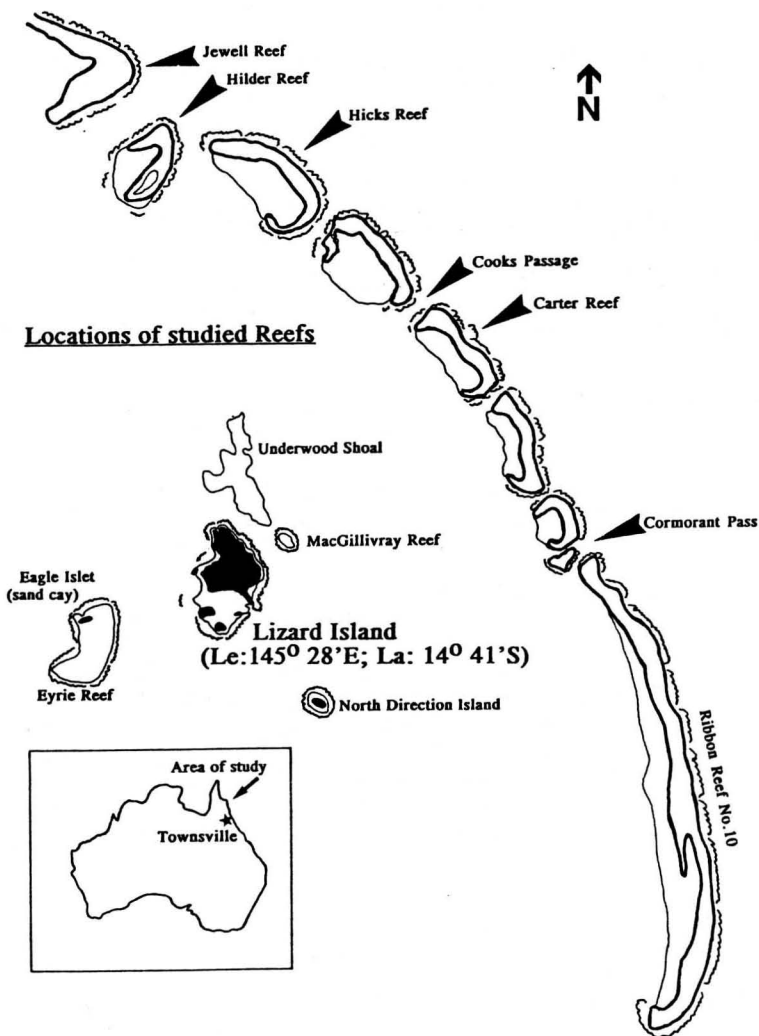


Fig. 1. Location of studied reefs of the Lizard Island Section. Lizard Island is situated in the Great Barrier Reef (Australia) at Le: 145° 28' E; La: 14° 41' S.

Geochemically the observed microbialites are composed of mainly high-Mg calcites and exhibit high positive  $\delta^{13}\text{C}$  (+3 to +4) values.

## 1 INTRODUCTION

The presented study of modern micritic crusts in reef caves is part of an investigation of surviving Cretaceous benthic communities in light degraded environments of reef habitats.

Within the simultaneously studied Lower Cretaceous reefs, in northern Spain (REITNER 1982, 1986, 1987) we have observed in all cases a close relationship of thrombolitic or stromatolitic micrite crusts with a benthic community characterized by coralline sponges. This relationship of microbialite crusts with sponges and further sessile benthic organisms was observed in shallow water cryptic habitats and within larger reef mound structures in deeper parts of the reef slopes ("sponge reefs").

The investigations of modern occurrences in reef caves which may represent a facies telescoping of deeper biofacies in shallower ones, could be a key to understand the formation of fossil sponge reefs.

The investigations began in 1990 with a pilot study in fringing reefs of Lizard Island (Great Barrier Reef) and reefs of the outer barrier for comparison. Main goals are to study this environment under normal conditions and for comparison under controlled artificial conditions in seawater running aquaria. Two reef caves were selected for longtime research and all experiments were carried out within these caves.

H. ZANKL (Marburg) has recently found nearly similar microbialites in cryptic habitats of reefs of St. Croix (US Virgin Islands, central Caribbean realm) (ZANKL 1993).

Comparative fossil examples were studied by NEUWEILER (1993) on middle Albian reefs of northern Spain and KEUPP et al. (this volume) for Jurassic ones. Both studies refer to the presented data.

Purpose of this study is to demonstrate the growing procedure of a modern type of cryptic, light independent microbialite, the interaction with associated benthos, and its significance as a key facies to understand fossil metazoan-micritic/microbialite reefs. To understand these very complex processes it is necessary to review and compile modern concepts of biomineralisation, biofilms, and e.g. the alkalinity question. Therefore mixing of own results and reviews is planned and intended!

Main goal of this study is creation of a working hypothesis to understand the processes of formation of micritic/microbial build ups ("mud mounds").

## 2 LOCATION OF STUDIED REEF AREAS AND SAMPLE SITES

The work was carried out at Lizard Island Research Station on Lizard Island (Le 145°28'E; La: 140°41'S) (Fig. 1).

The reefs studied are located in the northern part of the Great Barrier Reef (GBR) around Lizard Island within the Lizard Island Section of the GBR Marine Park.

The fringing reefs of Lizard Island are the main reef areas studied (Fig. 2). The investigations are focused on two reef caves within the fringing reefs of the Lizard Island Group. One of the selected reef caves is located at the southern corner of South Island in a water depth of 6-9m, and the second selected reef cave is located close to Bommie Bay on the northeastern side of Lizard Island in a water depth of ca. 10 m (Fig. 2). Within these two caves all life habitat controlled longtime experiments are carried out.

Additional investigations were made in reef caves of the "Washing Machine", Pidgin Point, and Crystal Beach (Fig. 2).

In the surroundings of the Lizard Island Group, reef caves were studied at North Direction Island, Eyrie Reef, and MacGillivray Reef ("Macs-Reef") (Fig. 1). Additional

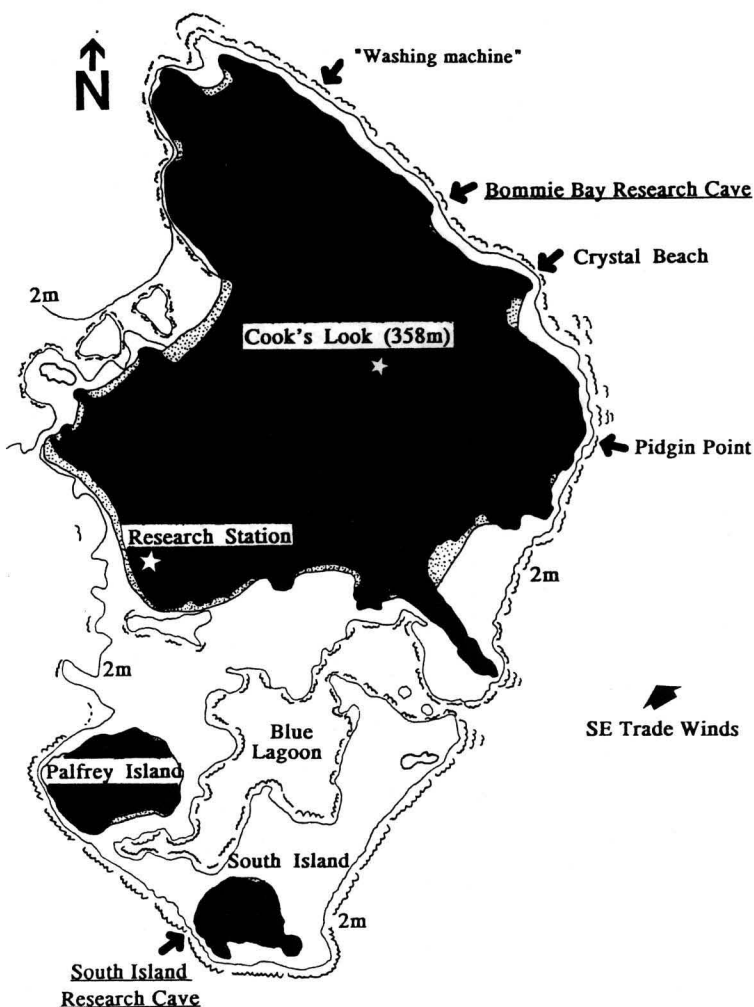


Fig. 2. Location of investigated reef caves around Lizard Island.

studies were carried out in reef caves and overhangs of the Outer Barrier. The studies were focused on Hicks Reef, Hilder Reef, Jewell Reef, and Ribbon Reef No.10 (fig.1).

### 3 MATERIAL AND METHODS

#### 3.1 Material

All specimens (organisms and rock samples) used for this study were collected at the sample sites and prepared for further investigations. In the caves the samples were taken from recognizable different facies types. All selected specimens were photographed and documented by using underwater video films. The investigations were focused on coralline sponges (*Astrosclera willeyana*, *Spirastrella (Acanthochaetetes) wellsi*, *Vaceletia crypta*, *Murrayona phanolepis*, and *Plectroninia neocaledoniense*) and microbialites. *Sp. (Acanthochaetetes) wellsi* and *Astrosclera willeyana* are the most common taxa and therefore selected for longtime experiments. Within the caves 5-10 specimens of each species were selected and labeled for in situ experiments.

From different types of microbialites samples were taken using a big (1.5 kg) hammer and the damaged parts on

the cave walls were labeled also to study the regeneration of the disturbed parts.

The initial growth of microbialites and settlement of biofilms and benthos were studied beside the regeneration of disturbed parts using artificial substrates.

From 160 selected specimens more than 500 rock thin-sections and histological sections were made. All specimens including the sections are deposited in the Institut für Paläontologie der Freien Universität Berlin.

#### 3.2 Methods

##### 3.2.1 In vivo fluorochroming of hard tissue of sponges and microbialites

In order to study growth and calcification rates of living specimens of two species of coralline sponges, the chaetetid *Spirastrella (Acanthochaetetes) wellsi* and stromatoporoid *Astrosclera willeyana*, and associated calcified microbialites were stained with different types of fluorochromes in vivo.

The specimens were stained principally with two types of fluorescent dyes, with the antibiotics tetracycline base (Achromycin; SERVA 35865), tetracycline HCL (Achromycin-HCL; SERVA 35866), 7-Chlorotetracycline-HCL (CTC, Aureomycin; SERVA 14200), and with the indicators for metal titration (fluorometric determination of Calcium) calcein (MERK 2315,  $C_{30}H_{26}N_2O_{13}$ ), and calcein- $Na_2$  (FLUKA 21030  $C_{30}H_{24}N_2Na_2O_{13}$ ). In all cases high concentrations of 250 mg/l seawater were used. The fluorescence dyes were injected into the living portions of the specimens, and they were covered with a plastic bag for an incubation time of 10-15 min. only.

The used fluorochromes are  $Ca^{2+}$  binding chelat complexes which are bound on the surfaces of the newly formed Ca-salt crystals. Calcein has for example 5 free carboxyl-groups ( $COO^-$ ) which bind  $Ca^{2+}$ . They allow a polychrome fluorescence labeling of the calcareous skeletons and microbialites. The polychrome labeling allows to calculate the growth rates and to recognize the loci of mineralization!

Calcein was first used as an intravital fluorescence tag to study the growing mammal bones (RAHN 1977). WILLENZ & HARTMAN (1985) has used it with success to study the growth rates of the aragonitic coralline sponge *Ceratoporella nicholsoni* from Jamaica (Caribbean). They used a concentration of 100mg/l and an incubation time between 12 and 24 hours and treated the specimen again after one week and six months. The sponge exhibited a growth rate of 200  $\mu m/a$ . We have done it more or less in the same manner, however, we used higher concentrations and less incubation time, but the results are similar. Especially the labeled specimens of the high-Mg calcite *S. (Acanthochaetetes) wellsi* exhibit a strong green fluorescence. Same results were observed within the microbialites, but a distinctive growing was not observed,

however, the loci of calcifications were localized.

The same procedure was performed with still living specimens in aquaria. The aquaria experiments were not directly comparable because the sponges were too stressed due to rapid temperature change. The calcification rates of the aquaria specimens were therefore much higher (1-3  $\mu\text{m}/\text{week}$ ) as observed in the natural habitat (1  $\mu\text{m}$ ) probably caused by increased stressed Ca-detoxification.

To localize the loci of mineralization, specimens fixed with buffered glutaraldehyde and stored in 70% ethanol can also be used. The Ca-binding proteins with seed crystals exhibit a similar fluorescence behavior which is different from any autofluorescence of different tissues types.

Best results in shorttime staining (15min) of living specimens within their natural habitat we got with Calcein- $\text{Na}_2$  fluorochrome ((FLUKA 21030  $\text{C}_{30}\text{H}_{24}\text{N}_2\text{Na}_2\text{O}_{13}$ ) (100mg/l). The yellow/green fluorescence is very prominent and marks few newly formed calciumcarbonate seed crystals.

The second group of fluorochromes which work successfully are different types of the antibiotic tetracyclines. Tetracyclines are used as antibiotic agents and were the first fluorochromes which allow a staining of Ca-bound hardtissues in vivo (MILCH et.al 1958). The fluorescence behavior was discovered because the growing teeth of young children which had got tetracyclines as drugs exhibit under UV-light a yellow fluorescence.

Tetracyclines are used widely for calcification and Ca-binding protein studies in vivo (FINERMAN & MILCH 1963 binding of tetracyclines to Ca; KOBAYASHI & TAKI 1969 sea urchins; BARNES 1981 corals). Aureomycin (CTC) was used to study intra- and extracellular Ca-ions especially to show the role of Ca during e.g. the moving of amoebae (GAWLITTA & STOCKEM 1980) and the growth of algae (HAUSSER & HERTH 1983).

For the here presented study the tetracycline-HCL and Aureomycin (CTC) exhibit the best fluorescence results. Especially the calcification areas of the microbialites could be detected with tetracycline-HCL. Aureomycin shows a strong fluorescence within newly formed skeletons of *S. (Acanthochaetetes)*. The main problem with these dyes is their antibiotic character. Sponge tissues are, as a rule, penetrated with symbiotic bacteria which play an important role in the metabolic pathways of a sponge. The tetracyclines are disturbing or inhibiting this procedure. WILLENZ & HARTMAN (1985) had no results using tetracyclines and they argue that the staining for more than 12 hours would be lethal for the symbiotic bacteria. Therefore we have used tetracyclines only for shorttime (10-15 min). Normally the staining results are visible within some minutes after incubation. The water flow through the sponge canal systems guarantees a rapid transport to the calcification loci.

The microbialites do not show this effect because microbes do not play a very important role during calcification.

The yellow/golden fluorescence is easy to distinguish from the autofluorescence of different tissue types.

The fluorochromed specimens were studied with an epifluorescence microscope ZEISS Axiophot. The filter sets used for calcein and tetracyclines are: high-performance

narrow-band pass filter BP 365/12 nm, LP 397 nm (UV-light, no. 487701); high performance wide-band pass filter BP 395-440, LP470 (blue violett, no. 487705).

To study acidic mucus substances (mucoproteins, glycoproteins, acidic mucopolysaccharids (= proteoglycans = glycosaminoglycans & proteins; glycosaminoglycane = Uron acid + aminosugars) which play an important role during biomineralisation, the fluorochrome acridine orange and non-fluorescent thiacine stainings (toluidine blue, methylene blue) were used. Acridine orange is an important fluorescence dye to recognize bacteria. Some specimens were stained with Acridine orange and Ca-chelating fluorochromes (calcein, tetracyclines) to localize  $\text{Ca}^{2+}$  concentrations within the acidic mucopolysaccharids. Acridine stainings were done with living tissues and microbialites as well as with glutaraldehyde/formol fixed ones. Acridine organe exhibits an orange fluorescence using a high performance wide-band pass filter (blue, BP 450-490, LP 520; no. 487709) (STRUGGER 1940, HICKS & MATTHAEI 1958).

Living sponge tissues (proteins) including collagenous supporting skeletons are easy to determine with the fluorochrome thiacine red. Using this dye, it was easy to recognize the very thin sponge crusts (50  $\mu\text{m}$ ) which grow in close contact with microbial biofilms, and which exhibit a strong staining behavior using acridine orange and/or toluidin blue, and methylene blue (acidic mucopolysaccharids!). Thiacine red exhibits a strong red fluorescence using a high performance wide-band pass long wave filter set (green, BP 515-565/LP 590; no. 487714) or in combination with acridine orange (blue, BP 450-490/LP 520) or in combination with tetracyclines (blue violet, BP 395-440/LP470).

In all cases autofluorescence behavior of different tissues and minerals gives additional information beside the artificial fluorescence. Many substances exhibit a strong autofluorescence as chlorophyll, collagen, and organic macromolecules enclosed in newly formed crystals (DRAVIS & YUREWICZ 1985). The best way to study autofluorescence is to use the longwave high-performance narrow-band pass filter BP546/12, LP590 (green, no. 487715). The fluorescence is red. The main problem is to get good micrographs. It is useful to reduce the shutter time of one point. Beside the longwave narrow-band filter, a high performance wide-band pass filter BP 450-490/LP520 (blue, no. 487709) gives very good information. The fluorescence is yellow. Especially the mineralization events in coralline sponges (e.g. *Vaceletia, S. (Acanthochaetetes)*) can be recognized (REITNER 1992, CUIF et al. 1990).

### 3.2.2 Non fluorochroming stainings

Beside fluorochromes classical staining techniques were used. Most investigated samples were block stained with basic fuchsine and sometimes differentiated with methylene blue. Additionally, pure basic fuchsine, methylene blue, and toluidine blue stainings were always used. The block staining was done on fixed specimens in 70% ethanol for a long period of 12-24 hours, because the migration of staining solutions in very strongly lithified microbialites and coralline sponges needs time. Each sample has its own best staining

duration, and it is useful to try various incubation times. For calcareous crusts 24 hours have proven sufficient. The sponges need less time and 1-12 hours are a mean times. After staining the samples are washed 3x in 70% ethanol or till no staining solution can be removed from the specimen anymore. The growing fronts and mineralizing portions of the microbialites are stained in various colors depending on the organic substances versus mineralization.

### 3.2.3 Fixing of sponges and microbialites

Most samples were fixed in buffered 4% glutaraldehyde (=glutardialdehyde) solution in seawater. Sodium cacodylate buffer (0.4 mol) was used (7.4 ph) in seawater also. Few were fixed in buffered 4% formol or in ethyl alcohol only. The specimens were stored at 8-4°C in a refrigerator for 1-2 days depending on their size. After fixation, the specimens were washed in running seawater for 1-2 hours to remove the glutaraldehyde. After this procedure the specimens were moved to ascending ethyl alcohol concentrations (20-30-50-70 %) each step with a minimum of 30 min. The specimens are kept in 70% ethyl alcohol for longtime storage.

Some selected small pieces were postfixed (after washing with seawater) with 2% osmium tetroxide solution (OsO<sub>4</sub>) in filtered seawater (for SEM and TEM investigations) for 1-3 hours, depending on the amount of organic matter. After postfixing the specimens were washed with 30% ethyl alcohol and later moved using ascending alcohol concentration and stored at 70%.

Specimens which were selected for biochemical studies were rapid dried or fixed in a saturated mercury chloride (HgCl<sub>2</sub>) solution.

## 3.3 Sample preparations

### 3.3.1 Hardpart microtome

The fixed specimens were block stained and afterwards embedded in araldite or epon (epoxy resins). The specimens are dehydrated to 100% ethanol and then moved into a mixture of propylene oxide and resin. This procedure is carried out until only resin is left in the tissue of the specimen and after 3 days in a stove at 30-60°C the araldite is polymerized and hard enough to cut with a microtome. Normally the hardtissues must be removed before sectioning to prevent all important data between softtissues and mineralized parts to be gone. With the described techniques it is possible to cut both with a hardpart microtome from LEITZ. The sections are of 50-15 µm thickness. If thinner sections are required (10-5 µm) the specimens must be presected in ca.100-1000 µm thick slices, re-embedded in resin, and manipulated with a grid free grinding machine.

### 3.3.2 Electron microscopy (TEM, SEM)

Samples for transmission electron microscope (TEM) studies (OsO<sub>4</sub>-fixed specimens) were demineralized first with EDTA to remove the calcareous skeletons, then with 5% HF to dissolve the siliceous spicules, embedded in epon, and cut with an ultramicrotome. Samples for scanning

electron microscope (SEM) studies were normally dried or critical point (CP) dried after 100% dehydration or virtually CP-dried with PELDRI II (Plano), which is easier to handle, and results are comparable normal CP. It was useful to break up the dehydrated specimens before drying after shock freezing with liquid nitrogen. SEM samples were coated with Au. Backscatter analyses were carried out on polished surfaces as well as EDAX-mapping and spot analyses (REITNER 1992).

## 3.4 Experiments within reef caves and aquaria

Within the two selected reef caves (South Island and Bommie Bay research caves) various experiments were performed, and longtime ones are still running.

Specimens were marked with plastic labels. The experiments began in February 1990 with an initial staining. In spring 1992 some of the 1990 specimens were marked again (80% of the labeled specimens were still in place). Some of them were picked up for control measurements.

Beside staining, different types of artificial panels were installed in the caves for longtime fouling experiments. Since 1990 two beton blocks and dead coral skeletons are being observed and the fouling is documented every year by underwater photography and video films. Important are also the observation of regeneration on freshly broken surfaces after rock sampling to understand the very slow growth rates of microbialites and biofilm development.

1993 we have done shorttime (2 weeks) experiments with wooden substrated, cleaned coral skeletons, and aluminium to study the settlement of initial biofilms. The panels were mounted on large SEM operating disks.

In seawater running aquaria living specimens of coralline sponges and associated microbialites were stored to control the results from natural habitats under artificial conditions. There are many technical problems to get stable conditions with the available aquaria system. The biological systems of the microbialites do not survive a period of more than 2 weeks, and experiments under controlled conditions are not possible at the moment. In vivo staining experiments within the first week, however, were very successful.

The underwater light measurements were carried out with a LICOR-sensor radiation meter (type LI-189 with a Squerical Quantum Sensor type LI-193SA).

## 4 DEFINITION OF "MICROBIALITE"

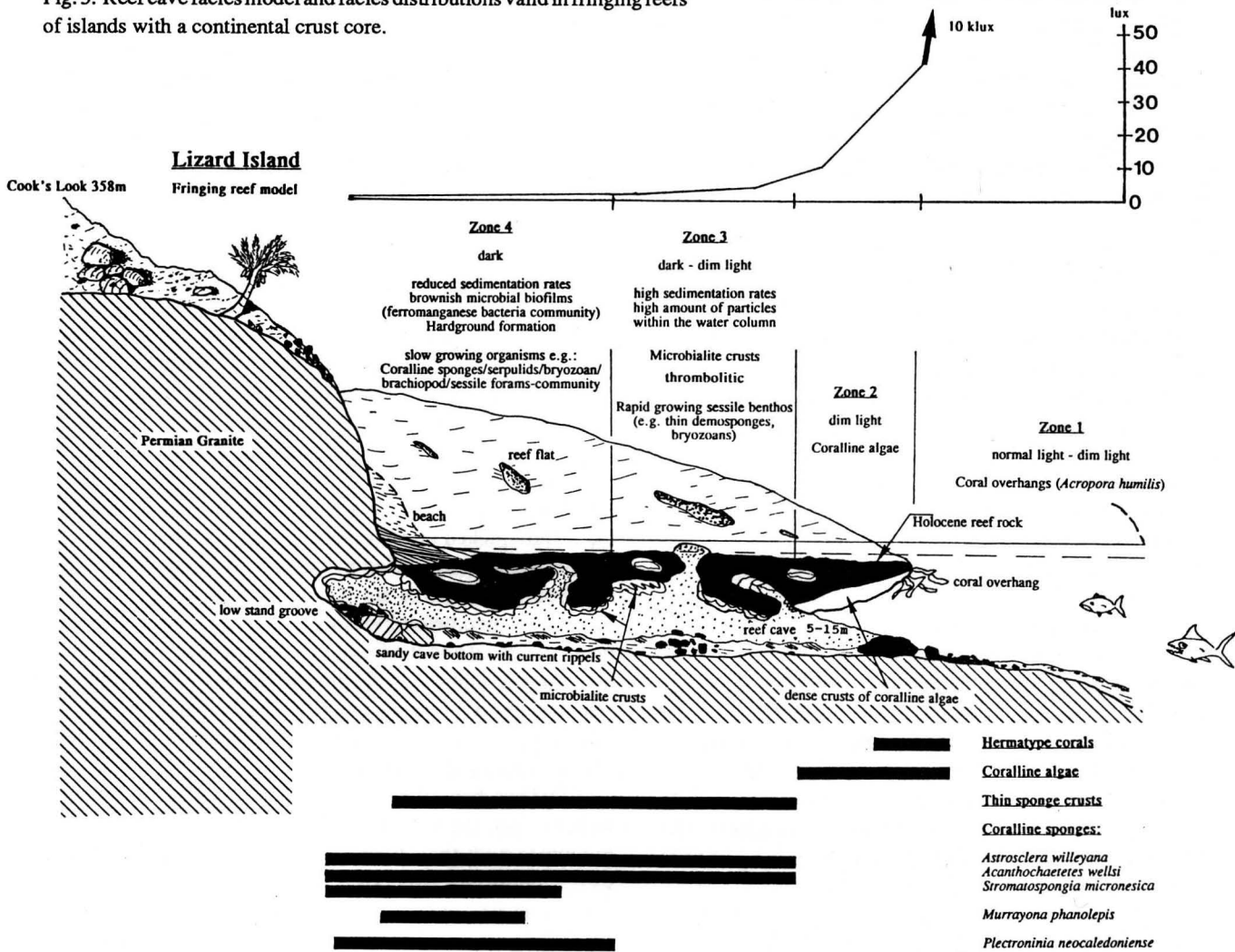
The term "microbialite" was introduced by BURNE & MOORE (1987: 241-242) to explain organosedimentary deposits of benthic microbial communities and binding of allochthonous material:

*"Microbialites are organosedimentary deposits that have accreted as a result of a benthic microbial community trapping and binding detrital sediment and/or forming the locus of mineral precipitation."*

BURNE & MOORE (1987) recommended to use the term only when the internal structure of a micrite body exhibits a fine more or less planar lamination.

This term is meanwhile used in a widespread manner and

Fig. 3. Reef cave facies model and facies distributions valid in fringing reefs of islands with a continental crust core.



include beside classical stromatolitic buildups all structures with laminated and/or thrombolitic micrites and related benthic metazoans and plantae. The main problem is that not all organic Ca-binding and mineralizing mucilages are in first order of microbial nature.

The term microbialite is partly substituting terms like "submarine micritic cements, micritic cements, and micrite crusts".

Within the presented paper the term "microbialite" includes two processes of formation: a direct formation via mineralisation of microbes such as bacteria and fungi cells and related slimes, and an indirect formation with no direct control by microbes only by calcifying organic macromolecules.

#### 4.1 Previous studies on microbialites - a short overview

Carbonate crusts with microbialitic features from the Great Barrier Reef (GBR) were e.g. described by MARSHALL (1983, 1986) from the One Tree Reef, and from the central area of the GBR E of Townsville. I.G. MACINTYRE, one of the protagonist of submarine lithification, has studied a lot of reefs in the Caribbean realm and has noted the importance of

more or less laminated micrite crusts and linked peloidal formation (e.g. 1977, 1978, 1984, 1985).

A very important paper was written by MACINTYRE & MARSHALL (1988) in which they summarize all known controlling factors and growing features of submarine more or less laminar micrites.

JONES & HUNTER (1991) were the first authors which have recognized the close relationship between a corallal facies and microbialites. They have observed in Late Pleistocene reef strata of Grand Cayman and San Salvador Island a vertical succession of corals, coralline red algae, and microbialites. They interpreted this succession as result of regressive conditions. The observed community sequence is very similar to the recently observed ones within Lizard Island reef caves, but the results and interpretations are contradictory.

Recent prominent deeper water microbialite crusts below 120 meter water depth were described by BRACHERT & DULLO (1991) from the Red Sea close to Port Sudan. These microbialite crusts exhibit a very close relationship with ones observed from Lizard Island.

Deep water microbialites and crusts from the Red Sea collected during the cruise 29 of the RV Sonne in 1984 were reported by STOFFERS & BOTZ (1990). These crusts are not

comparable with those ones described from shallower water levels.

## 5 CRYPTIC MICROBIALITES OF THE LIZARD ISLAND SECTION

### 5.1 Spatial facies distribution within shallow water reef caves of Lizard Island and North Direction Island

In all studied shallow water caves (5-15 m) around Lizard Island, North Direction Island, and Macs-Reef four main facies types could be distinguished. The caves are relatively narrow and have a mean horizontal distribution of 5-15 m (Fig. 3).

The light measurements are given in photometric lux ( $1 \text{ lux} = \text{quantum } 0.1 \mu\text{mol s}^{-1} \text{ m}^{-2}$ ).

**Zone 1** represents the entrance area with active coral growing and strong sun light conditions. The coral community is dominated by the branching form *Acropora humilis* which is forming overhangs. The measured light intensities at a sunny day at noon time varies from 2 klux within the open water to 600 lux close to the cave entrance.

**Zone 2** is light protected and is located under the *Acropora humilis* overhangs, and under cemented older reef rocks. This dim light area (5-10 lux) is characterized by very dense crusts of various coralline red algae dominated by the genera *Neogoniolithon*, *Lithophyllum*, *Tenarea*, *Peyssonella*, *Porolithon*, and *Lithoporella* (Pl. 1/1a,b; Fig. 3). The algae are associated with zooxantellate deeper water corals of the *Agaricia*-group. *Leptoseris* cf. *incrustans* is a thin platy coral common in this environment. This coral is normally adapted to deeper conditions (80-100m) and possesses special pigments to use remaining sun light in the deepness. Quite common are *Porites australensis* and *Synarea* sp. (KÜHLMANN 1983, FRICKE & SCHUHMACHER 1983, FRICKE & MEISCHNER 1985).

The measured light intensities were 50 lux close to the entrance with many *Agaricia* corals, 5-10 lux in the central red algae area, and 2-5 lux in the transition zone 2 to zone 3.

**Zone 3** starts immediately with some decimeter transition area only. The transition zone is characterized by rare single cell-layered thin smooth crusts of coralline red algae which may be related to *Melobesia*. The dim light of the transition zone is changed into more or less dark conditions (2-0.1 lux). On the roof of the caves, chimney-like openings are common through which little light (1 lux) and fine grained sediments come in from the reef flat under normal conditions (Pl. 2/2a,b; Fig.3). On the floor of the openings pebble sized debris of reef rocks are accumulated as a result of heavy storms. On the cave walls grow a lot of non-skeletalized branching organisms like hydrozoans and bryozoans which baffle fine grained sediments and larger microbial colonies bind sediment. The cave walls therefore exhibit a dense cover of sediment fixed by organisms. Rapidly growing sponges, bryozoans, serpulids, and ascidians are dominant faunal elements. Coralline sponges are restricted to sediment reduced areas. The observed microbialites are characterized by relatively thick crusts (5-6 cm) with a high amount of detrital material and many hints to anaerobic conditions

(below 1cm of the sediment surface dark sulfid rich sediments). Mean light values are 0.4 - 0.1 lux within this zone.

**Zone 4** represents the distal facies of the reef caves (Pl. 1/3, 4; Fig. 3). This area is completely dark (0.2 - 0.0 lux) and under normal conditions the water column is reduced in particles in contrast to zone 3. The sandy bottom exhibits sometimes current ripples which indicate increased water movements and currents during spring tides and storms. The caves and crevices are very narrow and branched at their distal ends. In most cases the granitic basement is not exposed, or the distal parts are more or less closed by a dense cover of microbialites. In few cases (South Island cave, North Direction Island cave) the most distal ends of the caves were reachable. These places are characterized by cemented large boulders of reef breccia (Pl. 1/4a). The reef breccia is restricted to grooves within the granite which may be interpreted as sea level low stand grooves (Fig. 3).

Coralline sponges and their linked benthos community play a dominant role, and they form small rigid reef mounds of about one meter diameter and 50 cm high (Pl. 1/3a, b). The coralline sponge community, apart from the common species *S. (Acanthochaetetes) wellsii* and *Astrosclera willeyana* is characterized, by the very cryptic species *Stromatospongia micronesica*, *Murrayona phanolepis*, and *Plectroninia neocaledoniense*. Further sponges are small lithistids (*Disco-dermia* sp., *Desmanthus incrustans*), *Rhabderemia sorokiniae*, *Didiscus placospongioides*, *Clathrina* sp., *Spongia* sp., *Agelas* sp., *Sycon* sp., and many very thin sponge crusts mostly related with the Poecilosclerida. The associated sessile rigid benthos is dominated by small brachiopods of the *Thecidellina congregata* group, *Frenulina sanguinolenta*, and *Argyrotheca arguta* (Pl. 1/3b, 4b) (cf. GRANT 1980, Enewetak Atoll) sessile foraminifera (*Homotrema rubrum*, *Carpenteria monticularis*, *Carpenteria* sp., *Miniacina* sp., div. agglutinating foraminiferas, e.g. *Placopsilina* sp.), hydrocorals (*Distichopora crisioides* and *Stylaster elegans*), ahermatypic corals (*Dendrophyllia* sp., *Tubastrea* sp.), bryozoans (*Celleporaria* div.sp., *Puellina innominata*, *Parasmittina* sp.), common hydroids (*Halopteris* sp.), crustose ascidians with many spicules, and serpulids.

The associated microbialites with a thickness of 2-3 cm are thinner than those from zone 3 resulting from less sedimentary input. Common are ferromanganese bacterial biofilms on the surfaces. The entire facies is comparable with a typical hardground facies.

## 5.2 Structure of cryptic microbialites

### 5.2.1 Outer surfaces

The studied microbialites show two distinctive surface types (Pl. 2/1a, b). It is possible to distinguish an upper surface type which is characterized by small sized (ca. 1-3 cm) irregular thrombolitic pillars which are often orientated in the direction of the main water current (Pl. 2/1a, c). The main water current is controlled by tides, and the prominent flow direction is from inside to outside of the cave system (Bernoulli effect). Therefore the pillars exhibit an

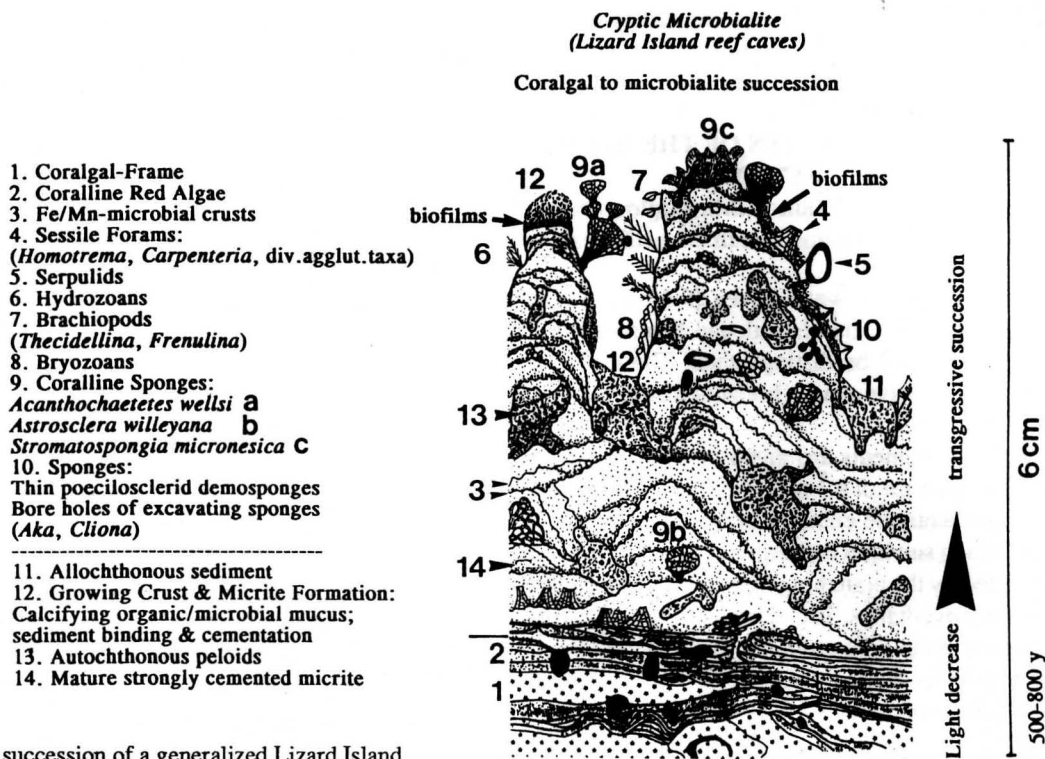


Fig. 4. Facies succession of a generalized Lizard Island type microbialite.

inclination to the cave entrances. The upper surface is often dominated by baffling organisms like branching hydrozoans, serpulids, bryozoans, foraminifera, and sponges. These baffling community is well developed in zone 3 (Pl. 2/2).

The second surface type is developed beneath protruding reef rocks and on the cave roofs, always protected against sedimentation (Pl. 2/1b; Pl. 3). The surfaces are flat and structured only by organisms (Pl. 4/6a, b). Only little sediment is trapped by slimy surfaces. Normally these surfaces are characterized by dark grey and brownish organic films either of microbial biofilms or thin sponge crusts (Pl. 1/3b, 4b; Pl. 3). Thrombolitic pillars are never observed. This sediment protected niche is dominated by slowly growing organisms like coralline sponges, boring sponges (*Aka*, *Cliona*), brachiopods, crustose bryozoans, and serpulids (Pl. 1/2b, 3b, 4b; Pl. 4/4, 5)).

This more encrusting and framebuilding community has a typical hardground character, as known from many fossil ones (cf. REITNER 1989: Mid-Cenomanian hardground of Liencres, northern Spain). This community is dominant in zone 4 and restricted in zone 3 to sediment protected areas.

### 5.2.2 Vertical facies succession

In all studied microbialite specimens the vertical facies succession is very characteristic and exhibits always the same structure (Pl. 2/1c, b; Fig. 4).

The vertical development of the microbialites starts with a coralgal facies. The core of the microbialite succession is mostly formed by prominent crusts of thin sheets deeper water corals of the *Agaricia*- and *Porites*-group alternating with dense crusts of crustose coralline red algae. All portions

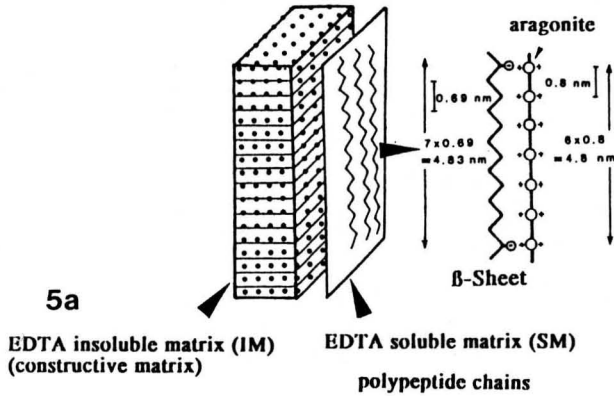
are heavily bored by lithophage bivalves which are still in situ (Pl. 2/1b). The bore holes are filled up by a white chalky very fine calcareous mud which is sometimes completely cemented! Corals exhibit often early diagenetic features like epitaxial, and isopacheous aragonitic cements. In some cases the coral skeletons exhibit features of a freshwater vadose diagenesis. Their aragonitic skeletons are altered into a low-Mg calcite granular calcite. These traces of freshwater diagenesis may be hints to a sea level low stand.

The genera/species distribution is identical with that of zone 2! The coralgal facies is sometimes terminated by thin single cell layered melobesiid coralline algae together with crustose foraminifera (*Homotrema*, *Carpenteria*, *Planorbulina*, *Acervolina*) in alternation with first occurrences of micrite crusts.

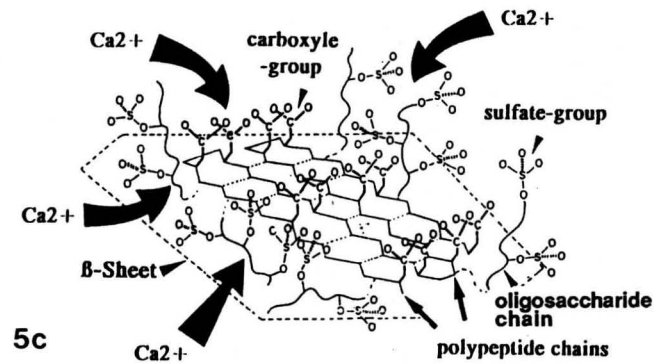
### Thrombolitic crusts (Pl. 2/1-3)

The thrombolitic crusts of the upper surfaces are three to six centimeters thick and structured by pillars and large interpillar openings. The pillars grow straightly upwards and become inclined in their younger portions. The inclination angle is between 15-30°. The thrombolitic pillars are structured by curved brownish laminae which are remains of Fe/Mn bacterial biofilms (Pl. 2/3). The more or less lense shaped space between the the Fe/Mn laminae is irregular, and the distances of the Fe/Mn-laminae vary from 1mm to 10mm. The carbonate is formed by a dense (aphanic) honey brown micrite with many allochemes (packstone) (Pl. 2/3). Common benthos are serpulids, bryozoans, and crustose foraminifera which grow predominantly on the Fe/Mn crusts. Coralline sponges are rare. The interpillar space is partly open or filled with organic mucus which is trapping detritus (Pl. 2/1c, 2, 3). The staining behavior of the mucus with basic

### Crystal seed formation via organic soluble matrices (modified "Matrix model" after SIMKISS (1986))



### Nucleation surface of an acidic glycoprotein (Calcium-binding macromolecule) (modified after ADDADI & WEINER 1989)



### Interface between a $\beta$ -sheet monolayer (SM) and the initial plane of a seed crystal (modified after MANN 1989)

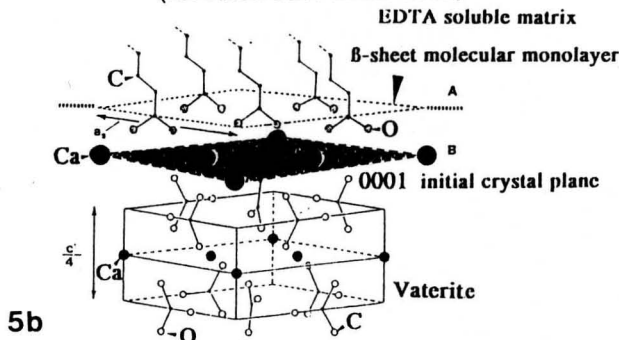


Fig. 5. Mineralization model via Ca-binding organic macromolecules.

5a. Ca<sup>2+</sup> binding function of a molecular monolayer ( $\beta$ -sheet, polypeptide chains of acidic macromolecules). This  $\beta$ -sheet is EDTA soluble (soluble matrix SM). The  $\beta$ -sheet needs a basement to organize. This basement is called constructive matrix. Most organic constructive matrices are EDTA insoluble (e.g. collagen).

5b. This graph explains the interface between  $\beta$ -sheet, initial plain (001) of calcium carbonate seed crystal, and mature crystal.

5c. This graph shows a simple  $\beta$ -sheet of an acidic glycoprotein with Calcium-binding carboxylate groups (COO<sup>-</sup>) and Calcium concentrating sulfate groups. This type of molecules controls often the crystal shape and if very acidic, they inhibit crystal nucleation.

red fuchsin and methylene blue exhibits the presence of mucoproteins (Pl. 2/1c, 2). The interpillar pores are often surrounded by Fe/Mn-biofilms (Pl. 2/4). The older portions of the microbialite are dense and only few interpillar openings remain. The open interpillar space is rapidly increases in the younger parts of the microbialite. Increasing sedimentary fluxes lead to a complete filling of the interpillar space, and the micritic crust is losing the typical thrombolitic structure.

#### Hardground-type microbialite

The micritic crusts in sediment protected spaces are condensed and exhibit a mean thickness of 1-2 cm (Pl. 2/1b, Pl. 3). If the reef rock basement is still in situ, the crust is growing directly on coral skeletons or on thin crusts of coralline red algae.

Thrombolitic features are normally not present, and the entire structure is more or less horizontal laminated and demonstrates a virtually stromatolitic character (Pl. 3/1, 6). The crusts are structured by many irregular Fe/Mn-laminae with average vertical distances of approx. 1 mm or less (Pl. 3/1-3, 6). The brownish autochthonous micrite exhibits a wackestone-packstone texture. The microbialite is intensively bored by boring sponges, predominantly by the haplosclerid sponge *Aka* (Pl. 3/4; Pl. 4/4), rarely by clionids and the genus *Cliothisa hancocki*. *Aka* is producing large (5-10 mm) cavities. The bore holes are occupied beside the

boring sponges by various non-boring sponges, or filled up with different organic mucus substances which trapping and bind detritus (Pl. 3/5). If the pores are closed autochthonous peloids may formed within the organic mucus (Pl. 4/3). The growth mode of the entire hardground-type microbialite is significantly controlled by the boring activity of sponges. The constructive benthos community is composed of the *Acanthochaetetes* community which includes various types of filter- and tentacle feeding organisms (Pl. 1/3b, 4b; Pl. 4/6).

#### 5.3 Interpretation

The observed vertical succession exhibits a diachronous facies change from a light dominated biofacies with zooxantellate corals and coralline red algae to a light independent community. This cryptic facies is dominated by microbialite calcareous crusts, and an aphotic framebuilding benthos community dominated by coralline sponges (*Acanthochaetetes* community). The vertical facies distribution is almost identical with the observed horizontal distribution in the reef caves!

The vertical facies succession from corals to thick coralline red algae crusts to microbialites indicates a transgressive event.

This community replacement sequence is always an indication of transgressive conditions and never for regres-

sions as discussed by JONES & HUNTER (1991).

Unclear is the entire age of the complete sequence because no U/Th and/or  $^{14}\text{C}$  data are available. However, the growth rates of the chaetid sponges *S. (Acanthochaetetes) wellsi* could be determined by using in situ staining fluorochromes. The observed rates vary between 50 to 120  $\mu\text{m}/\text{y}$  (mean 70  $\mu\text{m}/\text{y}$ ). Large specimens with a diameter of 5-6cm from North Direction Island have therefore an age of 700-800 years. The electron spin resonance (ESR) data from the same specimens resulted 550-600 y and more or less correspond with the biologically measured data. The main problem is that the Fe/Mn-biofilms have a strong corrosive ability and therefore more than 40% of the carbonate is dissolved! The dissolution is proved by corroded skeletal remains and rough surfaces of larger cavities, and tests of foraminifera within the micritic crusts. Comparable features are seen in stylolitic carbonates. Similar method of reconstruction of the entire thickness of stressed stylolitic rocks was used to calculate the dissolution amount. The microbialite sequence must have a maximum age of the beginning of the Holocene reef growth which began ca. 6000 years ago. The freshwater diagenetic features of some corals may support this idea. A big specimen (15 cm in diameter) of *Astrosclera willeyana* from 25 m water depth of Ribbon Reef No. 10 has a  $^{14}\text{C}$  age of approx. 3000 years and the measured ESR age exhibits a range from (2500-4400 y).

## 6 MICROBIALITE FORMATION

### 6.1 Microbialite mineralisation model based on organic macromolecules

During the last decade mineralisation concepts based on the interaction of acidic organic macromolecules with inorganic substances were developed, which allow the description of poorly understood mineralisation or biomineralisation events - seen in microbialites.

Basic work and reviews were done by DEGENS (1976, 1979, 1989), DEGENS & ITTEKOT (1986), DEGENS et al. (1967), LEADBEATER & RIDING (1986), LOWENSTAM & WEINER (1989), MANN et al. (1989), SIMKISS & WILBUR (1989), ADDADI & WEINER (1985, 1992), and WESTBROEK & de JONG Eds. (1983). Most of these studies are based on the biochemical analyses of macromolecules (proteins, mucoproteins, glycoproteins, proteoglycans) which are important components during mineralisation.

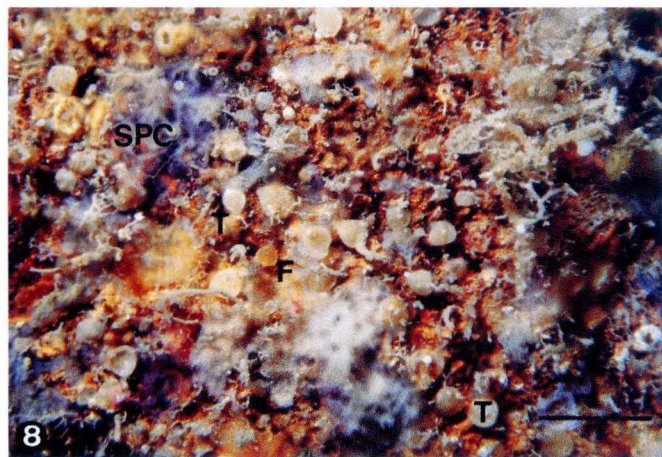
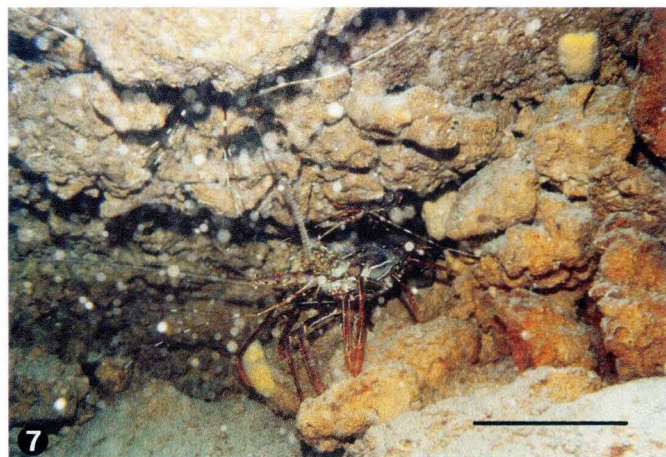
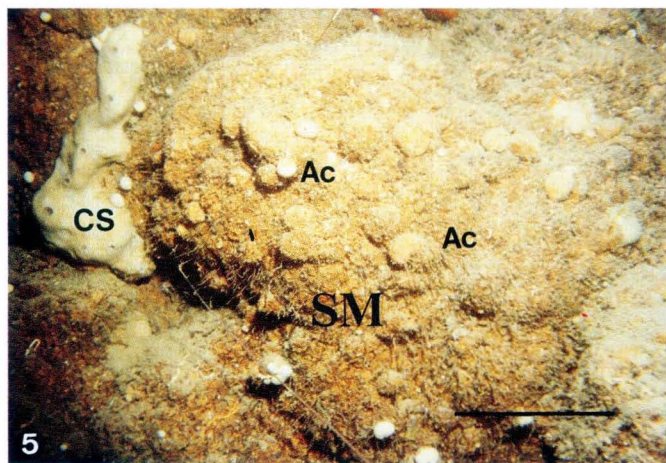
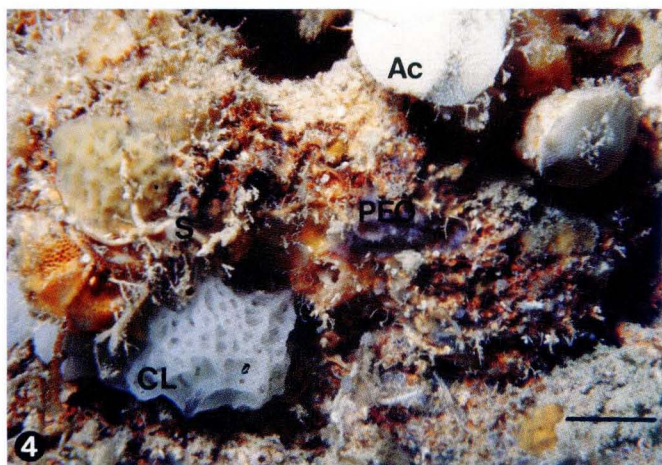
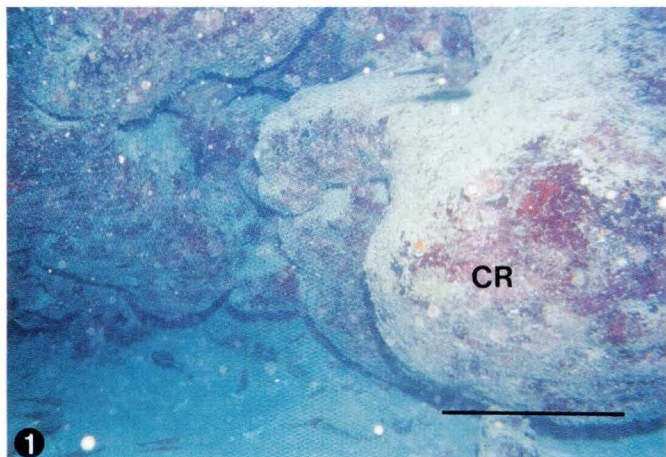
#### Theory of organic matrices (Fig. 5)

##### Acidic organic macromolecules

Organic macromolecules are normally polyanionic polymeres of dividing chains of smaller organic molecules like amino acids, sugars ect.. These very large molecules (< 100 kdaltons) are key structures during formation of metal salts such as  $\text{CaCO}_3$ . These organic macromolecules

#### Plate 1 Modern cryptic microbialite/metazoan facies of Lizard Island (Great Barrier Reef, Australia)

- Fig. 1. Reef cave entrance (Crystal Beach, Lizard Island, all figures) 10m waterdepth - Zone 2 (coralline algae crusts)  
 1a. Steep areas are completely covered by dense crusts of coralline algae (CR). The flat areas are covered by loose and bound sediment. Scale 1 m  
 1b. Detail of Fig. 1a (CR). Occasionally grow keratose sponges (SP: *Spongia* sp.) and bryozoa (B) on the algae crusts. Scale 5 cm.
- Fig. 2. Area below a roof chimney with high sedimentation rates -Zone 3. This zone is characterized by rapidly growing benthos (r-strategists).  
 2a. Carbonate sand and silt from the surface reef flat is baffled by bryozoa, hydrozoans, and sponges (SP). Scale 10 cm  
 2b. Transition area to Zone 4 with decreasing sedimentary input. It is characterized by diverse sponges communities which form small bioherms (5-20 cm) (Cl: *Clathrina*, Ac: *S. (Acanthochaetetes) wellsi*, PEO: pocilosclerid thin sponge crusts, S: serpulids) Scale 2 cm
- Fig. 3. Central part of Zone 4 which is characterized by slowly growing benthos (K-strategists) and brownish biofilm surfaces.  
 3a. Important frame builders are coralline sponges which form small sponge mounds (50cm)(SM) mostly constructed of *S. (Acanthochaetetes) wellsi* (AC) and *Astrosclera willeyana*. (CS: calcaronean sponge). Scale 20 cm  
 3b. Close up view of Fig. 3a. The surface is covered by brownish biofilms and exhibits remains of overgrown coralline sponges. On the biofilms grow *Spirorbis* and other serpulids (S), *S. (Acanthochaetetes)* (Ac), brachiopods (B), and ascidians (A). Scale 2 cm
- Fig. 4. Distal end of a reef cave (Zone 4) located in a sea level low stand groove within the granite basement of Lizard Island  
 4a. Cave walls exhibit cemented coral rubble. This rubble is interpreted as an early cemented beach rock and transgression lag deposits. The microbialites grow on the rubble. The sediment input is extremely reduced. Scale 20 cm  
 4b. Wall surface with numerous brachiopods (*Thecidellina* T, *Frenulina* F) and many thin sponge crusts (SPC). Scale 2 cm



can have 0.01 % to 5 % of the total mass of a biomineral (ADDADI & WEINER 1985; BERMAN et al. 1988). These entrapped molecules exhibit e.g. sometimes a strong autofluorescence behavior! (REITNER 1992).

It is possible to dissolve these molecules from Ca-phosphates or CaCO<sub>3</sub> crystals using EDTA or acetic acid. The common use is EDTA (ethylenediamine-tetraacetate or titriplexe III-solution) a Ca-chelating complex. A certain part of these molecules is EDTA soluble and these molecules are called "soluble matrix molecules (SM)" (Fig. 5). Beside these EDTA soluble substances there are EDTA insoluble organic substances which have more or less neutral charges and they are therefore polymerized. These macromolecules and related substances are called "insoluble matrix molecules (IM)" (Fig. 5, Pl. 6/1, 4). These substances play an important role as framebuilding matrices like collagen (Pl. 6/1; Pl. 7/1), cellulose, chitin, or silk proteins of the mollusca. In a broader sense insoluble matrices must not be insoluble organic molecules. Rigid mineralized surfaces can have the same function during biomineralization.

EDTA soluble molecules are extremely acidic, this means they have a significant amount of asparagin (asp) or glutamin (glu) acids. These two amino acids have two carboxyl-groups (COO-) in contrast to the other ones which have only

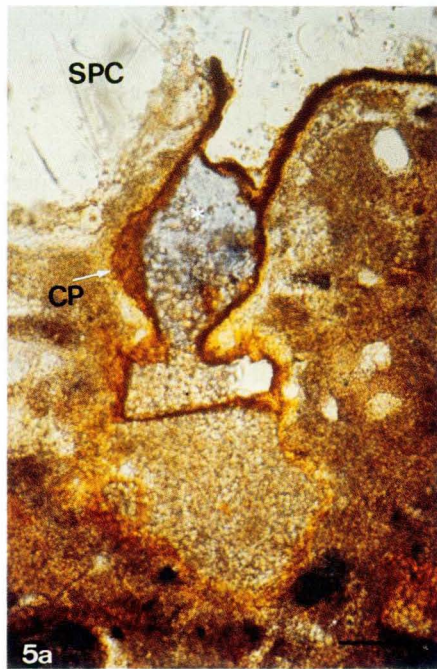
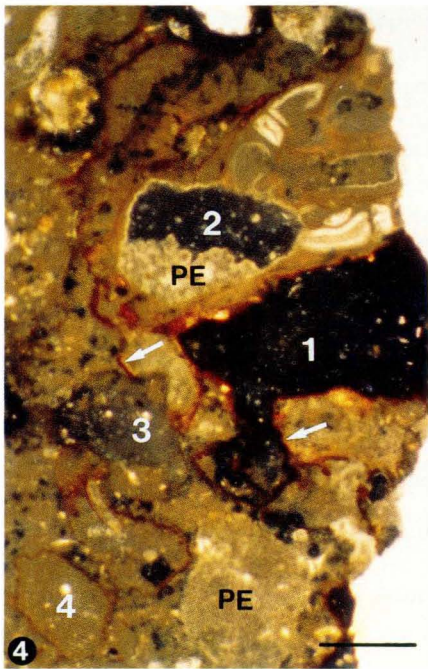
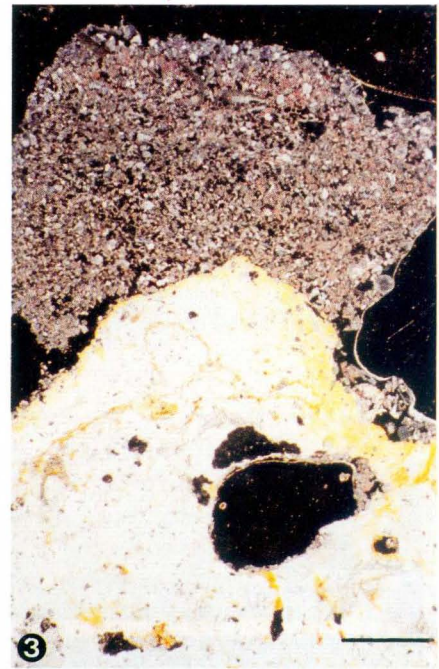
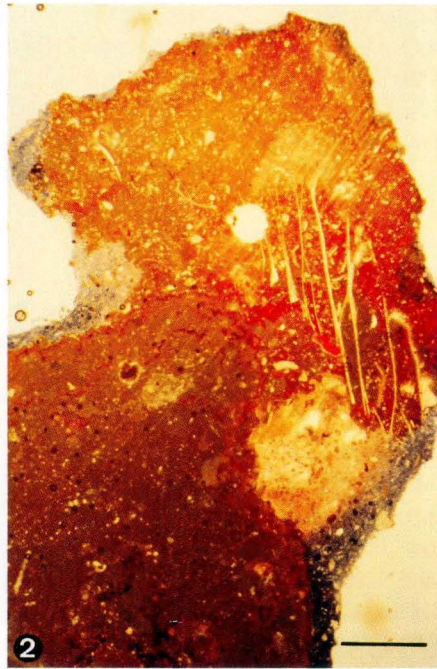
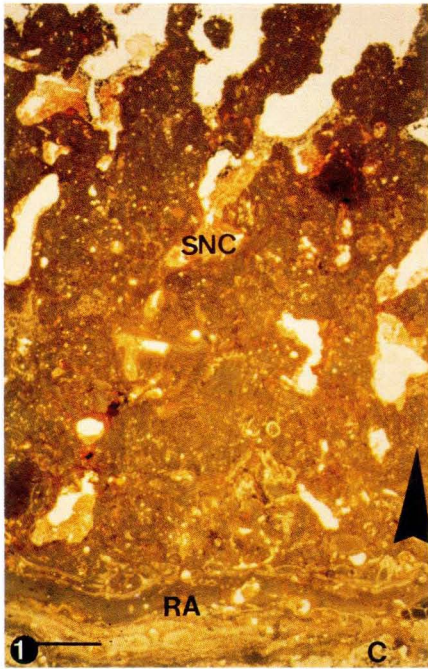
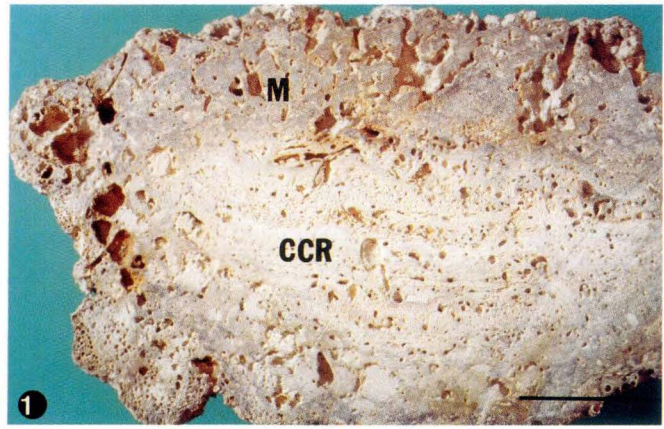
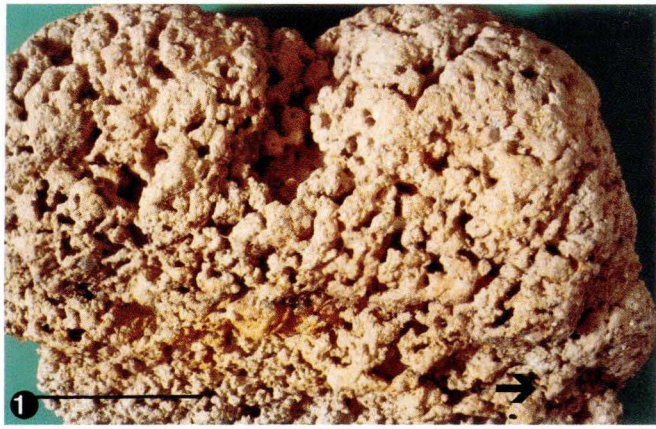
one. During protein synthesis one carboxyl group is eliminated forming peptide ligatures with one amino group and losing a water molecule. Proteins with a high amount of asp and glu acids are negatively charged because only one carboxyl group is neutralized. These proteins are proton donators (basophil). They are relatively small and light and exhibit mean weights of 10-30 kdaltons only (REITNER et al. in press). Common are saccharid groups which are covalently (glycosidic) linked with the acidic proteins forming glycoproteins. They have free carboxyl- and/or sulfate groups which are proton donators too (Fig. 5). Further acidic macromolecules are acidic mucopolysaccharids (= proteoglycans = glycosaminoglycans and proteins), glycosaminoglycane = Uron acid + aminosugars) and polysaccharids only.

### Seed crystal formation

The main problem of crystal formation is the nucleation process. SIGG & STUMM (1989) distinguish two types of nucleation processes, a homogenic nucleation and a heterogenic one. The homogenic nucleation is observed only under artificial conditions in extremely pure solutions and is not realized in natural environments. Most important for the presented study is the heterogenic nucleation. Nucleation happens spontaneously when very small extrane-

## Plate 2 Modern cryptic microbialite/metazoan facies of Lizard Island (Great Barrier Reef, Australia)

- Fig. 1. Characteristic thrombolitic microbialite structure of the Lizard Island reef caves of Zone 3 and 4  
 1a. Entire shape of a microbialite boulder. The irregular thrombolitic pillars are orientated in direction to the cave entrance (arrow) which proves a dominant directed water flow. The top surfaces do not show the pillar structure caused by higher sediment accumulation (zone 3). Scale 5 cm  
 1b. Section of a microbialite boulder (M) of zone 3 which exhibits a core of corals and coralline red algae (CCR). The upper surface of the boulder is overgrown by thrombolitic structures, the lower surface by the hardground-type microbialite. Scale 5 cm  
 1c. Stained thin section of a thrombolitic microbialite crust. The microbialite was block stained with red fuchsine to indicate remains of organic matter (e.g. proteins). The section starts with a coralgal frame (C). The corals are covered by thick crusts of coralline red algae (RA). The microbialite exhibits weakly cemented areas (SNC) which are red stained indicating organic mucus. Cementation occurs within the organic mucus. The arrow marks the decrease of light. Scale 1 cm
- Fig. 2. Thin section of the top area of a growing microbialite. The glutaraldehyd fixed microbialite was stained with red fuchsine and differentiated with methylene blue. This staining indicates a reactive protein dominance (red) and a reactive sugar dominance (blue). The intensity of the color is value of the maturity of the crust. The non-stained portions are completely cemented. Scale 2 mm
- Fig. 3. Thin section of a top area of a growing microbialite under dark field conditions. The uppermost portion is incompletely cemented and exhibits a cloudy structure. The interparticle space is filled by organic mucus. The particles are bind allochems. The bright area is an entirely cemented crust. Scale 2 mm
- Fig. 4. Growing mode of internal parts of a fixed microbialite. The Mg-calcitic crust is bored by sponges and the pore space is filled with methylene blue stained basophilic organic mucus. The inner surfaces are covered with Fe/Mn-microbial biofilms (arrows).  
 All observed microbialites are structured by these Fe/Mn-crusts!  
 The loss of the intensity of the blue color is a result of calcification events (1-4). Within the pore with stage 2 are early cemented peloids (PE) visible, a result of a direct microbial cementation. Scale 2 mm
- Fig. 5a. Growth mode of an upper portion of a fixed methylen blue microbialite below a thin poecilosclerid sponge crust (SPC). The small sediment pocket is internally covered with Fe/Mn-biofilms which have a corrosive potention, and a corrosion pattern is always recognizabale (CP). The Mg-calicte crystal seeds are growing within the blue stained basophilic sugar-rich organic mucus (star). Scale 1 mm
- Fig. 5b. Same specimen under x Nicols.



ous particles, molecules, ions, and foreign atoms are present within the solution. The extraneous particles have a catalysator effect which decreases the activating energy of crystal forming ions. This process is most successful when the catalysator (=nucleation) surfaces of the extraneous particles are very similar to the forming crystal seed (discussion in SIGG & STUMM 1989). An example for abiogenic calcites formed during heterogenic nucleation is the chalky fine grained calcite in freshwater lakes ("Seekreide"). Aragonite and vaterite need organic marker molecules as extraneous particles (ADDADI & WEINER 1985; WHEELER & SIKES 1989). The heterogenous crystal nucleation is a paradigm for seed crystal nucleation under control of acidic macromolecules (Fig 5, Pl. 5/4, 6; Pl. 6/4, 5). The negatively charged free COO- groups are trapping divalent cations such as Ca<sup>2+</sup>. This ability is of great significance for an organism because the process allows the elimination the cell toxic surplus of Ca<sup>2+</sup> and a directed transport via enzymes like calmodulin and membrane bound Ca<sup>2+</sup>-ATPase to loci where calcium is used as a physiological controlling factor.

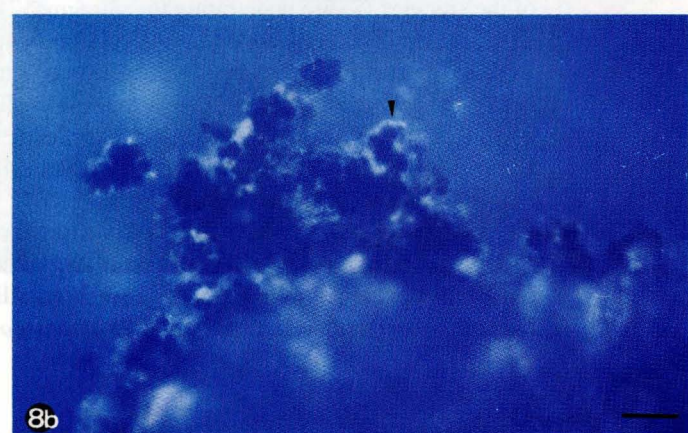
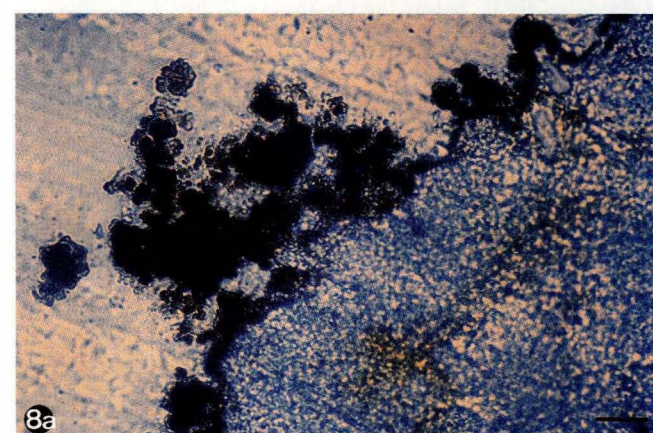
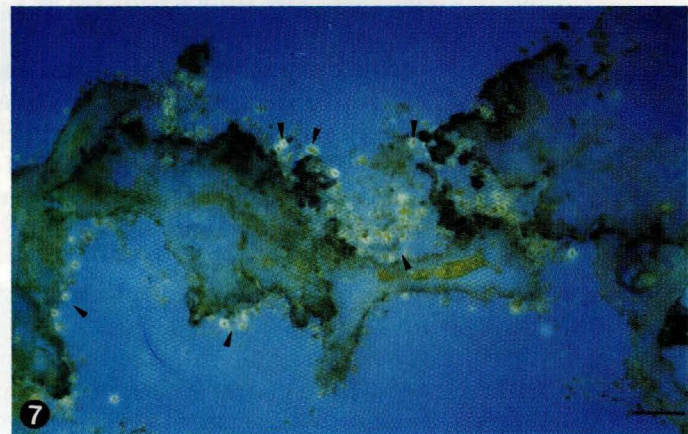
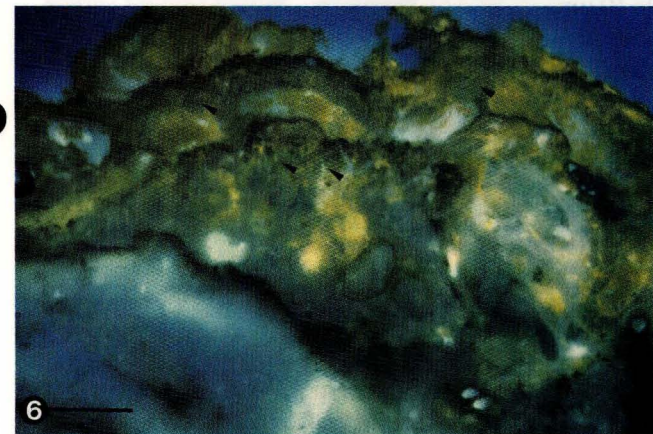
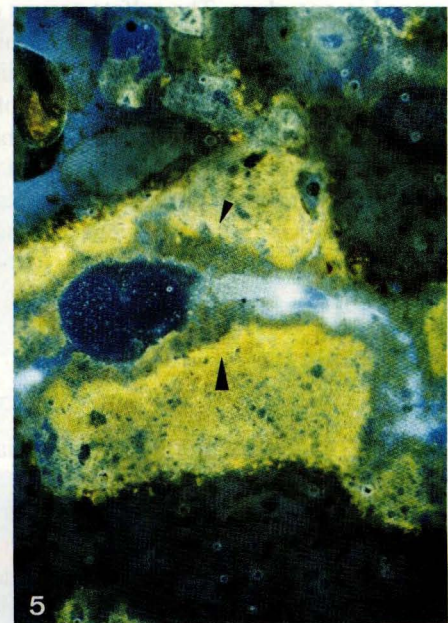
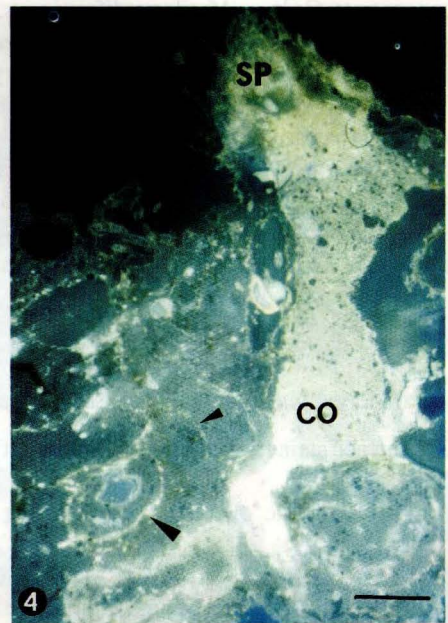
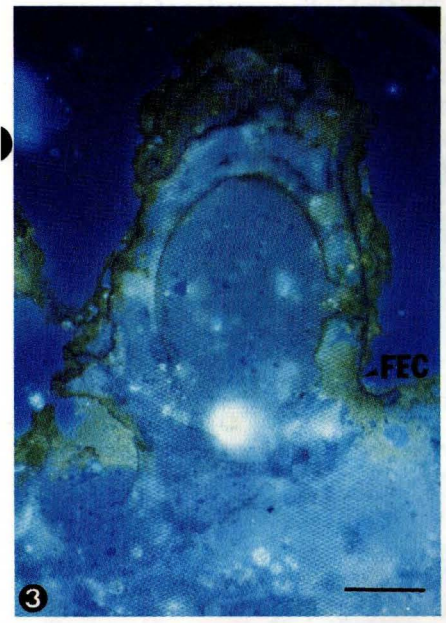
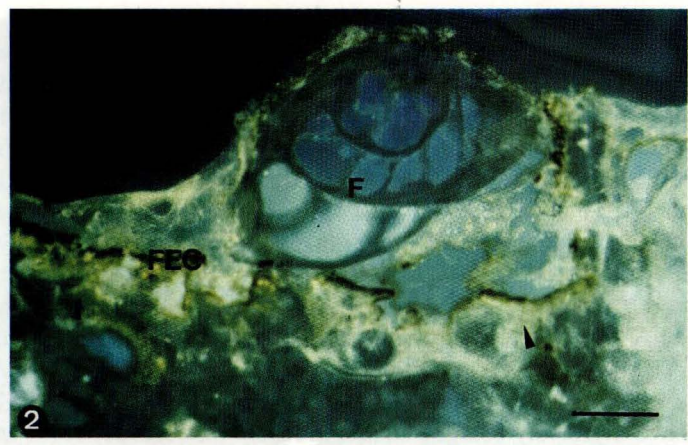
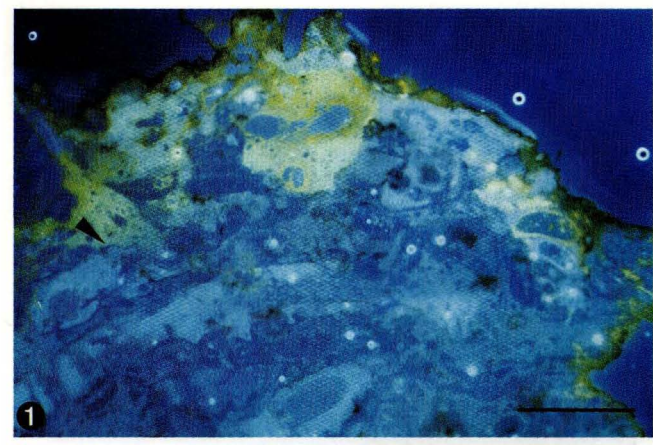
The binding ability of divalent cations by acidic macromolecules is an assumption for crystal nucleation. Important is the formation of a flat molecular monolayer of the acidic macromolecules in polypeptid ligatures chains. The chains are linked with H-bridges and must lay on a neutral non reactive surface (ADDADI et al. 1990). The monolayer and its basement are linked chemically weakly only. The CH<sub>2</sub>-chains of the monolayer are arranged in a faulted secondary structure which are called "β-sheet structure" (ADDADI & WEINER 1985, WORMS & WEINER 1986) (Fig. 5).

The monolayer of large acidic molecules represents the EDTA "soluble matrix", and the neutral basement is called "insoluble matrix".

The negatively charged COO- groups of the β-sheets may bind Ca<sup>2+</sup>. In certain cases the carboxyl groups of asp and glu in the β-sheets are arranged distally (far from the IM) in one plane. The trapped Ca<sup>2+</sup> ions have therefore the same direction. If the COO- groups have definite distances, the Ca<sup>2+</sup> ions form an initial crystal plane, e.g. the (001) plane which is perpendicular to C-axis of a CaCO<sub>3</sub> crystal.

Plate 3 Modern cryptic microbialite/metazoan facies of Lizard Island (Great Barrier Reef, Australia). Epifluorescence of in vivo labeled microbialites by different fluorochromes (Lizard Island, Bommie Bay reef cave, 15 m water depth). All specimens are fixed with glutaraldehyd and stored in 70% ethanol. The epifluorescence was carried out with a ZEISS Axiophot light microscope.

- Fig. 1. Calcein stained microbialite. The calcification fronts exhibit a strong yellow fluorescence which indicates a high amount of Ca<sup>2+</sup>-ions. The color gradient represents the decrease of free Ca<sup>2+</sup>-ions (arrows). Filter 05 High-performance wide-band pass filter blue violet, BP 395-440 LP 470. Scale 100 μm
- Fig. 2. Tetracycline-HCL stained uppermost portion of a microbialite crust. The Fe/Mn-biofilms demonstrate dark brownish crusts (FEC). Below this crust a yellow and a very bright fluorescence is present which proves reactive cementation fronts and the presence of free Ca<sup>2+</sup>-ions (arrows). The foraminiferal test (F) does not exhibit any fluorescence and is initially overgrown by a calcifying biofilm. Filter 05 High-performance wide-band pass filter blue violet, BP 395-440 LP 470. Scale 50 μm
- Fig. 3. Tetracycline-HCL stained uppermost portion of a microbialite crust. The Fe/Mn-biofilms demonstrate dark brownish crusts (FEC). The in statu nascendi calcifying biofilms overgrow a serpulid tube. The corrosive behavior of the Fe/Mn-biofilms is responsible for the irregular surfaces of the different growing stages. The calcifying areas exhibit a yellow fluorescence. Filter 05 High-performance wide-band pass filter blue violet, BP 395-440 LP 470. Scale 50 μm
- Fig. 4. Aureomycine (Chlorotetracycline) stained microbialite. The yellow fluorescence on the surface of the crust indicates Ca-rich cells and tissues of sponges (SP). Below one sponge the sediment-filled boring cavity shows a bright fluorescence of calcifying organic mucus (CO) between allochems. The mucus may be a product of decaying sponge tissue. The nearly completely cemented areas exhibit a strong increasing bright fluorescence to the inner margins (arrows). An intense microbial activity is located there. Filter 05 High-performance wide-band pass filter blue violet, BP 395-440 LP 470. Scale 50 μm
- Fig. 5. Tetracycline-Base stained small sediment trap with a high amount of calcifying proteins. The cementation fronts are clearly visible! (arrows). Filter 05 High-performance wide-band pass filter blue violet, BP 395-440 LP 470. Scale 100 μm
- Fig. 6. Calcein stained microbialite with many Fe/Mn-biofilms. The fluorescence is restricted to small areas and thin vertical filamentous structures (arrow) of traces of endolithic fungi borings. Filter 05 High-performance wide-band pass filter blue violet, BP 395-440 LP 470. Scale 50 μm
- Fig. 7. Tetracycline-HCL stained calcifying bacteria (arrows) on a Fe/Mn-biofilm. High-performance wide-band pass filter 05, blue violet, BP 395-440 LP 470. Scale 25 μm
- Fig. 8a. Active Fe/Mn-biofilm. The siderocapsid bacteria form grape-like structures. The basement exhibits typical corrosion features for this type of biofilm. Normal light
- Fig. 8b. Same specimen as 8a stained with calcein. The living biofilm (arrow) exhibits a strong bright fluorescence. The Fe/Mn grape-like aggregates are the product of a special respiration of these microbes under aerobic to disaerobic conditons. UV High-performance narrow-band pass filter 01; BP365/12 LP 397; Scale 10 μm



Carboxyl groups with bind  $\text{Ca}^{2+}$  ions form an interface between the acidic organic macromolecule and the inorganic crystal (Fig.5). The distances of the  $\text{Ca}^{2+}$  ions within the (001) plane determine the calcium carbonate mineral ( $4.99\text{\AA} = \text{calcite}$ ,  $4.96\text{\AA} = \text{aragonite}$ ,  $4.13\text{\AA} = \text{vaterite}$ ) (ADDADI & WEINER 1989, WHEELER & SIKES 1989).  $\beta$ -sheets of acidic macromolecules are soluble matrices which allow initial crystal plane formation (Fig. 5).

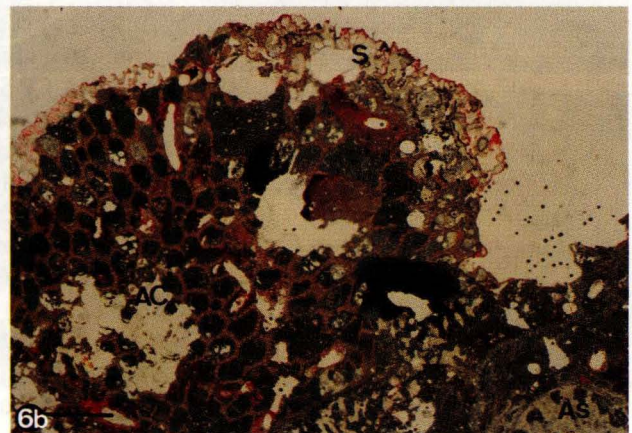
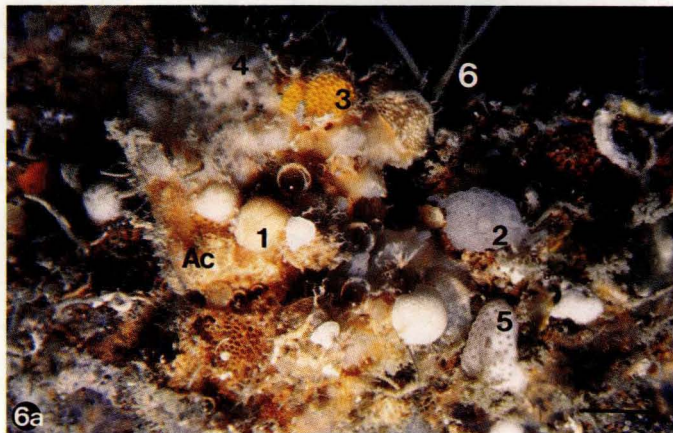
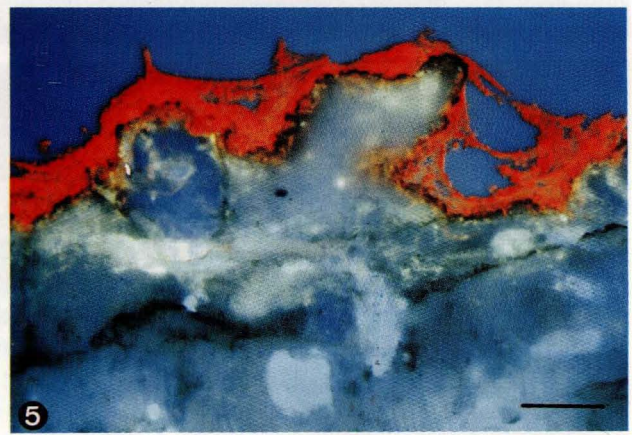
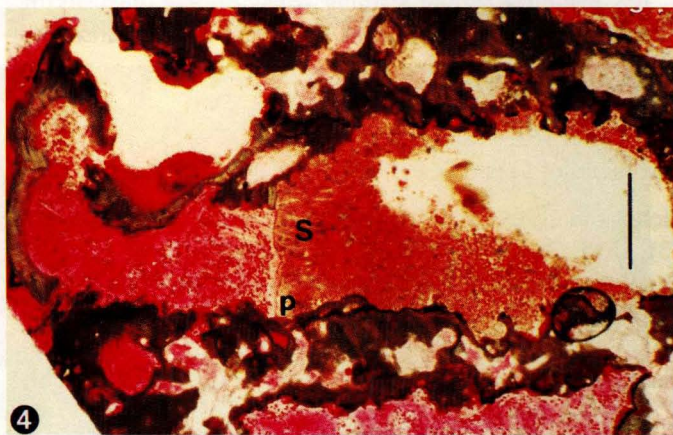
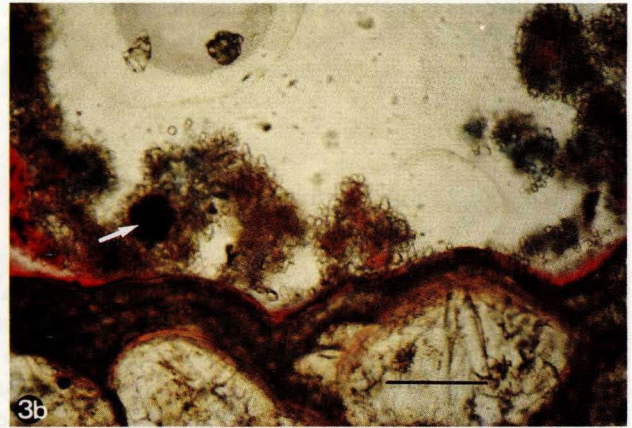
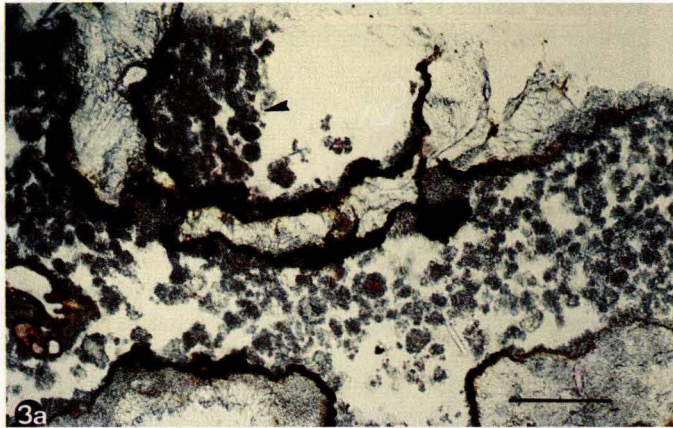
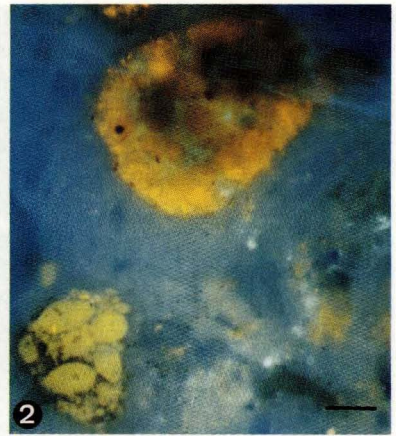
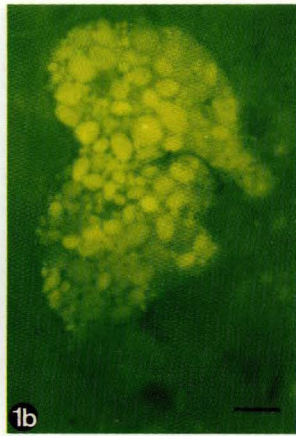
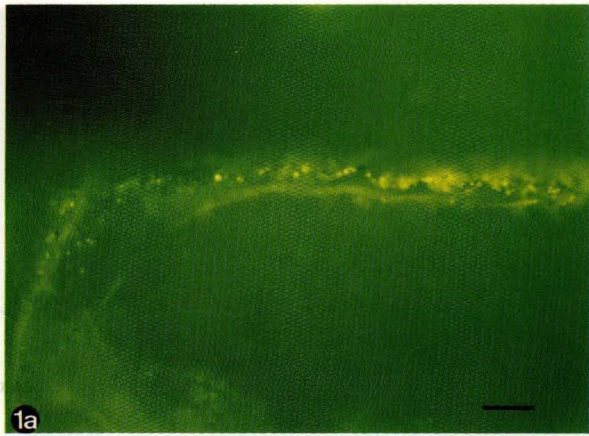
### Crystal growth

Very important for crystal growth are vertical side chains of  $\beta$ -sheets which are constructed of glycosidic linked acidic saccharid-groups mostly of oligosaccharids. These sugars have negatively charged sulfate groups which are not arranged in one plane. The sulfate groups concentrate  $\text{Ca}^{2+}$  ions, but they do not neutralize them! This phenomenon is visible in organic mucilages using Ca-binding fluorochromes (REITNER 1992). A spatial concentration of  $\text{Ca}^{2+}$  ions on the carboxyl groups of the  $\beta$ -sheet occurs which fixes the cations. The seed crystals are formed under control by the  $\beta$ -sheet and/or through the organisms. Rapid epitactically crystal growth is a result of Ca supersaturated seawater with  $\text{HCO}_3^-$  and  $\text{CO}_3^{2-}$  getting in contact with the crystal seeds.

However, crystal growth is limited or controlled by these very large and acidic macromolecules too (ADDADI & WEINER 1985, REITNER et al. in press). Most of the matrix formed crystals have strange forms like the aragonitic nacre of the mollusks. Extremely acidic macromolecules, predominantly glycoproteins may trap  $\text{Ca}^{2+}$  ions on certain crystal planes or on inhibit the formation of 001 planes. These very acidic types are inhibitors of any mineralisation, or they allow the crystal to grow only in selected directions (further discussion in ADDADI et al.(1990), BORBAS et al. (1991), and REITNER et al. (in press). Most successful crystal formation is realized in weak to medium acidic glycoproteins which have asp and glu concentrations of 25-30%. BERMAN et al. (1988) have compared the SM of irregular echinids with those one of *Mytilus californianus*. The Ca-binding proteins of the nacre of *Mytilus californianus* exhibit 46mol% asp+glu. This protein inhibits the crystal growth in direction of the c-axis. The SM proteins of the echinids exhibit only 29mol% of asp+glu which allow a much more regular growing of the stereom single crystals. The same phenomenon was observed during the high-Mg calcite formation in the sponge *S. (Acanthochaetetes) wellsi* (REITNER et al. in press).

The inhibition ability of very acidic macromolecules,

- Plate 4 Modern cryptic microbialite/metazoan facies of Lizard Island (Great Barrier Reef, Australia)
- Fig. 1a. Active biofilm of a microbialite surface stained with calcein. The calcifying microbes exhibit a strong yellow fluorescence (cf. Pl. 5/5).
- Fig. 1b. Large calcifying microbes within bore hole of a sponge exhibiting a strong green/yellow fluorescence (compare Pl. 5/7)
- Fig. 2. 1a, b High-performance wide-band pass filter 17 green, BP 485/20 BP 515-565. Scale 10  $\mu\text{m}$   
Same microbes as in fFig.1b stained with acridine orange, a microbe tracer. High-performance wide-band pass filter 05, blue violet, BP 395-440 LP 470. Scale 10  $\mu\text{m}$
- Fig. 3. Peloid formation  
3a. Large borehole of a sponge within a fixed microbialite. The internal surface is covered with a Fe/Mn-biofilm. The cavity is irregularly filled with Mg calcite spherulites (peloids) of various sizes. Newly formed peloids are loose and exhibit fuchsine and methylene blue stained cores, tracing proteins and complex sugars. In some cases bacteria cells are forming the peloid cores. The peloid organic cores (soluble organic matrices) are altered into a crypto-crystalline low Mg calcite. Marginally on the cores Mg calcite crystals grow. The peloids grow within organic slime pockets. If the muco-substances are resorbed, the peloids condense and grow together (arrow).Scale 100  $\mu\text{m}$   
3b. Detail of Fig.3a. The peloids grow on a biofilm. Peloids with dark cores are derived from microbes (arrow). Scale 50  $\mu\text{m}$
- Fig. 4. Sponge tissue decaying features (Aka, boring sponge). The living part exhibits a clear red color (red fuchsine staining). The dead parts of the sponge are separated by a prominent organic phragma (p). The boundary area of the living tissue is characterized by collagenous fibres, indicating the moving process of the tissue. Some of the spicules (S) are penetrating the phragma. The decaying tissue below the phragma exhibits a crumple structure which calcifies, may be via ammonification. Scale 100  $\mu\text{m}$
- Fig. 5. Double fluorochrome stained upper portion of a microbialite with calcein and red thiocine. Yellow calcein fluorescence indicates calcifying parts below the Fe/Mn-crust. The prominent red color fluorescence is in all cases typical of sponge tissues (here a poecilosclerid thin sponge crust). High-performance wide-band pass filter 05, blue violet, BP 395-440 LP 470. Scale 100  $\mu\text{m}$
- Fig. 6. Small sponge reefs (Zone 4, LIZ92/45)  
6a. Large *S. (Acanthochaetetes)* colony (Ac) is overgrown by *Spongia* (1), *Clathrina* (2), yellow poecilosclerid sponge (3), *Mycale* (4), ascidian (5), and hydrozoans (6). Scale 1 cm  
6b. Fuchsine stained thinsection of a small coralline sponge reef (Zone 4). *Astrosclera willeyana* (AS), *S. (Acanthochaetetes) wellsi* (AC), and *Stromatospongia micronesica* (S). Scale 5 mm



however, is limited when most of the negatively charged valences are neutralized. When this takes place, the now weakly acidic mucus mineralizes rapidly. The process described may explain the very rapid calcifications e.g. within the polysaccharid layers of bacteria (e.g. stromatolite formation, algae, foraminifera)

LOWENSTAM (1981) and WEINER et al. (1983) distinguished two different evolutionary grades of mineralisation processes. They distinguish a "biologically matrix mediated" and a "biologically matrix controlled" mineralization process. The matrix controlled process is the most complex and sophisticated one which forms functional skeletal elements.

For microbialite formation the matrix mediated mineralisation process is the most important one which explains calcium carbonate crystal formation without direct control of organisms but under presence of reactive medium to weak acidic macromolecules.

## 6.2 Calcifying soluble and insoluble matrices within microcavities and pocket-like structures

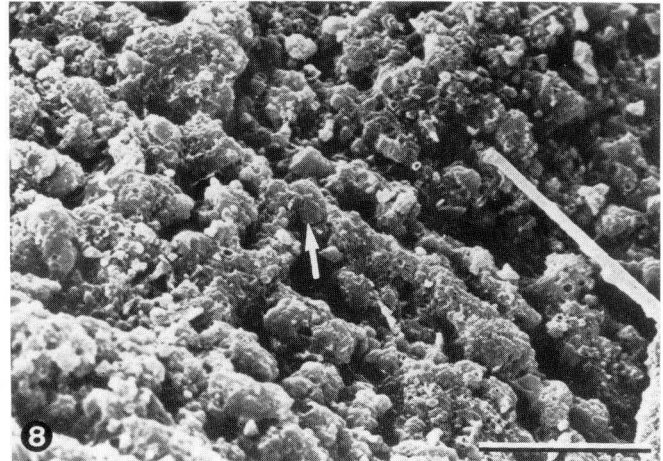
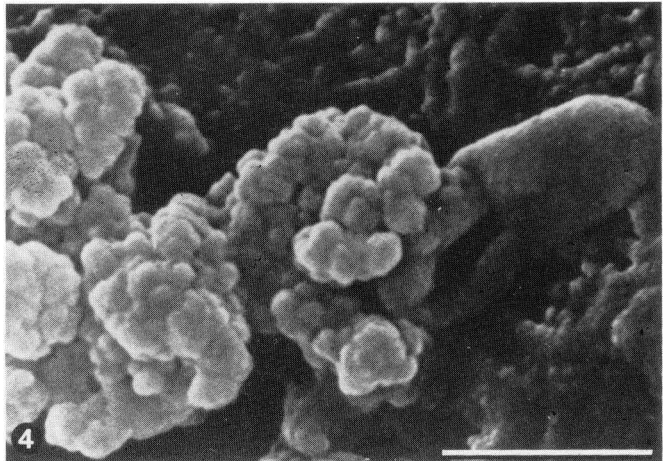
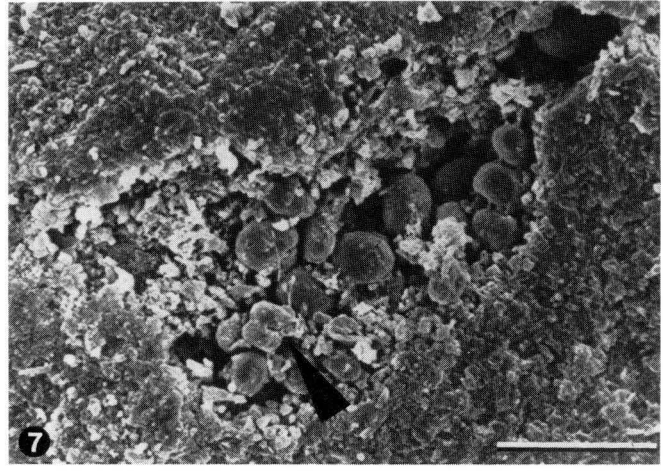
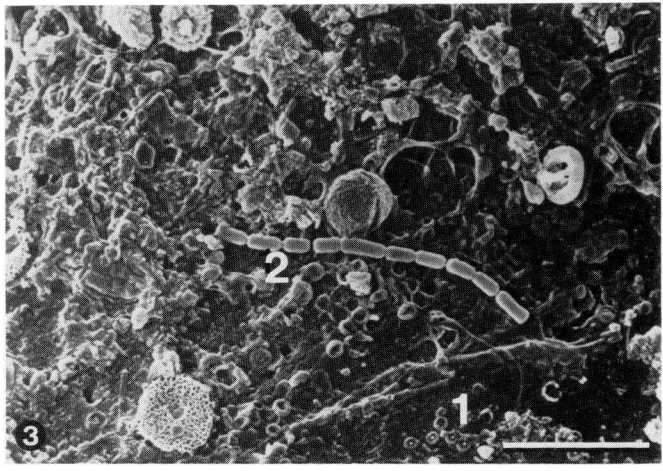
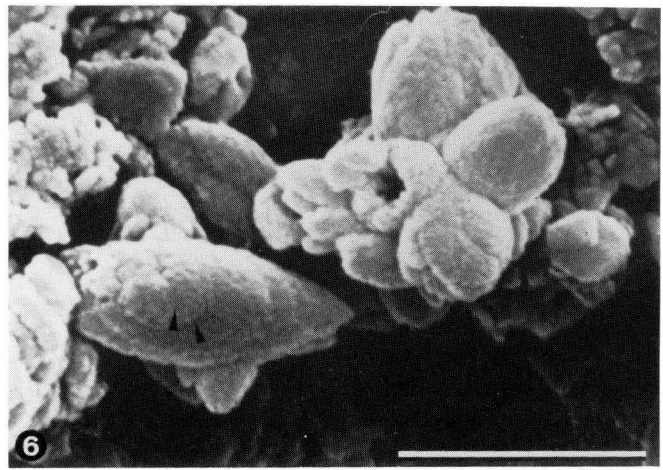
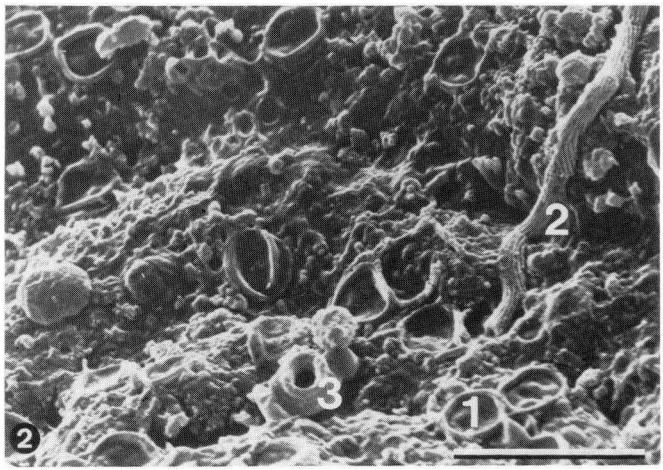
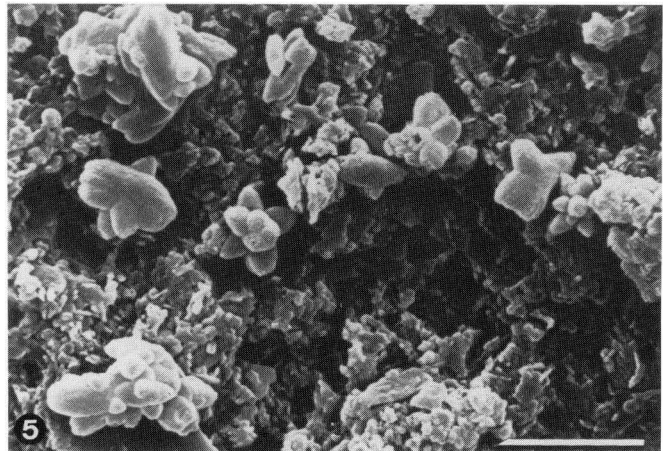
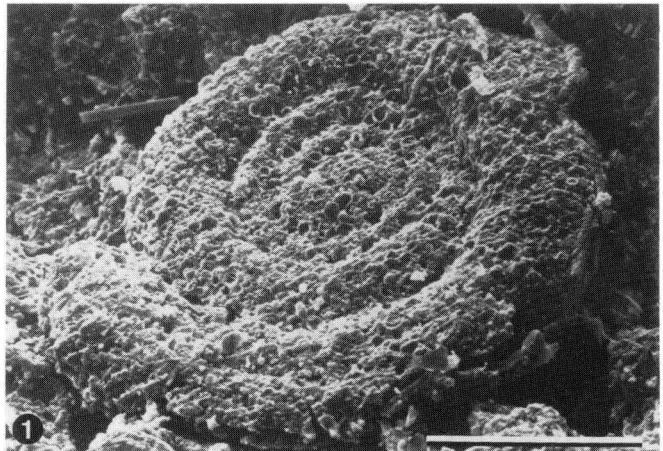
All studied microbialites do not show clear horizontal laminae as observed in true stromatolitic structures, except the Fe/Mn crusts which exhibit sometimes pseudo-stromatolitic features. They are constructed of irregular pocket structures (IPS) or microcavities of less than one millimeter to centimeter size which are limited and surrounded by brownish ferro-manganese crusts, short fibrous

Mg calcite cements, or by truncation surfaces linked with changes of the textural character of the pocket filling caused by the boring activity of sponges (Pl. 2/4, 5; Pl. 3/1, 5). The IPS and microcavities exhibit different generations of growth and maturity grades depending on the amount of organic substances (Pl. 2/2, 4; Pl. 3/5). They are filled with organic mucus and with trapped and bind fine grained detrital material (Pl. 2/3). It is possible to distinguish three different types of microcavity structures: 1. interpillar space of the thrombolitic microbialites (Pl. 2/1c), 2. fillings of the bore holes of excavating sponges (Pl. 2/5; Pl. 3/4), 3. detritus bind on the uppermost growing parts of thrombolitic pillars (Pl. 2/2, 3).

Pieces of formol or glutaraldehyde fixed microbialites were block stained with the non-fluorescent dyes basic red fuchsine, methylene blue, and toluidine blue O. Using these basophilic dyes, it was possible to stain the different organic mucilages. The staining behavior depends on the amount of organic substances and on the biochemical type. Most of the organic fillings of the pockets exhibit a red to pink staining which indicates a high amount of acidic proteins (Pl. 2/1c, 2). Acidic proteoglycane (sugar-) rich mucilages stain blue or lilac, sometimes pink, if using methylene blue and toluidine blue O (Pl. 2/2, 4, 5). This metachromatic effect (discussion in Böck 1989) indicates a dense storage of negative valences of carboxyl and sulphat groups! This observations are very significant because acidic proteins and proteglycans play a central role during mineralisation. All observed immature IPS exhibit a certain staining behavior. The intensity of staining at least depends on the grade of mineralisation.

## Plate 5 Modern cryptic microbialite/metazoan facies of Lizard Island (Great Barrier Reef, Australia)

- Fig. 1. Microbialite crust surface with *Spirillina* sp. which is initially overgrown by a microbial biofilm. Lizard Island Reef cave 15m water depth; Zone 4; (LIZ92/43). SEM; Critical Point dried (CP). Scale 50  $\mu$ m
- Fig. 2. Detail of the biofilm of Fig.1 exhibiting various collapsed non-mineralized microbes (1), fungi mycelles (2), and bound allochthonous coccoliths (3). Scale 10  $\mu$ m
- Fig. 3. Biofilm surface with different unknown bacteria (1) and cyanobacterium (Oscillatoriales) (2). The biofilm is formed by a ca. 100  $\mu$ m thick mucus. Lizard Island reef cave 10m water depth; zone 4; (LIZ92/50/1). SEM, CP. Scale 10  $\mu$ m
- Fig. 4. Burst rod-shape bacterium (type II) with wine grape-shaped seed aggregates of calcite crystals located on a biofilm. The calcite seeds have a diameter of ca. 20-50 nm). This type of calcite forming bacteria are relatively common. The chalky calcareous muds within borings are maybe linked with this type of bacteria. Lizard Island reef cave; zone 4; (LIZ92/50/1). SEM, CP Scale 1  $\mu$ m.
- Fig. 5. Spindle-shaped calcified bacteria (type I) cell colonies on a biofilm. These bacteria are common in biofilms with a high amount of fungi filaments. The sparry calcified cells are often trapped in small cavities and open bore holes. (Compare same species in Pl. 4/1a. under epifluorescence). Lizard Island reef cave; zone 4; (LIZ92/32). SEM, CP
- Fig. 6. Detail of Fig. 5. The calcified cells are hollow and exhibit in some cases remains of the murein layer. These specimens exhibit the calcified outer polysaccharid membrane layer. The calcite sheaths are formed by very small (20 nm) grains (arrow). Scale 2  $\mu$ m
- Fig. 7. Calcified coccoid bacteria in a sponge bore hole (type III). This type is formed under disaerobic conditions. The holes are closed by Fe/Mn-bacteria biofilms. (Arrow: dividing cells). (Compare same species in Pl. 4/1b under epifluorescence). Lizard Island reef cave; zone 4; (LIZ92/43). SEM, CP. Scale 20  $\mu$ m
- Fig. 8. Fe/Mn-bacteria biofilm. The coccoid Fe/Mn-bacteria (*Siderocapsa*?) are forming rows. A single coccoid cell (arrow) has a size of ca. 1-2  $\mu$ m. (Compare same species in plate 3, fig. 8a, b; under epifluorescence). Lizard Island reef cave; zone 4; (LIZ92/45). SEM, CP. Scale 20  $\mu$ m



Young IPS with acidic organic mucilages and a packstone fabric are semidurable and exhibit a strong blue color (Pl. 2/4, 5). Under X Nicols they exhibit only few mineralisation events (Pl. 2/5a, b). If metachromatic effects show a red/pink color, the consistence of the IPS is more or less durable (Pl. 2/2). Completely mineralized portions do not exhibit any staining. The newly formed micrite is honey brown.

TEM micrographs of these portions exhibit a lot of remains of collagenous fibres, fibre networks, sheets and further not clearly distinctable EDTA insoluble remains which represent the insoluble matrices (Pl. 6/1). Rod shaped bacteria are rarely observed (Pl. 6/1).

Fluorescence dyes were also used to localize the calcification fronts. The specimens were injected with Ca-chelating (=binding in chelate complexes) fluorochromes (tetracyclines, calcein) in vivo. Using these dyes it was possible to recognize the loci of calcification fronts in statu nascendi (Pl. 3/1-7). The acidic proteins, glycoproteins, and proteoglycans have a strong affinity to bind and trap divalent cations especially  $\text{Ca}^{2+}$ . They enrich these ions and within the basophilic mucilages (soluble matrices) grow seed nuclei of different Ca-salts. The used fluorochromes mask on the surfaces of the very small seed crystals  $\text{Ca}^{2+}$  or trapp free  $\text{Ca}^{2+}$  ions. The use of tetracyclines turned out as most successful. The calcifying mucilages exhibit a strong yellow fluorescence, using a high performance wide-band pass filter BP 395-440nm LP 470nm (blue-violet) or a high performance narrow-band pass filter set BP 365nm LP 397nm (UV) (Pl. 3/2-5, 7). Calcein exhibits with the same procedure a more or less green-yellow fluorescence (Pl. 3/1). The studied slimes in IPS have only a weak autofluorescence behavior.

The observations within the acidic mucilages of the IPS are very peculiar. The intense yellow fluorescence is restricted to spots and thin fronts (Pl. 3/7, 5). These spots are areas where  $\text{Ca}^{2+}$  ions are extremely enriched in very acidic mucus- or glycoproteins which inhibit calcification, still the concentration is too high and the acidity decreases. The thin fluorescing fronts are areas where seed crystals are formed

in statu nascendi when acidity decreases (Pl. 3/5). This phenomenon was also observed within very acidic glycoproteins of the calcium waste chambers of the coralline sponge *Vaceletia crypta* (REITNER 1992, GAUTRET & MARIN 1991).

The mineralizing process takes place via Ca-binding macromolecules (EDTA soluble matrices) which are rich in acidic aminoacids (asp 19.2 mol%, glu 12.8 mol%) and common insoluble matrices are mostly dislocated collagenous fibres (hypro 4-6 mol%) (first chromatographic analyses were made from microbialites of North Direction Islands by Dr. Pascale Gautret, Univ. Orsay, Paris Sud).

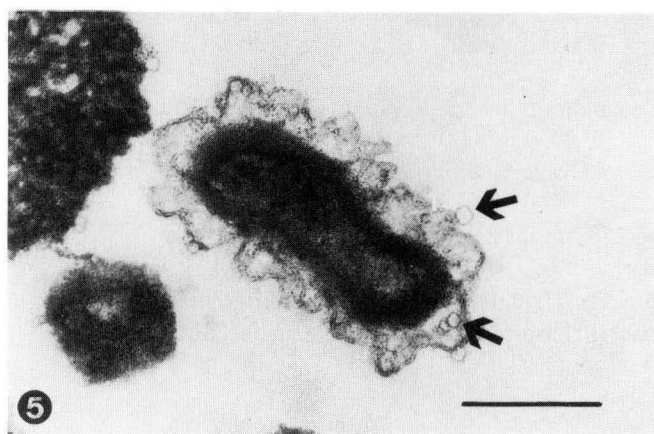
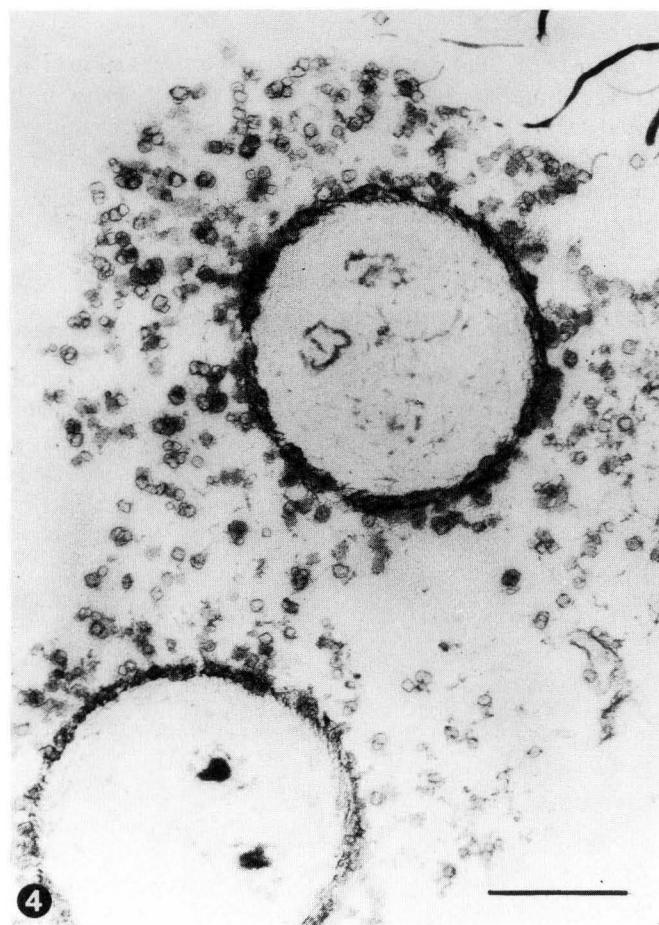
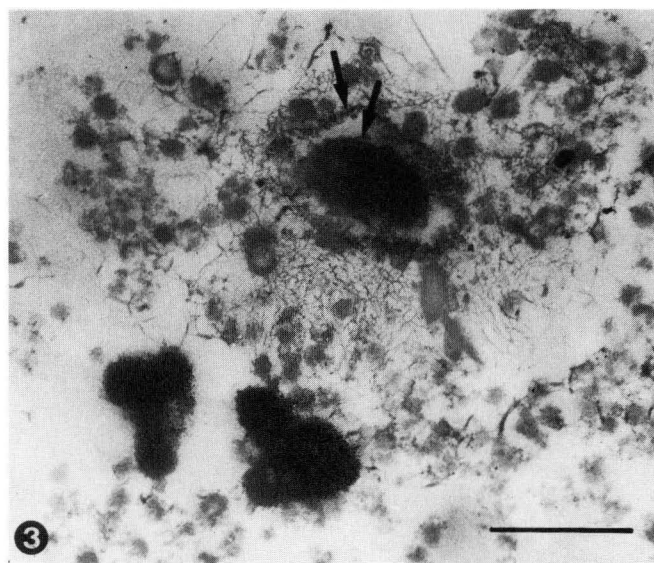
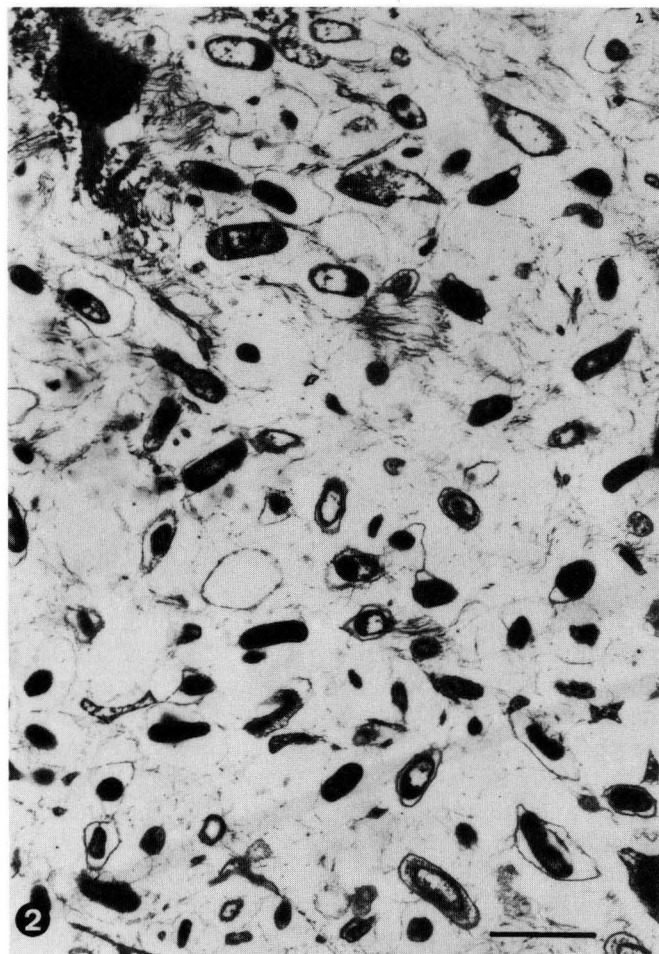
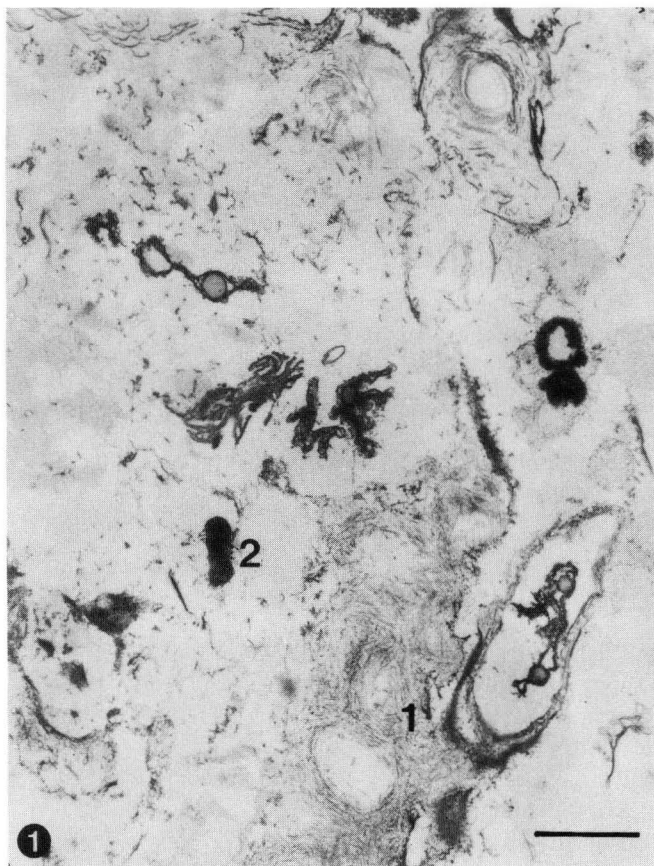
This mineralization is a typical irregular matrix mediated calcification process without any control by organisms.

### 6.3 In situ peloid formation

Some of the microcavities are filled with peloids only, and no further allochthonous material was observed. The peloids have a mean size of 20-60  $\mu\text{m}$  and they are irregularly distributed within the microcavities (Pl. 4/3a, b). The surfaces of the small cavities are covered by active Fe/Mn-biofilms (Pl. 4/3a). The holes are partly filled with mucus substances which exhibit a strong basophilic acidic character. The peloids grow within the mucus which exhibit a clumpy structure. The clumpy structures are the starting points of peloid formation. All observed peloids possess a core of these clumps which have a diameter of 10-20  $\mu\text{m}$ . The peloid cores exhibit a strong mainly blue staining, using a dye mixture of basic fuchsin and methylene blue (Pl. 4/3b). On the surfaces of the cores an euhedral dentate Mg calcite rim is always observed which does not exhibit any staining behavior. Within medium mature peloids the organic core exhibits a microcrystalline framework of anhedral Mg calcite crystals. The calcite crystals grow inside of the mucus. Using Ca-binding fluorochromes, the same fluorescence behavior is seen as observed in the larger slime pockets (IPS). The more or less irregular distribution of

#### Plate 6 Modern cryptic microbialite/metazoan facies of Lizard Island (Great Barrier Reef, Australia)

- Fig. 1. Structural EDTA-insoluble matrices of the surfaces of Lizard Island microbialites. The insoluble matrices are commonly formed by collagenous fibres and combined sheets (1). Sometimes bacteria are present (2). LIZ92/45; Transmission Electron Microscope (TEM) No. 37909. Scale 10  $\mu\text{m}$
- Fig. 2. Biofilm with Vibrionaceae-type bacteria some with loosely bound membranes intercalated in very thin fibres (collagen). LIZ92/32, TEM No.: 37383. Scale 5  $\mu\text{m}$
- Fig. 3. Electronic dense Fe/Mn-bacteria from a Fe/Mn-crust (not stained with  $\text{OsO}_4$ !). Cell and outer membranes exhibit the same dense structures (arrows). Probably the cells are not vital. The grey portions are probably remains of the soluble matrices of Fe/Mn seeds produced by microbes. They are connected with a thin collagenous fibre network. (Compare Pl. 5/8, Pl. 3/8). LIZ92/45; TEM No.: 36599. Scale 2  $\mu\text{m}$
- Fig. 4. Filaments of unknown origin (maybe fungia) with a dense inner layer of rhombic crystal seeds (maybe calcite) and a diffuse outer layer with scattered rhombic crystals. The crystal seeds are surrounded by an insoluble organic sheet. The grey inner portions of the seed crystals are probably remains of the soluble organic matrix. LIZ92/32; TEM No.: 36596. Scale 1  $\mu\text{m}$
- Fig. 5. Single rod-shaped bacteria with a faulted outer membrane containing small vacuoles (arrow) which exhibit the same size and shape as seen in the calcite seed crystals in Fig. 4. Probably these vacuoles have contained metabolic Ca waste. LIZ92/45; TEM No.: 37869. Scale 500 nm



peloid concentrations is a result of the clumpy structures of the organic mucus. The clumpy structure may be a result of decaying of organic slimes, but no traces of bacteria were observed by using SEM and TEM analyses. The cores of the observed peloids are definitely no bacteria remains! The insoluble matrices are very small ( $>1\mu\text{m}$ ) electron dense particles of unknown origin.

The peloid problem is widely discussed and variable hypothesis exist. MACINTYRE (1985) has summarized the different ideas on the origin of peloidal formation. He favors an abiogenic chemical precipitation of Mg calcite peloids. MARSHALL (1983) discussed the possibility that Mg calcite crystal nucleation takes place when seawater is passing through cavities and the crystals rapidly grow on these nuclei to form a microcrystalline fabric (peloid cores!). The often observed geopetal structures of peloids were interpreted as a mechanical sorting caused by flow regimes. MARSHALL (1983) and MACINTYRE & MARSHALL (1988) have discussed peloid nuclei settling down to the floor of the microcavity which may explain the geopetal filling. However, the so-called geopetal filling is in most cases an artefact which results from the clumpy structure of the organic mucus and the insoluble matrix. The newly formed peloids were bound by remaining mucilages and often concentrated on the roof or on the side walls of a cavity which have the function of insoluble matrices (Pl. 4/3a,b). The binding mucus becomes sometimes calcified, and a dense crusts of cryptocrystalline Mg calcite is precipitated. More or less geopetal fillings with many unconformities and cryptocrystalline crusts are observed within larger microcavities. However, these cavities are filled with calcifying mucilages and no water movement is indicated.

CHAFETZ (1986) discussed a different model and interpreted the marine peloids as a product of bacterially induced calcification. He has used etched surfaces for study and came to the result that bacteria are responsible for peloid formation. Main arguments are the presence of bacterial fatty acids (LAND & GOREAU 1970, LAND 1971 have found

saturated, straight-chain 16-carbon acid which is characteristic for bacteria) and brownish color of the peloid cores an indicative of organic matter.

His conclusions are very close to my recent observations. But the peloid cores do not exhibit bacteria remains according to TEM histology, SEM analyses, and staining. The observed presence of bacterial fatty acids is not contradictory. Most of the observed slimes are a product of bacterial decaying processes.

The cores of marine peloids are formed within clumpy basophilic (acidic) organic mucilages (mucoproteins). The later euhedral Mg calcite rim grows under the presence of remaining Ca-binding mucus epitactically on the peloid core.

The peloid formation is also a product of matrix mediated crystallisation.

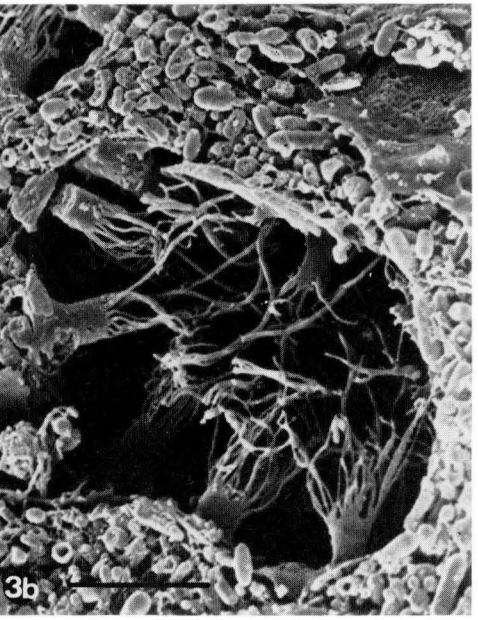
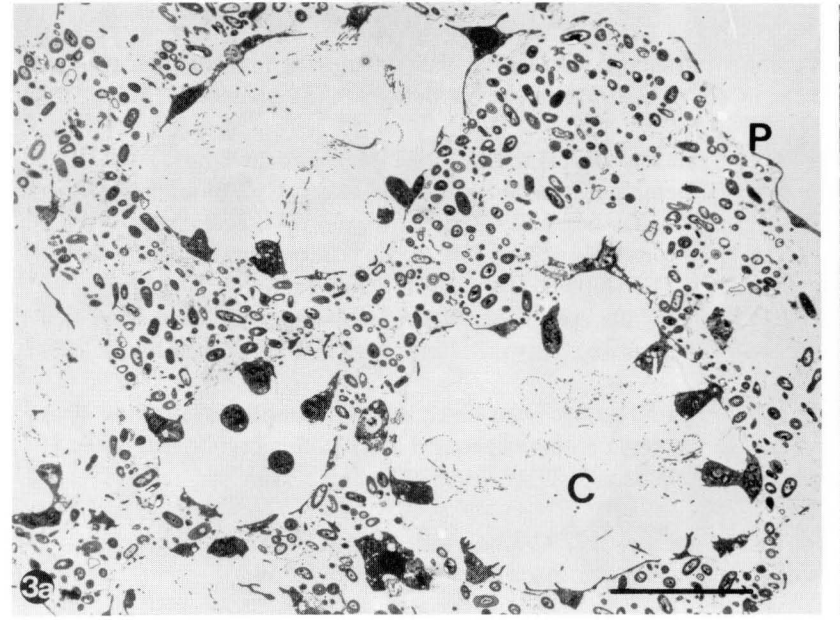
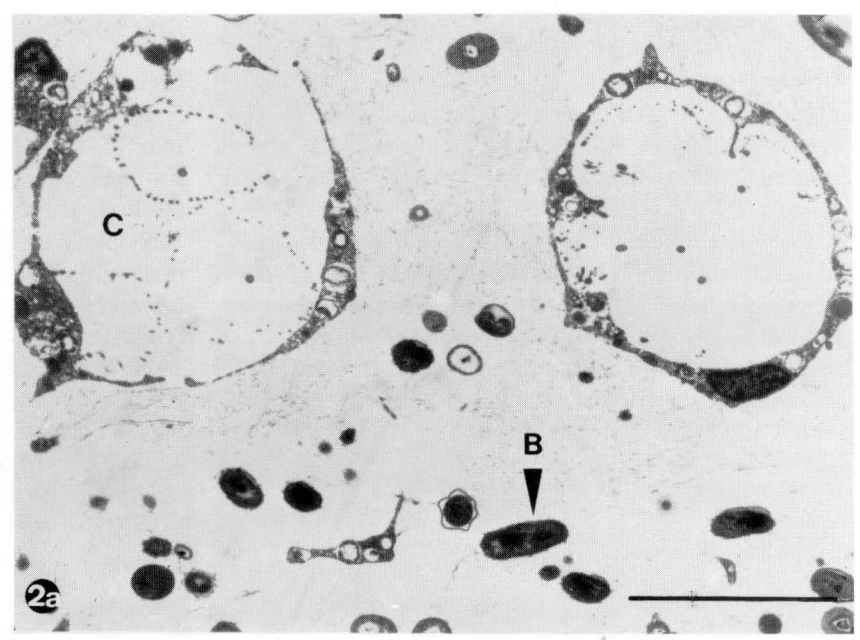
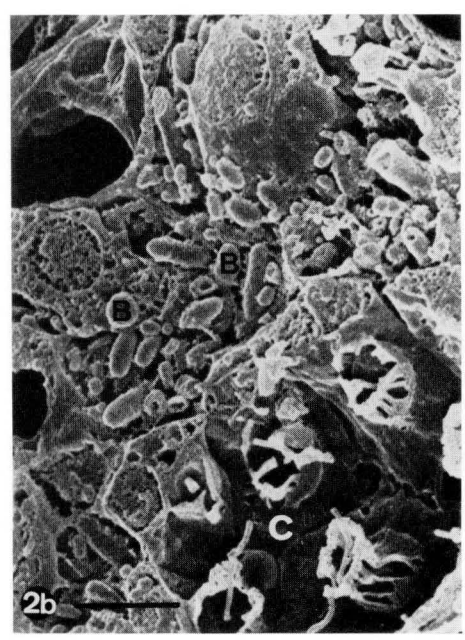
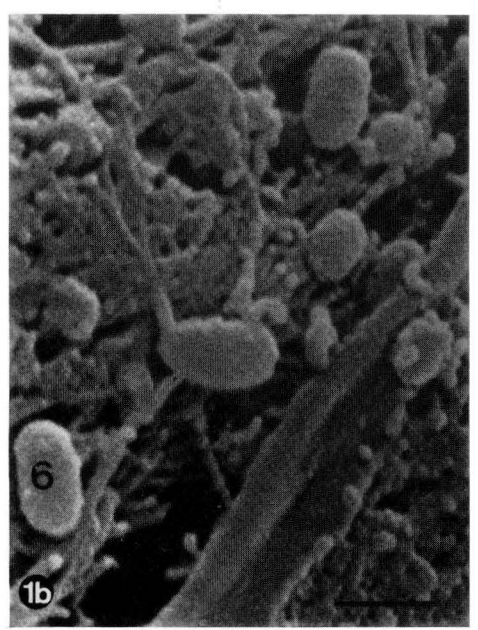
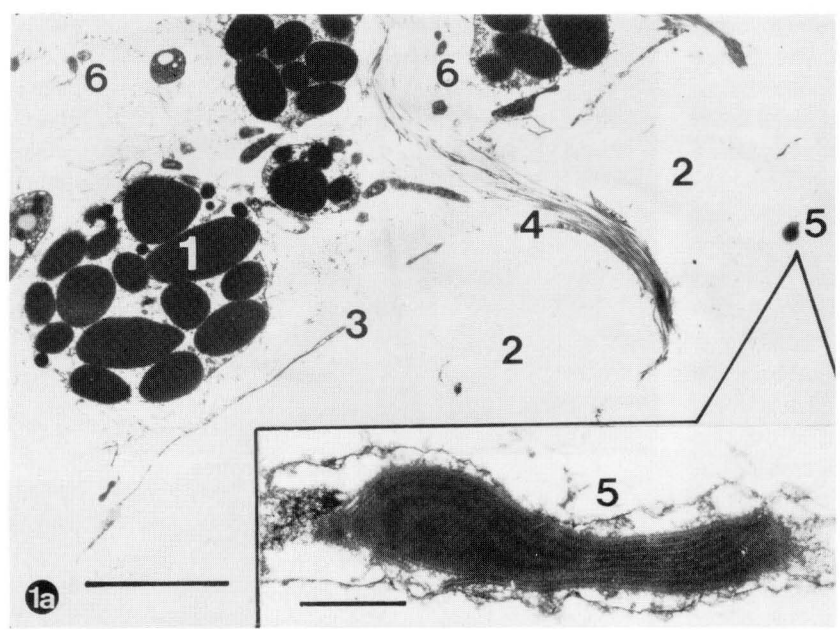
#### 6.4 Sponge tissue diagenesis - micropeloid formation

The hardground type microbialites are intensively bored by sponges, mainly (ca. 90%) by *Aka* cf. *coralliphaga* which forms larger cavities of some millimeter to 1cm centimeter size. Different types of *Cliona* (e.g. cf. *viridis*) produce smaller cavities often arranged like pearl chains. The bore holes of the sponges are settled by the boring sponges itself or occupied by a secondary settlement of sponges, mainly of poecilosclerids, hymedesmiids, and axinellids, but never by coralline sponges or Calcarea.

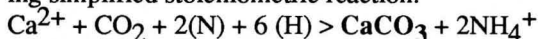
In many cases the sponge tissues exhibit a different staining behavior if using basic fuchsin. The bore holes are often separated by intensively stained organic phragmas which separate the living part from the dead part of the sponge (Pl. 4/4). The phragmas are normally penetrated by the spicules of the sponge which indicate that the dead portion is related to the sponge. The living cells of the sponge tissue exhibit a normal fuchsin red staining, whereas the dead portions of the sponge are stained in a dark brownish/

#### Plate 7 Modern cryptic microbialite/metazoan facies of Lizard Island (Great Barrier Reef, Australia)

- Fig. 1. *Spirastrella (Acanthochaetetes) wellsii* (HARTMAN & GOREAU 1975)  
 1a. Large collagenous fibres forming cells with many huge vacuols filled with reserve material (Icg-cells) (1) of the lower dermal layer. Boundary between the decalcified Mg-calcite basal skeleton (2) is marked by a basopinacoderm (3). The pinacoderm is penetrated by collagenous anchor fibres (4). Within the basal skeleton a boring facultative heterotrophic cyanobacterium of the *Anabaena*-group is common (5). Within the mesohyl collagenous fibre network a very small rod-shape bacterium is common (6). LIZ92/8; TEM No.: 36637. Scale 10  $\mu\text{m}$  and 2  $\mu\text{m}$   
 1b. Very small bacteria (6 in 1a) within the intercellular space (mesohyl). SEM, CP. Scale 500 nm
- Fig. 2. *Astrosclera willeyana* LISTER 1900  
 2a. Choanosom with small choanocyte chambers (C) and bacteria within the intercellular space (B). LIZ92/45; TEM No.: 35948. Scale 5  $\mu\text{m}$   
 2b. SEM micrograph of 2a. (C: choanocyte chambers; bacteria (B)). SEM, CP. Scale 2  $\mu\text{m}$
- Fig. 3. *Vaceletia crypta* (VACELET 1977)  
 3a. Choanosom with medium sized choanocyte chambers (C) and many intercellular different bacteria (e.g. Vibrionaceae) which are probably facultative anaerobe. (P: basopinacoderm); LIZ90/320; TEM No.: 35932. Scale 5  $\mu\text{m}$   
 3b. SEM micrograph of 3a. SEM, CP. Scale 5  $\mu\text{m}$



red manner. Under x Nicols these portions exhibit a strong birefringence of newly formed calcite crystals. The sponge tissue is degraded into a irregular clumpy structure during decaying (Pl. 4/4). These clumps become mineralized in the same manner as observed within the peloid formation. Using thiacine staining dyes as methylene blue and toluidine blue O, the decayed organic matter is stained into a dirty blue and exhibits therefore a strong basophilic behavior. The calcifying soluble matrix is extremely enriched with sulphated organic matter (proteoglycans, glycoproteins) which concentrate  $\text{Ca}^{2+}$  ions. An important source for  $\text{Ca}^{2+}$  ions in this particular case are lysing cells of the sponges and bacteria. The mineralisation takes place under aerobic and disaerobic to anaerobic conditions. Fe/Mn-bacteria films at the side walls of the cavities are common. The soluble matrices of acidic proteins and sugars initiate the seed crystal formation within the small glumpy structures. Insoluble matrices are still preserved collagen fibres of the sponge mesohyle and may be murein sheets of bacteria. The decaying proteins via bacteria allow a supporting further calcification process via ammonification (BERNER 1968). Ammonification is the process by which ammonia is released from the organic matter by microbes. Ammonification occurs under aerobic and anaerobic conditions. Decaying proteins increase the carbonate alkalinity as a result of ammonia and  $\text{CO}_2$  due to bacterial decomposition (simplified reactions:  $2\text{NH}_3 + \text{CO}_2 + \text{H}_2\text{O} > 2\text{NH}_4^+ + \text{CO}_3^{2-}$ ;  $\text{NH}_3 + \text{CO}_2 + \text{H}_2\text{O} > \text{NH}_4^+ + \text{HCO}_3^-$ ). The sulfate-groups of the glycoproteins are partly reduced to sulfide via sulfate reducing-bacteria  $2\text{CH}_2\text{O} + \text{SO}_4^{2-} > \text{H}_2\text{S} + 2 \text{HCO}_3^-$ ). Pyrite is sometimes observed within axial canals of sponge spicules and very rarely within the decaying tissue. This indicates occasional anaerobic conditions. The increased alkalinity supports the calcification. Calcification via ammonification may result by following simplified stoichiometric reaction:



Matrix mediated seed crystal formation and calcification via ammonification is one model to explain the calcified decaying sponge tissues. The endproduct is an irregular clumpy micropeloidal structure which is very common within the studied microbialites and in ancient sponge reefs! The spicules of the recently decaying sponges are partly altered into calcite!

It is now evident that the clumpy peloids, which are missing the characteristic euhedral Mg calcite rim of the "normal" peloids, are in situ calcified remains of decaying sponge tissue! (but only partly comparable with the "Verwesungsfällungskalk" of FRITZ 1958).

## 6.5 Biofilms and microbes

It is taken for granted that microbes play an important role in forming a microbialite structure. In all publication dealing with this topic it is obvious to the authors that microbes are directly responsible for carbonate crust formation, e.g. JONES & HUNTER (1991) discuss that filamentous cyanobacteria are responsible for microbialite formation, CHAEFETZ & BUCZYNSKI (1992) have shown that non thylakoid bearing bacteria play central role by the lithification of intertidal microbial mats. KRUMBEIN (1976, 1979), GERDES & KRUMBEIN (1987), and BURNE & MOORE (1987) listed different ways and types of microbial rock formation. In most cases phototrophic procaryotes are made responsible as a main resource of calcium carbonate formation. The role of bacteria which induce the precipitation of calcium carbonate is discussed since the first decades of our century (e.g. DREW 1911, KELLERMAN 1915, KELLERMAN & SMITH 1914). More recently the investigations were focused more on artificial bacterial cultures to study the pure  $\text{CaCO}_3$  products (e.g. KRUMBEIN 1974, MORITA 1980, GREENFIELD 1963, CARROLL et al. 1966, NOVITSKY 1981, BUCZYNSKI & CHAEFETZ 1991,

## Plate 8 Modern cryptic microbialite/metazoan facies of Lizard Island (Great Barrier Reef, Australia)

### Fig. 1. *Murrayona phanolepis* KIRKPATRICK 1910

1a. View on the broken surface of the calcinean sponge with dermal plate spicules (1), inner dermal layer with triradiate calcitic spicules (2), and choanosomal high-Mg calcite basal skeleton (3). LIZ90/284; SEM. Scale 500  $\mu\text{m}$

1b. TEM section of the boundary between the choanosom (1) and the decalcified basal skeleton (2) with fibres. The boundary layer is formed by many empty membrane bounded vesicles (3) (partly fixation artefacts). Some of the vesicles are dark (4) and exhibit bacteria affinities. LIZ92/8; TEM No.: 36741. Scale 5  $\mu\text{m}$

1c. Detail of a dark vesicle from Fig. 1b which is probably a special bacterium. The outer membrane is faulted, and exhibits sometimes empty small vesicles. TEM No.: 36756. Scale 500 nm

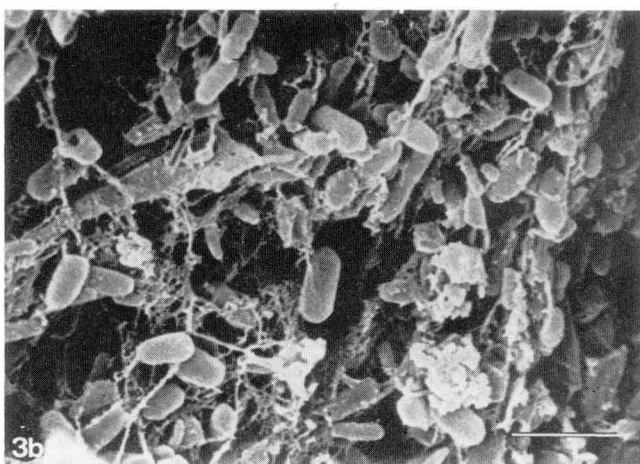
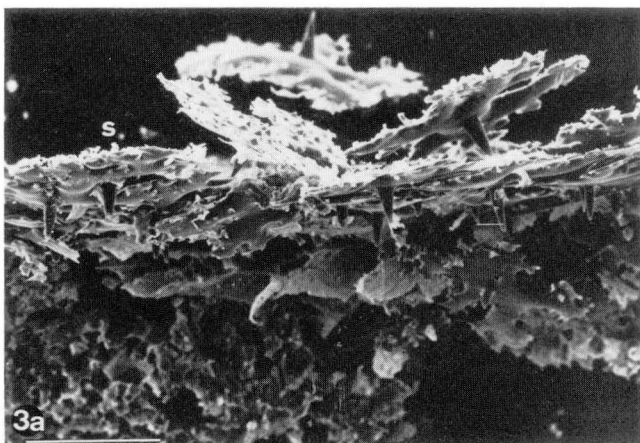
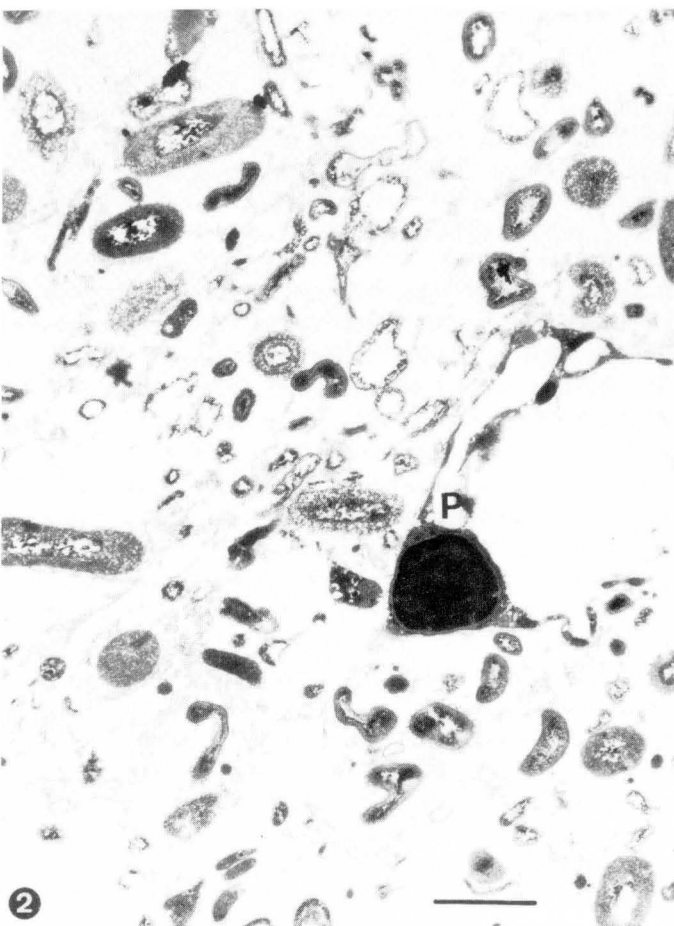
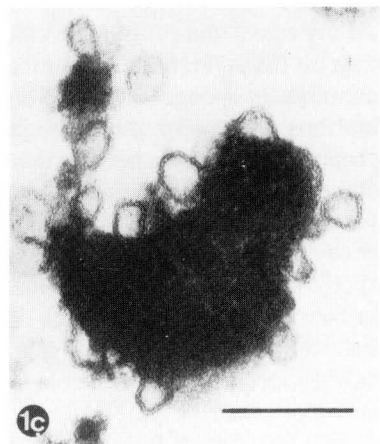
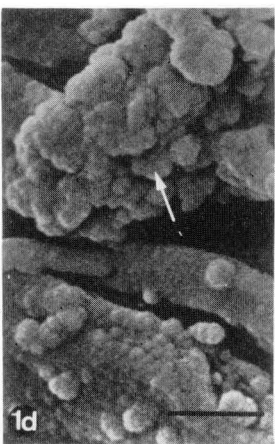
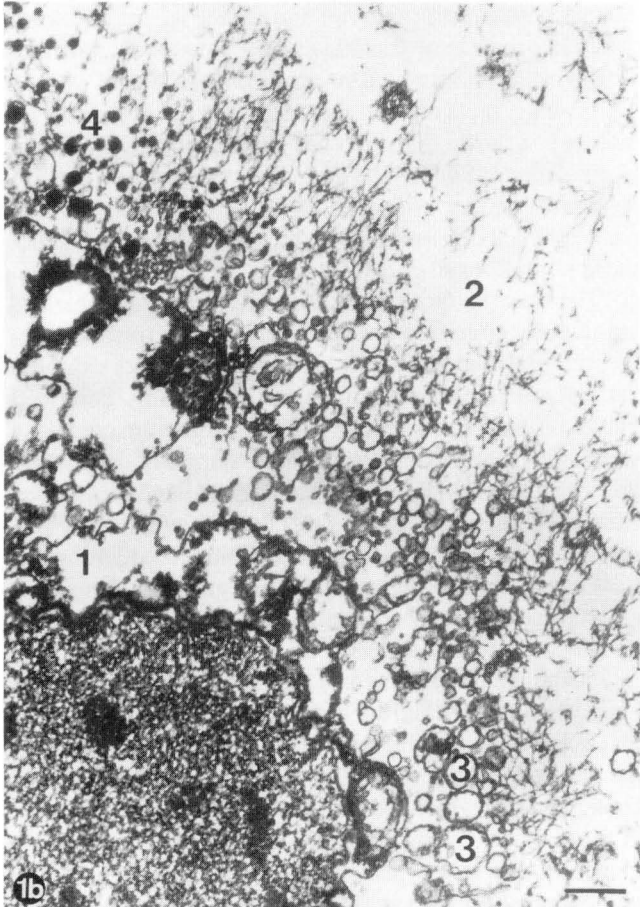
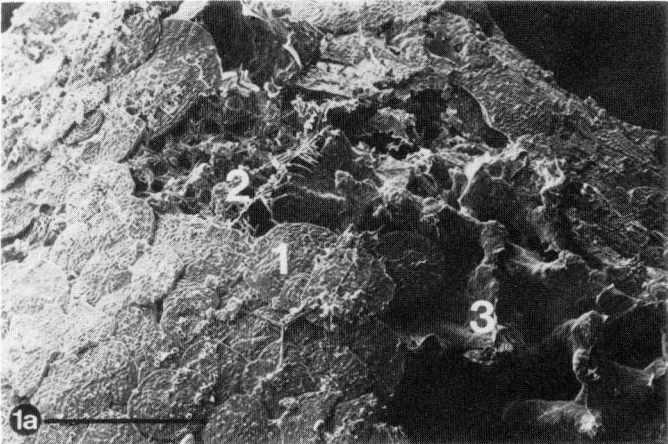
1d. SEM micrograph of the outer membrane of the special bacterium exhibiting very small Mg-calcite granules (20-50 nm) (arrow) which have the same as the empty membrane vesicles of fig. 1c. SEM. Scale 500 nm

Fig. 2. TEM section of a very thin (100  $\mu\text{m}$ ) poecilosclerid sponge crust which shows similarities to biofilms. These morphological types of "bacterio-sponges" are very common in zone 3 and 4 within cryptic reef caves. (P: endopinacocyte with a large nucleus); LIZ92/45 zone 3; TEM No.: 37903. Scale 3  $\mu\text{m}$

### Fig. 3. *Discodermia* sp.; lithistid demosponge

3a. Dermal layer with phyllotriaene dermal spicules. LIZ92/32, zone 4; SEM; CP. Scale 100  $\mu\text{m}$

3b. Common rod-shape bacteria within the intercellular space (mesohyle). Scale 2  $\mu\text{m}$



CHAFETZ 1986, and many others). Many of the observed calcified products of bacteria exhibit a dumbbell structure with brush crystals with a size between 10-50  $\mu\text{m}$ !

Investigations on well fixed material of cryptic microbialites has shown that microbes play a secondary role only as mineralizing agents, and their direct influence on  $\text{CaCO}_3$  formation is minor. However, they play an important role on the active (=living) surface of the microbialites and sometimes in small cavities.

The entire surfaces of all observed types of microbialites are initially covered by variably diverse microbial single- and multilayered sheets. These microbial sheets exhibit a vertical structure known from so-called "biofilms" described by WILDERER & CHARACKLIS (1989). Biofilms are complex structures of microorganisms which normally occupy the entire surfaces sometimes in a patchy distribution also. They can have a thickness of 100  $\mu\text{m}$ . A biofilm-reactor is a self-organized system compartment in which the microorganisms have a high ability to survive and grow. Biofilms have always a certain vertical structure and consists of microbial cells which are embedded in an organic polymere matrix (mucilages, slimes) formed by microbes. Biofilms are principally two-layered and they need in most cases an impermeable substratum of solid material to settle upon (Fig. 6). On the substratum, e.g. a lithified microbialite crust, a basis layer is located which is called base film (Fig. 6). This layer is more or less firm and contains microbial cells, exoenzymes, different types of bind allochthonous particles, and extracellular polymeric substances (EPS) which hold the cells together on the substrate. The EPS have a central function, because this is an open porous system filled with moving water through which liquids and particles of a certain size can move and be transported. Larger particles are entrapped this way in the base film. Within the base film the metabolic processes happend. The second layer is called surface film (Fig. 6) and normally exhibits a very rough topography. The surface film is an interface between the base film and the surrounding water or bulk liquid in the sence of ROSENBERG (1989) and WILDERER & CHARACKLIS (1989). The surface film exhibits a more or less firm portion similar to the base film which shows the rough topography. Between the the more or less firm base film extrusions a liquid phase is present which contains biofilm metabolites, microbial cells, inert substances, and at least allochthonous particles. The bulk liquid or normally surrounding watermass compartment supplies the biofilm reactor via eddy diffusion.

In special cases the substratum is semipermeable and porewaters which are moving within the substratum may supply the biofilm reactor or decayed and/or metabolic products are delivered to the substratum space!. This process plays an important role during microbialite formation because this may explain the transport of Ca-binding organic macromolecules to the loci of later mineralisation.

Various biofilms are observed on the microbialite surfaces and the bioactivity is visible using fluorochromes in vivo and in fixed material (Pl. 3/1-3; Pl. 4/1, 5). Calcifying bacteria were detected with tetracyclines and non-calcifying

ones with acridine orange and thiacine red (Pl. 3/7; Pl. 4/1.). The very common Fe/Mn-bacteria exhibit a strong fluorescence using calcein (UV) (Pl. 3/8a, b). The great variability of the biofilms is seen when studying Critical Point or PELDRI II dried specimens (Pl. 5). All biofilms exhibit strong fluorescence behavior, and it is possible to recognize the interaction with the substrates (Pl. 3/2; Pl. 4/5). It is the rule that all observed biofilms have an interaction with the porewater systems and microcavities of the microbialite which are filled with calcifying mucilages. The observed biofilms are always a system of bacteria, fungi, and sometimes protozoans like foraminifera. Algae are never observed within the dark environments. The base films are thin with a thickness of only 10-12  $\mu\text{m}$ , and they are stabilized by entrapped allochthonous collagenous fibres. The bacteria, mainly round and rod-shaped ones, are commonly linked with the fibres (Pl. 6/2). Similar features are seen within the mesohyle of sponges and it is very difficult to distinguish biofilms from very thin sponge crusts with only few choanocyte chambers per area unit (Pl. 8/2). The interfaces of the base films to the liquid film are very different and not yet extensively studied. Some of the observed surfaces are knobby and very irregular to extend the surface planes. The knobby structure is caused by microbes near the internal surface (Pl. 5/2). On the surface films many different often stalked microbes and fungi hyphen are present which are linked with the interior surface layer (Pl. 5/2, 3). Some of the microbes which are lying on the surface layer were primarily enriched in the overlaying liquid phase. The surface films have sometimes small openings (1  $\mu\text{m}$ ) like ostias in sponges. Within the base films pores were observed too, which may be identical with the "extracellular polymeric substances" postulated by WILDERER & CHARACKLIS (1989) (Pl. 5/5). They are part of a pore system through which natural products as liquids and non-liquids are transported.

### 6.5.1 Calcified microbes

Within the base film of few biofilms special types of calcified bacteria and filamentous structures were observed.

One calcified bacteria type (I) is relatively common (Pl. 5/5, 6). Single specimens exhibit a spindle like shape of 1-2  $\mu\text{m}$  size. Normally they occur in rosettes like aggregates. Broken individuals are hollow and the cavity is covered by an organic phragma which may be a remain of the murein sheet. The complex membrane layer of the bacterium is completely mineralized by a low-Mg calcite. The calcite exhibits an extremely fine grained structure due to aggregates of seed crystals of 50-80 nm. This bacteria type is sometimes enriched in small cavities.

The calcification on the membranes of a gram negative bacterium was described by MORITA (1980). Divalent cations ( $\text{Ca}^{2+}$ ,  $\text{Mg}^{2+}$ ) are linked with protruding acidic polysaccharid chains of the outer membrane. The cations are reacting either with metabolic  $\text{CO}_2$  which reacts in sea water e.g. with ammonia and amines to  $\text{HCO}_3^-$  and  $\text{CO}_3^{2-}$  (s. ammonification) increasing the alkalinity or with  $\text{HCO}_3^-$  and  $\text{CO}_3^{2-}$  from sea water. MORITA (1980) has evidenced this process with  $^{14}\text{C}$ -marked aspartate.

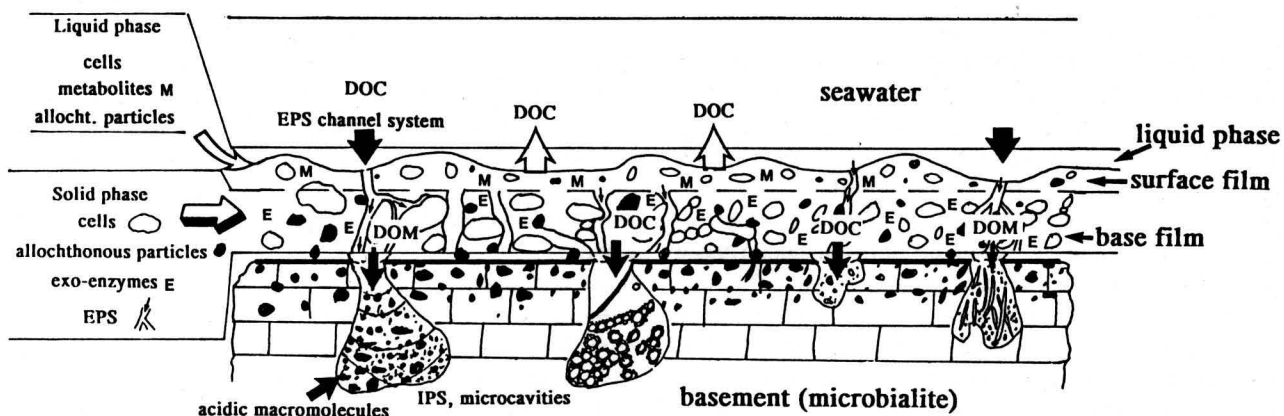


Fig. 6. Biofilm model after WILDERER & CHARACKLIS (1989) adapted to microbialites. The biofilm is a reactor which takes up from the ambient seawater DOC and rigid particles via EPS channel systems. The reactor filters and produces DOM and DOC, e.g. waste products, and releases it back to the seawater or into the open system of the upper microbialite (microcavities, irregular pocket structures (IPS)). Some products are acidic macromolecules which enhance mineralization. Organic matter released into the seawater is a nutrient supply for closely related filter feeding benthos as "bacterio-sponges".

Another type (II) of calcifying bacterium produces fine grained calcareous particles (100-200 nm) when decaying (Pl. 5/4). The non-calcified bacterial cell envelope is cracked and the fine grained calcified particles surround the cell envelope.

A third type (III) of calcifying rod-shape microbe was observed in microcavities (Pl. 5/7). This type exhibits a strong fluorescence when using acridine orange, and this is often surrounded by brownish non fluorescent small ferroan-rich particles (Pl. 4/1b, 2). This form is very large (10-15  $\mu\text{m}$ ), and the calcified body exhibits the same aggregates of seed crystals as seen in bacteria type I. The taxonomic affinities are unknown.

Calcified filamentous structures are common, and they play in microbialites of zone 3 a significant role. The filaments are not related to cyanobacteria. They have diameters between 4-15  $\mu\text{m}$ . No traces of thylakoid membranes were observed studying TEM sections (Pl. 6). Two types of mineralized filaments were observed. Both types exhibit an internal layer with tangentially arranged crystals. One type exhibits elongated irregularly arranged aragonitic crystals in the second outer layer, and the other type exhibits small rhomboedric calcite seed crystals which grow in a mucilage (Pl. 6/4). In TEMs the seed crystals are surrounded by insoluble matrix layers and they exhibit inside grey parts which may be remains of soluble matrices which are protected during decalcification with EDTA.

However, the observed calcifying microbes play only an insignificant role during the microbialite formation. But the activity of the biofilms may control the transport of calcifying organic substances to the microcavities underneath the biofilms via the EPS systems.

The particle trapping ability of the basal films within the biofilms explains in an excellent way the formation of the thrombolitic pillars of the microbialites of zone 3.

The base films can be mineralized because the main physiological processes occurred there. Base films are firm mucus layers with a lot of insoluble substances, and decaying base films have a strong ability to mineralize as detected

by Ca-binding chelating complexes. MORITA (1980) has observed under artificial condition that decreasing amount of living bacteria cells increase the amount of calcium carbonate precipitation. He suggested that this process is not microbial but is supported by microbial activities.

#### 6.5.2 Fe/Mn biofilms

All observed microbialite types exhibit numerous brownish to black/brownish thin crusts. They are more or less horizontally orientated and show a pseudo-stromatolitic structure. Nearly all inner surfaces of microcavities and some areas of the upper surfaces of the microbialites show these crusts (Pl. 3; Pl. 4/3a, 4, 5). EDAX and X-ray diffraction analyses have shown that light brownish crusts are rich in Fe (goethite) and the darker ones have a significant amount of Mn (Mn oxides). They are also enriched in clay minerals. The surfaces of the Fe/Mn crusts are extremely irregular and sometimes forming grape-like structures. High magnifications show clumpy aggregates of spherical elements with a size of 2-5  $\mu\text{m}$  (Pl. 3/8; Pl. 5/8)). Using calcein stained specimens, the surface of the clumpy aggregates exhibits a strong fluorescence under UV-light (Pl. 3/8). This fluorescence indicates a microbial activity, and the microbes are seen in TEM sections as well as under SEM (Pl. 6/3; Pl. 5/8)). Some of the bacteria have affinities with the taxon *Siderocapsa* sp.. Within zone 4 of the reef caves, this type of biofilm is very common on the surface of the reef cave walls and it is responsible for the dark brownish color (Pl. 1/3b,4b). In this area the film is growing under oxygen rich conditions. In some cases living Fe-biofilm surfaces were detected in microcavities which are may be reduced in oxygen. Thick ferroan hydroxyid crusts were observed in microcavities of zone 3 linked with thrombolitic facies. Mn and Mo rich portions were only observed in zone 4. All Fe/Mn-crusts exhibit at their base corrosive structures (Pl. 2/4; Pl. 3/3, 6). Parts of the calcified microbialites and organisms are dissolved and exhibit strong corrosive patterns ("pseudo-

stylolitic"). The microbialites in zone 4 have lost by this way more than 40% of the lithified volume! They exhibit an extreme dense pattern of Fe/Mn crusts. In one 4 cm thick crust over 100 larger isochronous Fe/Mn crusts were counted.

Corrosion is an electrochemical process characteristically of all metals except noble ones caused by the flow of electrons from one metal to another if an electrolyte is present. Dissolution (= corrosion) occurs at the anode and at the cathode the electrons are consumed. An important cathodic reaction in aerated solution at nearly pH 7 is an oxygen reduction. VIDELA (1989) describes the principal processes of microbiological corrosion which allows to explain the observed dissolution phenomena. The observed metal biofilms, the underlying calcium carbonate crusts, and the sea water is a natural electrochemical cell. The calcium carbonate crusts have an anode and the biofilms have a cathode function. VIDELA (1989: 309, fig.4) has observed colloidal hydrated iron oxide spheres as a corrosion product after settlement of marine *Vibrio* bacteria on steel. These goethite spherules are very similar to those ones in the brownish crusts and may be interpreted also as a corrosion product at the cathode. The calcium carbonate corrosion increases the alkalinity and may support the calcification in closely related microcavities and thin underlying areas despite of their dissolution ability!. In all cases below active Fe/Mn-biofilms  $\text{Ca}^{2+}$  is enriched detected by Ca-chelating fluorochromes (Pl. 3/2, 6). This observation may explain the extreme slow growth of the microbialite.

At present, an environmental interpretation of Fe/Mn-biofilms is still difficult. It is obvious that these crusts occur at certain times and cover the complete surfaces of the microbialite and bury all sessile organisms (Pl. 3/2). Environmental crises as eutrophic events might cause a rapid growth of this biofilm type. This idea is supported by the linked formation of crypt cells in *S. (Acanthochaetetes) wellsi* as a special surviving strategy.

## 6.6 Geochemistry and stable isotopes

### 6.6.1 Geochemical parameters

The first geochemical results of lithified microbialites show a dominance of high-Mg calcites with 12-16 mol%  $\text{MgCO}_3$  and 2000-2500 ppm Sr. The analyses were carried out with EDX, x-ray diffraction, and electron microprobe. Low-Mg calcites are present in bulk analyses and probably related to allochems (bivalves, brachiopods). However, some calcified bacteria sheets exhibit low-Mg calcites too (EDAX). Aragonite is rare and related to allochems (ascidian sclerites, coral remains) except some calcified filaments which exhibit an autochthonous aragonite.

Calcifying organic rich areas in microcavities or decaying sponges exhibit high amounts of S and P and sometimes Ba. The sulfur is related to Ca-binding sulphate groups of glycoproteins and P is related to calcium phosphates and free P of lysing cells. Silicon is detected in high amounts at certain places related to sponge spicules and clay minerals. Mn and Fe are enriched significantly in the Fe/Mn-microbialites sometimes associated with certain amount Mo.

### 6.6.2 Cements

Cements are rarely observed within the microbialites. An acicular equant aragonitic marine cement was observed in coral skeletons of the coralgal cores of the microbialite only. Within this facies a granular calcite cement is rarely present and is interpreted as an early diagenetic fresh water cement.

Some microcavities exhibit a rim of short dentate Mg calcite cement which exhibit a strong fluorescence using tetracyclines (Pl. 3/4). Margins of some boring sponge cavities are covered with a short fibrous Mg calcite cement which may be related to the sponge metabolic activity (Ca-detoxification). However, this phenomenon has not been studied up to now. Other typical marine cements play no significant role during microbialite early diagenesis.

### 6.6.3 Stable isotopes

For further characterisation of the calcium carbonates, the  $\delta^{13}\text{C}$  and  $\delta^{18}\text{O}$  ratios of some microbialites were studied. All measured data from Mg calcites of a microbialite crust from the Bommie-Bay research cave (Lizard Island) exhibit high positive  $\delta^{13}\text{C}$  (+3 - +3.84) and  $\delta^{18}\text{O}$  (-0.37 to -1.1). The  $\delta^{13}\text{C}$  and  $\delta^{18}\text{O}$  values expected for equilibrium inorganic precipitation of calcite in surface waters of the northern Great Barrier Reef are approximately +2,2% and -1% respectively. (WEBER & WOODHEAD 1970) (Fig. 7). The equilibrium values for Mg calcites must be corrected of +0,06%/mol  $\text{MgCO}_3$  (TARUTANI et al. 1969). Therefore, the observed microbialites are precipitated close to the expected equilibrium values. This is evident also for most of the associated coralline sponges. The high-Mg calcite of *S. (Acanthochaetetes)* and minchinellid sponges (*Plectoninia*) as well as aragonitic ones (*Astrosclera*, *Vaceletia*) fall within this range (REITNER 1992). The aragonitic ones exhibit higher positive values due to the fractionation during aragonite precipitation. Calculated aragonite equilibrium values are +4 to +5%  $\delta^{13}\text{C}$  and -1.6 to -1.8%  $\delta^{18}\text{O}$ . These data must be corrected -1.8 for  $\delta^{13}\text{C}$  and -0.6 for  $\delta^{18}\text{O}$  values (TARUTANI et al. 1969).

The observed data within one in detail measured profile of a microbialite exhibit some significant changes of the isotope values (Fig. 8). The coralgal cores exhibit a mean of light  $\delta^{13}\text{C}$  values. The coral core has a corrected value of a mean of -0.8  $\delta^{13}\text{C}$  and -0.43  $\delta^{18}\text{O}$  which is characteristic of hermatypic corals. The overlaying coralline red algae have moderately positive values of  $\delta^{13}\text{C}$  (+1). The lowermost microbialite layer has intermediate heavy carbon values. All following data are in a range between +3 and +3.5  $\delta^{13}\text{C}$ . The heaviest value was measured in portion where Fe/Mn-crusts are very common (point 9 in Fig. 8). This may be a hint for eutrophic conditions. Non-lithified portions of the microbialite e.g. in microcavities exhibit relatively light  $\delta^{13}\text{C}$  values (+1 to +1.5) (Fig. 7). Semi-lithified areas have moderate high  $\delta^{13}\text{C}$  values (+2.5) (Fig. 7). The measured initially formed peloids fall also in the field of lithified microbialites (Fig.7).

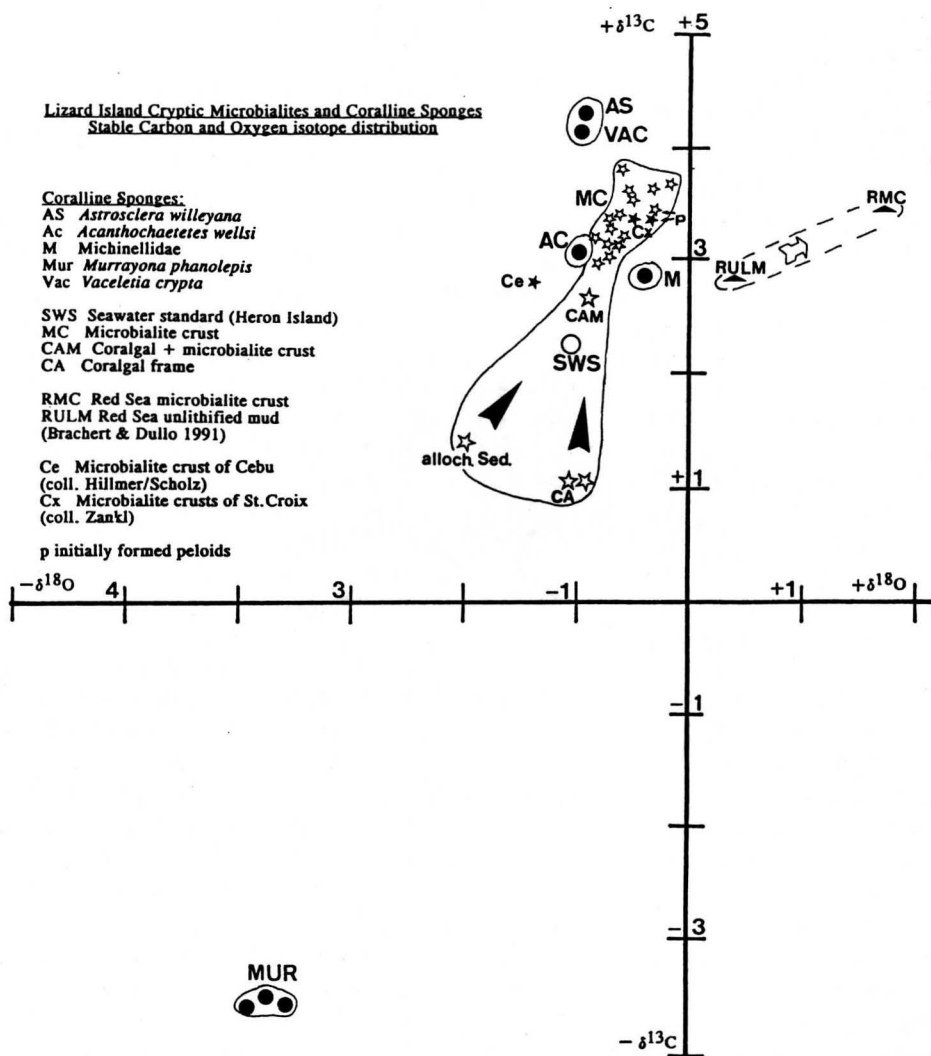


Fig. 7. Distribution pattern  $\delta^{13}\text{C}$  and  $\delta^{18}\text{O}$  (v. PDB) of modern cryptic microbialites from Lizard Island, St. Croix and Cebu (Philippines), and coralline sponges.

The shift from light  $\delta^{13}\text{C}$  values (+1) to heavy ones (+3.5) within mature microbialites is a result of a slow calcification (McCONAUGHEY 1989). Sponges and microbialites exhibit more or less the same stable isotope fractioning behavior. The observed values are very close to an expected equilibrium. A problem is that normally biologically precipitated carbonates are in disequilibrium with the ambient sea water. In coralline sponges, a moderate biological control of calcification is observed, and disequilibrium should occur (REITNER 1992, REITNER et al. in press). Only one species of the reef caves is in disequilibrium, the high-Mg calcite pharetronid *Murrayona phanolepis*, exhibits extremely light  $\delta^{13}\text{C}$  (-3.5 to -4) and light  $\delta^{18}\text{O}$  (-3.5) values (Fig. 7). The calcification in this particular case occurs under the control of symbiotic bacteria which explains the strong vital effect (REITNER 1992).

The microbialite formation occurs under the control of different organic substances (matrix mediated calcification). But in all cases the calcification is extremely slow (ca. 100  $\mu\text{m}/\text{y}$ ) and  $\text{CO}_2$  resource is from dissolved inorganic carbon (DIC) of the surrounding sea water.

In all studied cases no photosynthetic fractionated carbonates were detected except those from coralline algae (point 3 in Fig. 8). This observation fits with the histological data.

All published isotope data of modern microbialites have more or less the same values (KEUPP et al. 1993). Isotope analyses from fossil occurrences exhibit the same distribution patterns as in modern ones (discussion by NEUWEILER (1993) and KEUPP et al. (1993)).

## 7 PROPOSED RELATIONSHIP BETWEEN "BACTERIO-SPONGES" AND BIOFILMS OF CRYPTIC MICROBIALITES

### 7.1 Bacteria in sponges

Very important constituent of the reef cave inhabitants are thin sponge crusts which covering the living biofilms of the microbialites (Pl. 1/4b; Pl. 5/5). The sponges have a thickness of 50-100  $\mu\text{m}$  only and it is very difficult to make any taxonomic determinations. Probably most of them are new species or only poorly known taxa. More than 80% are related to the poecilosclerida a major taxon of the Demospongiae. Calcareous sponges are rare and observed non-rigid genera are *Sycon*, *Leucetta*, and *Clathrina* (Pl. 4/4a). Rigid pharetronid type species are *Plectroninia neocaledoniense*, *P. hindei*, and the calcinean *Murrayona phanolepis*. Coralline sponges with demospongiid affinities are the stromatoporoid *Astrosclera willeyana*, new species of *Astrosclera*, the chaetetid *Spirastrella* (*Acanthochaetetes*)

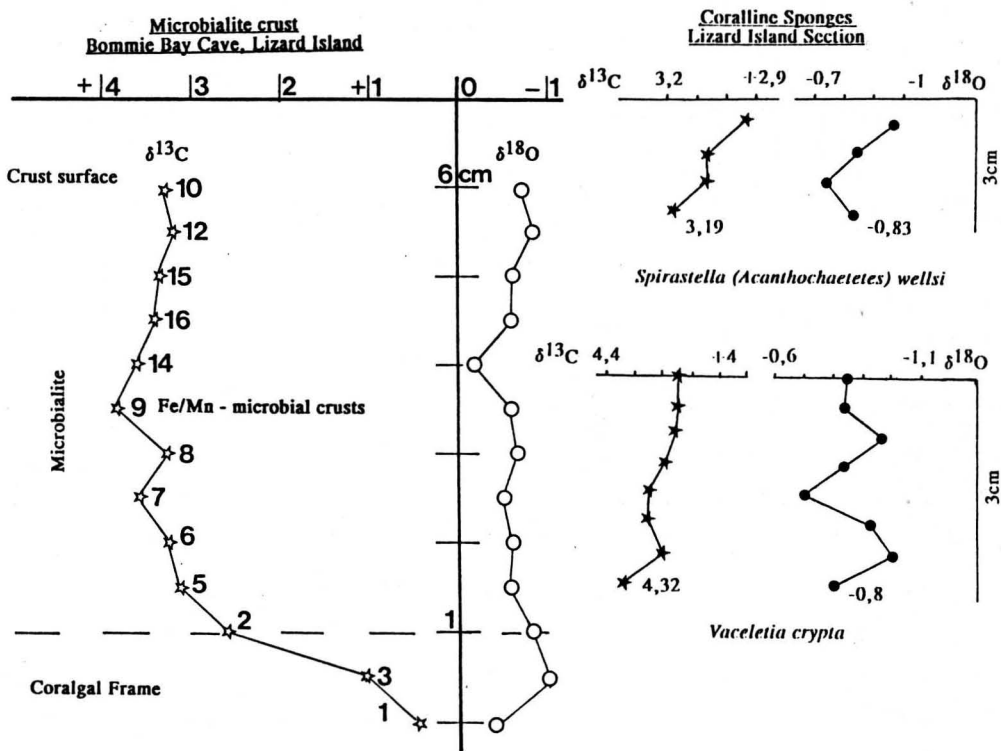


Fig. 8. Stable carbon and oxygen isotope profile from a Bommie Bay research cave microbialite (versus PDB standard). The major change is visible from 3 to 2 which marks the beginning of microbialite formation. 1 represents the coral core (*Agaricia*), and 3 overlaying coralline red algae. From 2 to 9 the  $\delta^{13}\text{C}$  values increase. 9 marks dense bundles of Fe/Mn-crusts maybe caused by eutrophism. 9 to 14 exhibits a slight decrease of  $\delta^{13}\text{C}$  values which are probably linked with the growing amount of light  $\text{CO}_2$  in the seawater caused by an increasing input of light carbon via burned fossil carbon (e.g. fuel). Same patterns were detected in large (250 y/old) coralline sponges (DRUFFEL & BENAVIDES 1986 for *Ceratoporella nicholsoni*, Caribbean). For comparison the isotope profile of a nearly 100 y old (calculated by measured growth rates) *Vaceletia crypta* specimen from Ribbon Reef No.10 (25 m water depth) which exhibits a slight increase of light carbon. Same feature is seen in a more or less same aged *S. Acanthochaetetes* from the Bommie Bay research cave (REITNER et al. in press)

*wellsi*, new species of *Spirastrella* (*Acanthochaetetes*) and *Stromatospongia micronesica* a sponge with chaetetid/stromatoporoid affinities. The spinctozoans *Vaceletia crypta* and *V. cf. crypta* are restricted to the outer barrier reefs and never observed within inner island related reefs.

All of these sponges exhibit various amounts of heterotrophic bacteria (Pl. 7/8). Especially the peocilosclerid thin sponge crusts and the coralline sponges, except *S. (Acanthochaetetes)* (Pl. 7/1) have bacteria which constitute 50% and more of the biomass of the sponge individual (Pl. 7/2,3; Pl. 8/2, 3)! This data based on the amount of bacteria versus sponge cells per area unit in different anatomical parts of the sponge (dermal layer, choanosome). The others have a mean amount of bacteria (10-20% of the sponge biomass). This observation is of particular interest because sponges are "bacteria containers", and the amount of microbes within the sponges is much more higher as in the biofilms. Most of the sponge related bacteria are symbiotic. SANTAVY et al. (1990) differ between a small population of bacteria, which is more less similar with the ambient seawater and which may play a role as a food resource of the host, and a large population of heterotrophic bacteria which are restricted to the sponge and do not occur in the surrounding seawater. These bacteria are most likely true symbionts.

Most of the papers published are dealing with phototrophic cyanobacterians in sponges and their role within the reef community (SARA 1971, VACELET 1971, WILKINSON 1979, 1983, WILKINSON & FAY 1979).

The role of the enormous amount of heterotrophic bacteria is hardly understood and only few investigations were made on these in sponges (SANTAVY et al. 1990, WILKINSON 1978 a,b; VACELET 1970, 1971, 1975). The main problem is that most of the bacteria in sponges are not culturable by the methods employed. SANTAVY et al. (1990) could only culture 3-11% of the bacteria inhabiting the coralline sponge *Ceratoporella nicholsoni* from Jamaica. The description of symbiotic bacteria is therefore limited to morphological details documented by electron microscopy.

The heterotrophic bacteria are concentrated within the intercellular mesohyle of sponges. They are enriched within mesohyle zones of the choanosomal layers (Pl. 7/2a, 3a).

## 7.2 Heterotrophic bacteria within studied cave sponges

*Vaceletia crypta* exhibits the highest density of of mesohyle bacteria (VACELET 1977) and the observed types are very similar to those ones described by SANTAVY et al. (1990) from *Ceratoporella nicholsoni* (Pl. 7/3a, b). The

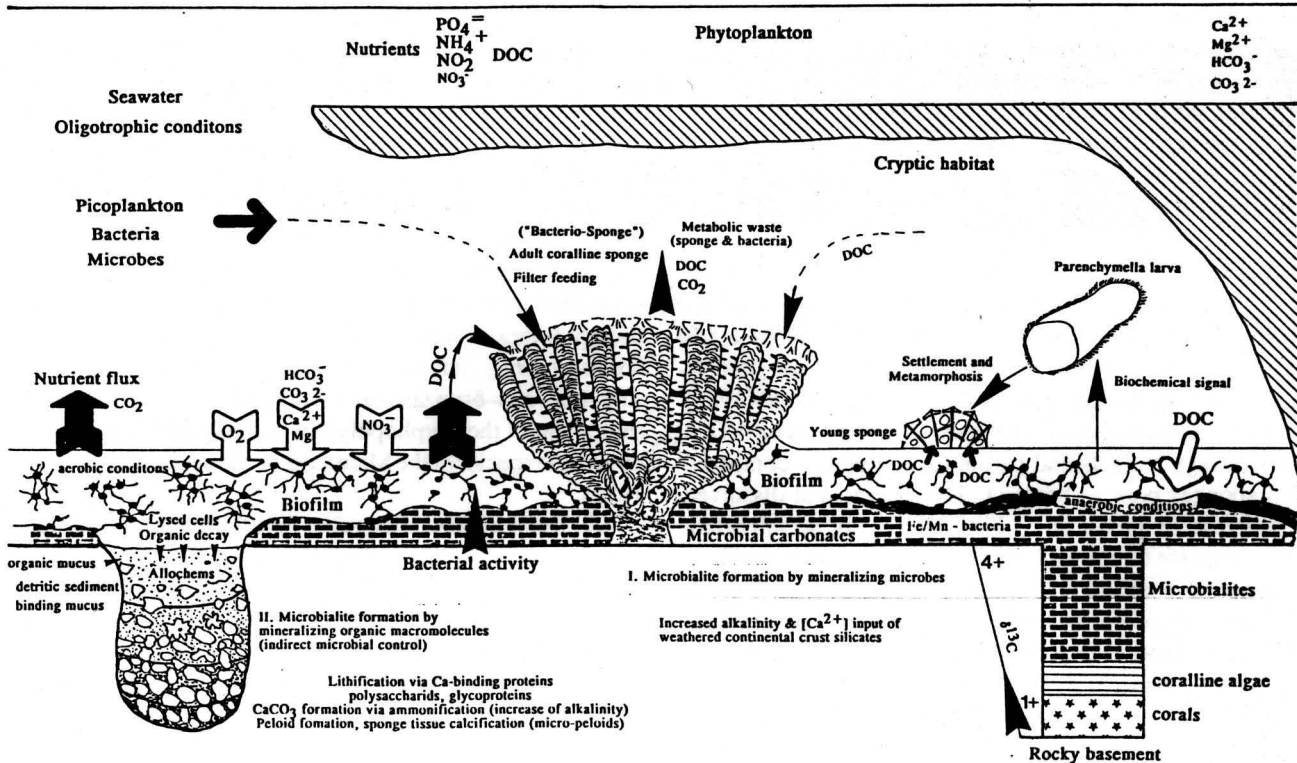


Fig. 9. Proposed relationship between "bacterio-sponges" and biofilms.

This hypothesis summarizes the proposed ideas on a relationship between microbial films and sponges and try to explain the often linked microbialite formation within dark cryptic habitats.

The basic ideas is following the external microbial activity supports the nutrient supply to the sponges and their symbiotic bacteria via dissolved organic matter and carbon and further deliver biochemical signals for the settlement of sponge larvae. The whole system is more or less self controlling and is characteristic of K-strategists.

This model may explain also the formation of fossil extended sponge/microbial reefs (partly "mud mounds"). The relationship between sponges and biofilms is not restricted to cryptic niches. It was also observed in vast sponge accumulations (sponge mounds) of the Arctic Seamount Vesterisbanken (HENRICH et al. 1992).

determined bacteria are closely resembling the family Enterobacteriaceae. Most of the observed forms show a gram-negative cell wall structure detected by gram-staining. Many of the bacteria are related to the taxa *Vibrio* and *Aeromonas*. Nearly the same bacterial populations were detected in *Astrosclera willeyana* (Pl. 7/2a, b), the thin poecilosclerid sponge crusts (Pl. 8/2), and within the lithistid demosponge *Discodermia* (Pl. 8/3a, b). All of these sponges have prominent developed mesohyle spaces and a network of thin fibres (mostly collagenous ones) between which the bacteria are located (Pl. 7/2a, 3a). All of these sponges are characterized by small choanocyte chambers (*Astrosclera willeyana* 10-15  $\mu\text{m}$  - Pl. 7/2a, b, *Vaceletia crypta* 15-20  $\mu\text{m}$  - Pl. 7/3a, b, *Discodermia* 15-20  $\mu\text{m}$ , thin sponge crusts 10-15  $\mu\text{m}$  - Pl. 8/2) and a decreased abundance of choanocyte chambers per area unit. The most reduced abundance of choanocyte chambers, only one chamber per 100  $\mu\text{m}^2$ , was observed in some thin poecilosclerid sponges.

Within *S. (Acanthochaetetes) wellsi* symbiotic bacteria observed are small (>1  $\mu\text{m}$ ) and rare ovoids (Pl. 7/1a, b). The choanocyte chambers are very large, 40-50  $\mu\text{m}$  in diameter. Within the calcareous basal skeleton endolithic heterotrophic cyanobacterians of the *Anabena* group are common (Pl. 7/a).

Completely different are the bacteria in the calcinean

pharetronid *Murrayona phanolepis* (Pl. 8/1). This still undetected bacteria type plays a significant role during calcification of the Mg calcite basal skeleton. The ovoid to round shaped bacteria (1-2  $\mu\text{m}$ ) exhibit outer membrane bound vesicles of 100 nm size in which calcium carbonate is secreted (Pl. 8/1c). It cannot excluded that these vesicles are may be overprinted fixation artefacts. However, in SEM micrographs small seed  $\text{CaCO}_3$  crystals (Pl. 8/1d) were observed, which exhibit the same size as the vesicles. The bacteria are concentrated at the boundary between living tissue and basal skeleton (Pl. 8/1b), and probably they are controlling the mineralization of the basal skeleton. One possibility is that the calcified bacteria are aggregated together and build initially the basal skeleton. This process is evidenced by the light  $\delta^{13}\text{C}$  (-3.5) and  $\delta^{18}\text{O}$  (-3.5) values of the skeleton which exhibit a strong bacterial metabolic fractioning Fig. 7).

### 7.2.1 Proposed function of symbiotic heterotrophic bacteria

Only little is known about the function of heterotrophic bacteria in contrast to the phototrophic ones (WILKINSON 1978a,b, 1983; WILKINSON & FAY 1979). Most of the ob-

served and cultivated bacteria from sponges are facultative anaerobes able to metabolize a wide range of components. The described ones in *Ceratoporella nicholsoni*, which are very similar to those studied, are able to ferment sucrose and fucose but exhibit an inability to ferment glucose which is typical for the most aeromonads. Within all observed Lizard Island coralline sponges high amounts of fucose and galactose were detected which indicates the fermenting processes (REITNER 1992). Therefore the bacteria may play a role during polysaccharid mucus formation. Important is the observation that bacteria take up dissolved amino acids (WILKINSON & GARRONE 1980) and bacteria are able to degrade sponge collagen (WILKINSON 1979). REISWIG (1981) has observed that bacteria rich sponges have a gross deficit in the energy budgets and partial carbon uptake compared with sponges poor in bacteria. This means that dissolved organic carbon produced by bacteria must be an important nutrient source for the sponge. The fermentative metabolism of the symbionts and delivered DOC allows the sponge to survive ecological crisis when the pumping rates are decreased. SANTAVY et al. (1990) have postulated that anaerobic zones may enhance the calcification of the basal skeleton of *Ceratoporella* maintaining an acidic environment. Sometimes I have observed an uptake of symbiotic bacteria by archaeocytes within *Astrosclera willeyana* but in most cases the phagocytized bacteria are not identical with symbiotic ones. Comparable observations for example were made by REISWIG (1990) within further sponges. He has observed in situ feeding in two shallow-water hexactinellid sponges. The one species *Rhabdocalyptus dawsoni* uses only dissolved organic carbon (DOC) and the other species *Aphrocallistes vastus* feeds bacteria. Both types take up organic matter in colloidal form.

In conclusion the natural products of symbiotic bacteria in sponges play a primary role as a nutrient source, control metabolic processes, remove metabolic waste, and may enhance calcification. The facultative anaerobic character of most of the symbiotic bacteria allows the sponge to survive environmental disturbances.

### 7.2.2 Hypothetic relationship between "bacterio-sponges" and biofilms

The pumping activity of sponges supplies in first order the symbiotic bacteria with dissolved organic carbon (DOC) because they are the dominant part of the sponge biomass. Sponge accumulations need therefore a resource of DOC and dissolved organic matter (DOM) to supply their symbiotic bacteria. Bacteria themselves produce high amounts of DOM, and therefore the closely related external biofilms may play a role as bacteria food producing "farms". It is obvious that the observed biofilms on the microbialites are tightly linked with sponges (Pl. 4/5). The coralline sponges are restricted to areas within the caves where Fe/Mn microbial biofilms are present and pharetronid calcareous sponges are linked with non-Fe/Mn-bacteria bearing biofilms. This may explain why many investigated reef caves are free of coralline sponges because the sponge related biofilms are

missing. The sponge larvae settlement may depend on the type of biofilms. Different types of biofilms may release biochemical signals to attract the larvae to settle down and metamorphose. This hypothesis is supported by the observation that young small coralline sponges are restricted to certain Fe/Mn-biofilms. Similar larval behaviour was described from some bryozoan and serpulid larvae by STEBBING (1972). He has observed that both organisms prefer to settle on the younger part of the large brown alga *Laminaria* which is covered by special types of biofilms. Same experiments and observations were made by RYLAND (1959) and CRISP & RYLAND (1960). SCHOLZ (this volume) describes the relationship between bryozoans and microbial mats. The stolon settlement in the scyphopolyp of *Aurelia aurita* is induced by a single species of the Micrococcaceae bacterium (SCHMAL 1985).

A further important aspect of biofilm/metazoan relationship is the interaction of the settled organisms with the substrate. Within some thin sponge crusts it was observed that the basopinacoderm is linked with the base film of the underlying biofilm. The interface exhibits a strong fluorescence detecting free  $Ca^{2+}$  ions and the presence of acidic polysaccharid slimes. SOULE (1973) has observed that a simple acid proteoglycane is responsible for the biological adhesion of bryozoa to the substrate.

Comparable observations of the relationship between metazoans and microbial films were made within arctic deep water spiculite mats and sponge mounds of the Vesteris-banken Seamount (HENRICH et al. 1992). Observed sponge larvae, young bryozoans, and serpulids settled only on spicules which are covered by microbial films. The internal spiculite mats are extremely enriched in biofilms and therefore an important food resource (DOC and DOM). An adapted strategy was recently observed by the author in many deep water sponges (e.g. the hexactinellid *Rhabdocalyptus dawsoni* - see above!, the demosponges *Polymastia sol*, and *Thenea abyssorum*) which have many external microbial films surrounding protruding spicules. These external bacterial gardens are a very sophisticated nutrient supply! .

The proposed relationship between sponges and biofilms in cryptic reef caves is summarized in Fig. 9. This model tries to explain the circuits between biofilm activity, sponge development, and microbialite formation.

From a functional viewpoint sponges and biofilms are very closely related. This may explain why microbes and sponges always play a central role e.g. in carbonate buildup formation since the beginning of the Cambrian (REITNER in prep.).

## 8 PROBLEMS OF MICROBIALITE FORMATION - THE ALKALINITY QUESTION

The investigation of reef caves in the Lizard Island Section has shown that microbialite formation does not occur in all caves studied. The microbialites occur only in fringing reefs of continental islands (e.g. Lizard Island, North Direction Island, South Island) which have an island core formed by an Late Permian granite. Microbialites were

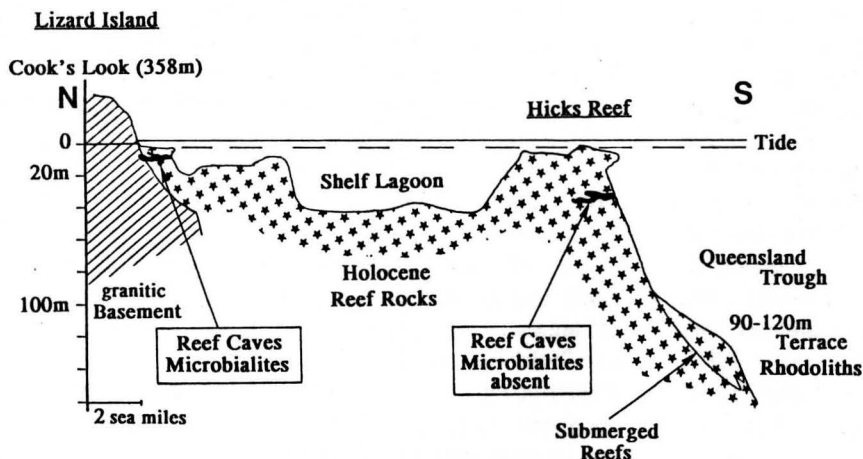


Fig. 10. Simplified N-S profile Lizard Island Hicks-Reef

Microbialites occur only in reefs which are linked with continental island (e.g. Lizard Island). Weathering silicates as feldspars and freshwater influx increase the carbonate alkalinity which favors calcification of microbialites.

Microbialites are nearly absent in reef systems without continental influx (e.g. reefs of the outer barrier).

also observed in mid-Holocene cores of reef islands close to the mainland of Australia (e.g. Nymph Island). The reef caves of the outer barrier are free of microbialites except in some cases when very thin crusts of different origin are present only. The link of microbialites with continental crust islands supports the idea that an increased carbonate alkalinity enhances calcification. However first results of alkalinity measurements exhibit no significant increase of carbonate alkalinity [ $\text{HCO}_3^-$ ]; [ $\text{CO}_3^{2-}$ ] in the ambient reef cave water. A slightly increased alkalinity was measured only on microbialite surfaces of zone 3 within the caves. This internal alkalinity increases partly under anaerobic conditions via ammonification.

We have done the measurements during the dry season only (measurements during the wet season are in progress). It is postulated that during the wet season carbonate alkalinity increases by an intense weathering of silicates of the Permian granite or through input of weathered product of silicates. The microbialites exhibit periodically a concentration of kaolinite, a clay mineral which is a product of feldspar weathering. Weathering of e.g. plagioclase increases carbonate alkalinity (KEMPE et al. 1989, KEMPE & DEGENS 1985). Freshwater with a high carbonate alkalinity is during the wet season running into the reef cave systems and increases slightly the carbonate alkalinity which favors the calcification of the microbialites. In many supratidal places of Lizard Island where granite boulders weather the reef debris, remains of continental rocks, glass bottles, and beer cans are strongly cemented by thick microbialitic/micritic crusts. The reef systems close to the mainland exhibit the same type microbialitic/micritic crusts. These reefs may be influenced by higher concentrations of [ $\text{HCO}_3^-$ ] and [ $\text{CO}_3^{2-}$ ] by river transport from rain forest areas which exhibit a strong silicate weathering.

The reefs of the outer barrier are not influenced by silicate weathering and therefore no microbialites occur in reef caves although the same biofilms and linked benthos community are present (Fig. 10).

Comparable and supporting observations were made by ZANKL (this volume) from reef caves of St. Croix (Caribbean). St. Croix is a continental island and silicate weathering occurs.

In reef caves of the Bahamas and linked deeper slope

areas no microbialites of the Lizard types were observed (REITNER unpublished data) because no continental crust is exposed. BRACHERT & DULLO (1991) have described Lizard Island-type microbialites from deeper parts (120m) of Red Sea reefs close Port Sudan in neighborhood of crystalline basements.

If this observation is confirmed that the influence of silicate weathering may be correlated with freshwater influx supporting the formation of microbialitic crusts - this phenomenon would be an important controlling factor for microbialite formation. NEUWEILER and KEUPP et al. (1993) have argued partly in the same manner. NEUWEILER for example has discussed that an increase of carbonate alkalinity via silicate weathering from the Spanish mainland by river systems, cold seeps and brines of salt solutions of diapirs, and weathering of carbonates (paleokarst) are responsible for the wide distribution of microbialite reefs in the Middle Albian of northern Spain.

### 9 ARE MODERN MICROBIALITES FROM LIZARD ISLAND A MODEL FOR ANCIENT SPONGE REEFS? - A PERSPECTIVE

Investigated microbialites and combined benthos of Lizard Island are found in cryptic and dark reef cave systems. Similar observations were made by JACKSON et al. (1971) in Caribbean reef caves, VACELET & VASSEUR (1965, 1971) in reefs of the island Madagascar, and BASILE et al. (1984) of the Enewetak Atoll. The observed benthos community is completely different from the normal photic shallow water reef habitat and represents a deeper water community which occurs normally in water depth from ca. 100-250m. The cave systems have environmental conditions which allow the telescoped deeper water faunas to live within these protected areas. The cave and channel systems within the cemented reef bodies are very widespread and the surfaces are vaster than the outer active growing zones of the coral reefs. The cave and pore systems are successively filled up by the growing of cryptic sessile benthos and, if present, by microbialites. Therefore also ancient reef bodies must demonstrate commonly this facies type.

Very close affinities to the modern ones were recognized within Albian coral reef platforms of northern Spain (REITNER

1987, 1989, REITNER & ENGESER 1987, NEUWEILER this volume). The best studied example is the Late Albian Albeniz-Eguino carbonate platform. This platform exhibits an outer barrier of coral reefs, an open lagoonal reef system with rudists, and deeper water micritic reef mounds with sponges. The platform is paleogeographically situated on a tilted crust segment in the front of a larger deltatic system.

The most important observation in this respect is that the cryptic surfaces are occupied by a microbialite facies and the benthic community which has a great taxonomically correspondence with the modern ones (*Acanthochaetetes*-community) (REITNER 1987, 1989, REITNER & ENGESER 1987). The microbialites in the caves exhibit the same vertical facies successions as observed in modern ones (cf. KEUPP et al. 1993).

The deeper water micritic/microbialitic sponge mounds ("mud mounds") were located in a reconstructed waterdepths of 80-150m at the platform margins. They demonstrate the same microbialite facies and benthic successions as seen within the shallow water reef caves today. This sponge mound facies is of widespread distribution at the platform margins and it migrates towards the coral facies as a result of rapid subsidence of the reef platform.

The maximum distribution of sponge reef mounds in Albian platforms is explained by transgressive events (starting phase of the "Cenomanian"-transgression) (further discussion see NEUWEILER this volume).

Comparable microbialite facies successions were studied in Jurassic sponge reefs (KEUPP et al. this volume), in late Cretaceous and Eocene ones of the southern Pyrenees, and within early Carnian sponge reefs of the Cassian Formation of northern Italy.

As a perspective and concept for further studies is postulated that within most Phanerozoic micritic reef mounds ("mud mounds") sponges and associated microbes (symbionts and external ones linked to biofilms) play a central role and control the mound formation. All micritic reefs should demonstrate this community type.

## 10 CONCLUSIONS

1. The investigated modern microbialites from Lizard Island are mainly a product of matrix mediated calcification via acidic organic macromolecules and baffled detritus. The calcifying organic substances were detected by using histochemical methods.
2. Microbial biofilms cover the surfaces of the microbialites and control the input of dissolved organic substances. They also control the settlement and distribution of benthic organisms. The slimy surfaces of biofilms are able to fix detritus. Biofilm based layers can mineralize and in few cases calcified microbes were observed.
3. The microbialites show two structural types: a thrombolitic one growing under relatively high sedimentation rates, and a more laminar to structurless one under reduced sedimentary influx (hardground-type).

4. All types are structured by Fe/Mn-microbial crusts. These crusts have a strong corrosive potential caused by electrochemical anode dissolution. In some microbialites more than 40% of the volumen is corroded. The brownish layers exhibit a pseudostromatolitic feature.

5. The studied caves have four main facies zones:

Zone 1: entrance area with normal reef corals (*Acropora*)  
 Zone 2: dim light area with deeper water zooxantellate corals (*Agaricia*, *Leptoseris*) and thick crusts of coralline red algae.

Zone 3: dimlight to dark area with slightly increased sedimentation rates and thrombolitic microbialite formation in comparison with zone 4. Coralline sponges are present but rapidly growing benthos is dominant (r-strategists).

Zone 4: dark conditions with reduced sediment particles in the water column, hardground-type microbialite and the *Acanthochaetetes*-community (k-strategists).

6. The vertical succession of the microbialites demonstrates a transgressive character.

7. Geochemically the microbialites are high-Mg calcites and the stable isotopes show a micrite formation close to the isotopic equilibrium of sea water.

8. The growth of microbialites within the investigated reefs is most probalby controlled by silicate weathering which increases the carbonate alkalinity. Therefore microbialitic crusts were only observed in reefs linked to continental islands (e.g. Lizard Island). In reefs of the outer barrier no microbialites were found.

9. The modern microbialites and associated organisms from the Lizard Island Section are very similar to those from Tertiary and Cretaceous occurrences.

## ACKNOWLEDGEMENTS

I thank the co-directors Dr. L. Vail and Dr. A. Hoggart at the Lizard Island Research Station as well as Terry Ford and Lois Wilson, the crew of the RV "Sunbird", for extensive help and support. The investigations were permitted by the Great Barrier Reef Marine Park Authority (G92/041; G93/046;). The Deutsche Forschungsgemeinschaft is acknowledged for financial support (Re 665/1-2, 4-1,2). I wish to thank Dr. Erlenkeuser (Univ. Kiel) and Dr. Joachimski (Univ. Erlangen) to carry out the stable isotope analyses and I acknowledge Prof. Franke (FU-Berlin) for the X-ray diffraction and electron microprobe analyses. The ESR-analysis were carried out by Dr. Eisenhauer (Heidelberg), and Dr. P. Röpstorf (Berlin) has done the TEM preparations, both are gratefully acknowledged. Many thanks to the Berlin Lizard Island working group, Dipl. Geol. Neuweiler, Prof. Keupp (all Berlin), Prof. Dullo (Kiel), Dr. Scholz (Hamburg), Prof. Hillmer (Hamburg), and Prof. Zankl (Marburg) for critical discussions, comments and leaving comparative material. Dr. Mehl and P. Böttcher (both Berlin) kindly

improve the language and make helpful suggestions. Very constructive reviews by Prof. Schlichter, and an anonymous reviewer are gratefully acknowledged.

## REFERENCES

- ADDADI, L. & WEINER, S. (1985): Interactions between acidic proteins and Crystals: Stereochemical requirements in biomineralization. – Proc. Natl. Acad. Sci. USA, **82**, 4110-4114
- & -- (1989): Stereochemical and Structural Relations between Macromolecules and Crystals in Biomineralization. – In: MANN, S.; WEBB, J. & WILLIAMS, R. J. P. (eds.): Biomineralization. – 133-156, Weinheim (VCH)
- & -- (1992): Kontroll- und Designprinzipien bei der Biomineralisation. – Angew. Chemie, **104**, 159-176, Weinheim
- ADDADI, L.; BERMAN, A.; MORADIAN-OLDAK, J. & WEINER, S. (1990): Tuning of Crystal Nucleation and Growth by Proteins: Molecular Interactions at Solid-Liquid Interfaces in Biomineralization. – Croatica Chem. Acta, **63**, 539-544, Zagreb
- BARNES, D.J. (1981): Improved measurement of coral calcification by sequential incubations with tritiated tetracycline and 45-calcium. – Proc. 4th internat. Coral Reef Symp., Manila, **2**, 249-255, Manila
- BASILE, L.L., CUFFEY, R.J. & KOSICH, D.F. (1984): Sclerosponges, Pharetronids, and Sphinctozoans (relict cryptic hard-bodied porifera) in the modern reefs of Enewetak Atoll. – J. Paleont., **54**, 636-650, Tulsa
- BERMAN, A.; ADDADI, L. & WEINER, S. (1988): Interactions of sea-urchin skeleton macromolecules with growing calcite crystals - a study of intracrystalline proteins. – Nature, **331**, 546-548, London
- BERNER, R.A. (1968): Calcium carbonate concretions formed by the decomposition of organic matter. – Science, **159**, 195-197, Washington
- BORBAS, J. E.; WHEELER, A. P. & SIKES, C. S. (1991): Molluscan Shell Matrix Phosphoproteins: Cirrelation of Degree of Phosphorylation to Shell Mineral Microstructure and to In Vitro Regulation of Mineralization. – J. Exp. Zool., **258**, 1-13
- BRACHERT, T. & DULLO, C. (1991): Lamina micritic crusts and associated foreslope processes, Red Sea. – J. Sed. Petrol., **61**, 354-363, Tulsa
- BUCZYNSKI, C. & CHAFETZ, H. S. (1991): Habit of Bacterially induced Precipitates of Calcium Carbonate and the Influence of medium Viscosity on Minerology. – J.Sed.Petrol., **61**, 226-233, Tulsa
- BURNE, R. V. & MOORE, L. S. (1987): Microbialites: Organosedimentary deposits of benthic microbial communities. – Palaios, **2**, 241-254, Tulsa
- CARROLL, J. J., GREENFIELD, L. J. & JOHNSON, R. F. (1966): The Mechanism of Calcium and Magnesium Uptake from Sea Water by a Marine Bacterium. – J. Cell. and Cop. Physiol., **66**, 109-118
- CHAFETZ, H. S. (1986): Marine Peloids: A Product of Bacterially induced Precipitation of Calcite. – J. Sed. Petrol., **56**, 812-817, Tulsa
- CHAFETZ, H. S. & BUCZYNSKI, C. (1992): Bacterially induced Lithification of Microbial Mats. – Palaios, **7**, 277-293, Tulsa
- CRISP, D. J. & RYLAND, J. S. (1960): Influence of filming and of surface texture on the settlement of marine organisms. – Nature, **185**, p. 119, London
- CUIF, J.-P., GAUTRET, P., LAGHI, G. F., MASTANDREA, A., PRADIER, B. & RUSSO, F. (1990): Recherche sur la fluorescence UV du squelette aspicaire chez les démosponges calcitiques Triasiques. – Geobios, **23**, 21-31, Lyon
- DEGENS, E. T. (1976): Molecular mechanisms on carbonate, phosphate and silica deposition in the living cell. – Topics in curr. Chem. **64**, 1-112
- (1979): Why do organisms calcify?. – Chem. Geol., **25**, 257-269, Amsterdam
- (1989): Perspectives on Biogeochemistry. – 423 p., Berlin (Springer)
- DEGENS, E. T., CAREY, F. G., SPENCER, D. W. (1967): Amino-acids and amino-sugars in calcified tissues of portunid crabs. – Nature, **216**, 601-603, London
- DEGENS, E. T. & ITTEKKOT, V. (1986): Ca<sup>2+</sup> -Stress, biological response and particle aggregation in the aquatic habitat. – Netherlands. J. Sea Res., **20**, 109-116
- DRAVIS, J. J. & YUREWICZ, D. A. (1985): Enhanced carbonate petrography using fluorescence microscopy. – J. Sed. Petrol., **55**, 795-804, Tulsa
- DREW, G. H. (1911): The action of some denitrifying bacteria in tropical and temperate seas, and the bacterial precipitation of calcium carbonate. – J. Mar. Biol. Assoc. U.K., **9**, 142-155
- DRUFFEL, E. R. M. & BENAVIDES, L. M. (1986): Input of excess CO<sub>2</sub> to the surface ocean based on 13C/12C ratios in a banded Jamaican sclerosponge. – Nature, **321**, 58-61, London
- FINERMAN, G. A. M. & MILCH, R. A. (1963): In vitro Binding of Tetracyclines to Calcium. – Nature, **196**, 486-487, London
- FRICKE, H. & MEISCHNER, D. (1985): Depth limits of Bermudan scleractinian corals: a submersible survey. – Mar. Biol., **88**, 175-187, Berlin
- FRICKE, H. & SCHUMACHER, H. (1983): The depth limits of Red Sea stony corals: an ecophysiological problem (a deep diving survey by submersible). – Pubbl. della Staz. Zool. de Napoli I Mar. Ecol., **4**, 163-194, Naple
- FRITZ, G. K. (1958): Schwammstotzen, Tuberoide und Schuttbreccien im Weißen Jura der Schwäbischen Alb. – Arb. Geol. Paläont. Inst. TH Stuttgart, N.F., **13**, 118 p., Stuttgart
- GAUTRET, P. (1989): Premières données sur les masses moléculaires des composés organiques associés aux squelettes aspicaire de spongiaires calcifiés (Démosponges et Calcarea). – C. R. Acad. Sci. Paris, **309** (ser. II), 1083-1088, Paris
- GAUTRET, P. & MARIN, F. (1990): Composition en acides aminés des phases protéiques solubles et insolubles du squelette calcaire de trois Démosponges actuelles: *Ceratoporella nicholsoni* (HICKSON), *Astroclera willelyana* LISTER et *Vaceletia crypta* (VACELET). – C. R. Acad. Sci. Paris, **310** (ser. II), 1369-1374, Paris.
- GAWLITTA, W., STOCKEM, W., WEHLAND, J. & WEBER, K. (1980): Pinocytosis and Locomotion of Amoebae. – Cell and Tissue Res., **213**, 9-20, Berlin
- GERDES, G. & KRUMBEIN, W. E. (1987): Biolaminated Deposits. – Lecture Notes in Earth Sciences, **9**, 283 p., Berlin
- GRANT, R. E. (1980): Brachiopods of Enewetak Atoll. – In: DEVANEY, D. M., REESE, E. S., BURCH, B. L. & HELFRICH, P. (eds.), The Natural History of Enewetak Atoll; Vol.II.- 77-84, Honolulu
- GREENFIELD, L. J. (1963): Metabolism and concentration of Calcium and Magnesium and precipitation of Calcium carbonate by a marine bacterium. – Ann. N. Y. Acad. Sci., **130**, 23-45, New York
- GUNTORPE, M. E., SIKES, C. S. & WHEELER, A. P. (1990): Promotion and Inhibition of Calcium Carbonate Crystallization in Vitro by Matrix Protein from Blue Crab Exoskeleton. – Biol. Bull., **179**, 191-200
- HAMILTON, W. A. & CHARACKLIS, W. G. (1989): Relative Activities of Cells in suspension and in Biofilms. – In: CHARACKLIS, W. G. & WILDERER, P. A. (eds.): Structure and Function of Biofilms. – 199-219; Dahlem Konferenzen (Wiley)
- HAUSSER, I. & HERTH, W. (1983): The Ca<sup>2+</sup>-Chelating antibiotic, Chlorotetracycline (CTC), disturbs multipolar tip growth and primary wall formation in *Micrasterias*. – Protoplasma, **117**, 167-173, Berlin
- HENRICH, R., HARTMANN, M., REITNER, J., SCHÄFER, P., STEINMETZ, S., FREIWALD, A., DIETRICH, P. & THIEDE, J. (1992): Facies belts and Communities of the Arctic Vesterisbanken Seamount (Central Greenland Sea). – Facies, **27**, 71-104, Erlangen
- HICKS, J. D. & MATTHAEI, E. (1958): A selective fluorescence stain for mucin. – J. Pathol. Bacteriol., **75**, 473-476

- RYLAND, J. S. (1959): Experiments on the selection of algal substrates by polyzoan larvae. – *J. exp. Biol.*, **36**, 613-631
- SANTAVY, D., WILLENZ, Ph. & COLWELL, R. R. (1990): Phenotypic Study of Bacteria Associated with the Caribbean Sclerosponge, *Ceratoporella nicholsoni*. – *Appl. Environment. Microbiology*, **56**, 1750-1762
- SARÀ, M. (1971): Ultrastructural aspects of the symbiosis between two species of the genus *Aphanocapsa* (Cyanophyceae) and *Icrinia variabilis* (Demospongiae). – *Mar. Biol.*, **11**, 214-221, Berlin
- SCHMAL, G. (1985): Bacterially induced stolon settlement in the scyphopolyp of *Aurelia aurita* (Cnidaria, Scyphozoa). – *Helgoländer Meeresuntersuchungen*, **39**, 33-42, Hamburg
- SCHOLZ, J. (1993): Self-organization in Reefs: Observations on Bryozoans and Microbial Mats. – *Facies*, **29**, this volume
- SIGG, L. & STUMM, W. (1989): *Aquatische Chemie*. – 388 pp., Zürich (VDF).
- SIMKISS, K. (1977): *Biominalisation and Detoxification*. – *Calcif. Tiss. Res.*, **24**, 199-200; Berlin (Springer)
- (1986): The processes of biomineralization in lower plants and animals - an overview. – In: LEADBEATER, B. S. C. & RIDING, R. (eds.): *Biominalisation in Lower Plants and Animals*. – The Syst. Assoc. Spec. Vol. **30**, 19-38, Oxford
- SIMKISS, K. & WILBUR, K. M. (1989): *Biominalization. Cell Biology and Mineral Deposition*. – 337 pp., San Diego (Academic Press)
- SOULE, J. H. (1973): *Histological and Histochemical Studies on the Bryozoan-substrate Interface*. – In: LARWOOD, G. P. (ed.): *Living and fossil Bryozoa*. – 343-347, London (Academic Press)
- STEBBING, A. R. D. (1972): Preferential sttlement of a bryozoan and serpulid larvae on the younger parts of *Laminaria* fronds. – *J. mar. biol. Ass. U.K.*, **52**, 765-772
- STOFFERS, P. & BOTZ, R. (1990): Carbonate crusts in the Red Sea: their composition and isotope geochemistry. – In: ITTEKOT, V., KEMPE, S., MICHAELIS, W. & SPITZY, A. (eds): *Facets of modern biogeochemistry*. – 242-252, Berlin (Springer)
- STRUGGER, S. (1940): *Fluoreszenzmikroskopische Untersuchungen über die Aufnahme und Speicherung des Acridinorange durch lebende und tote Pflanzenzellen*. – *Jena. Z. Naturwiss.*, **73**, 97ff., Jena
- TARUTANI, T., CLAYTON, R. N. & MAYEDA, T. K. (1969): The effect of polymorphism and magnesium substitution on oxygen isotope fractionation between calcium carbonate and water. – *Geochim. Cosmochim. Acta*, **33**, 987-996, Oxford
- VACELET, J. (1970): Description de cellules à bactéries intranucléaires chez des éponges *Verongia*. – *J. Microscopie*, **9**, 333-346
- (1971): L'ultrastructure de la cuticule d'éponge cornées du genre *Verongia*. – *J. Microscopie*, **10**, 113-116
- (1975): Etude en microscopie électronique de l'association entre bactéries et spongiaires du genre *Verongia* (Dictyoceratida). – *J. Microscopie Biol. cell.*, **23**, 271-288.
- VACELET, J. & VASSEUR, P. (1965): Spongiaires des grottes et surplombs des récifs de Tuléar (Madagascar). – *Rec. Trav. Stat. mar. Endoume, Suppl.* **4**, 71-123, Marseille
- & -- (1971): *Eponge des récifs coralliens de Tuléar (Madagascar)*. – *Téthys, Suppl.* **1**, 51-126
- VIDELA, H. A. (1989): Metal Dissolution/Redox in Biofilms. – In: CHARACKLIS, W. G. & WILDERER, P. A. (eds.): *Structure and Function of Biofilms*. – 301-320; Dahlem Konferenzen (Wiley)
- WEBER, J. N. & WOODHEAD, M. J. (1970): Carbon and Oxygen Isotope Fractionation in the Skeletal Carbonate of Reef-Building Corals. – *Chem. Geol.*, **6**, 93-117, Amsterdam
- WEINER, S., TRAUB, W. & LOWENSTAM, H. A. (1983): Organic matrix in calcified exoskeletons. – In: WESTBROEK, P. & de JONG, E. W. (eds.): *Biominalization and Biological Metal Accumulation*. – 205-224, Amsterdam (Reidel)
- WESTBROEK, P. & de JONG, E. W. (eds.) (1983): *Biominalization and Biological Metal Accumulation*. – Amsterdam (Reidel)
- WHEELER, A. P. & SIKES, C. S. (1989): Matrix-Crystal interactions in CaCO<sub>3</sub> Biomineralization. – In: MANN, S., WEBB, J. & WILLIAMS, R. J. P. (eds.): *Biominalization*. – 95-131, Weinheim (VCH).
- WILDERER, P. A. & CHARACKLIS, W. G. (1989): Structure and Function of Biofilms. – In: CHARACKLIS, W. G. & WILDERER, P. A. (eds.). – *Structure and Function of Biofilms*. – 5-17; Dahlem Konferenzen (Wiley)
- WILKINSON, C. (1978a): Microbial associations in sponges. II. Numerical Analysis of Sponge and Water Bacterial Populations. – *Mar. Biol.*, **49**, 169-176; Berlin
- (1978b): Microbial associations in sponges. III. Ultrastructure of the in situ Associations in Coral Reef Sponges. – *Mar. Biol.*, **49**, 177-185; Berlin
- (1979): Nutrient translocation from symbiotic cyanobacteria to coral reef sponges. – *Coll. Internat. CNRS, Biologie de spongiaires*, **291**: 373-380, Paris
- (1983): Net Primary Productivity in Coral Reef Sponges. – *Science*, **219**, 410-411, Washington
- Wilkinson, C. & Fay, P. (1979): Nitrogen fixation in coral reef sponges with symbiotic cyanobacteria. – *Nature*, **279**, 527-529, London
- WILKINSON, C. & GARRONE, R. (1980): Nutrition of marine sponges. Involvement of symbiotic bacteria in the uptake of dissolved carbon. – In: SMITH, D. C. & TIFFON, Y. (eds.): *Nutrition in the lower metazoa*. – 157-161, Oxford (Pergamon)
- WILKINSON, C., GARRONE, R. & HERBAGE, D. (1979): Sponge collagen degradation in vitro by sponge-specific bacteria. – *Coll. Internat. CNRS, Biologie de spongiaires*, **291**, 361-364, Paris
- WILLENZ, Ph. & HARTMAN, W. D. (1985): Calcification rate of *Ceratoporella nicholsoni* (Porifera: Sclerospongiae): An *in situ* study with calcein. – *Proc. 5th Internat. Coral Reef Congr., Tahiti 1985*, **5**, 113-118
- WILLIAMS, R. J. P. (1989): The Functional Form of Biominerals. – In: MANN, S., WEBB, J. & WILLIAMS, R. J. P. (eds.): *Biominalization*. – 1-34, Weinheim (VCH).
- WORMS, D. & WEINER, S. (1986): Mollusk shell organic matrix: Fourier transform infrared of the acidic macromolecules. – *J. Exp. Zool.*, **237**, 11-20
- ZANKL, H. (1993): -- *Facies* **29**, this volume

Manuscript received March 3, 1993

Revised manuscript accepted July 26, 1993